# NORWEGIAN DEFENSE UNIVERSITY COLLEGE/ ROYAL NORWEGIAN NAVAL ACADEMY

# Bachelor thesis

Propulsion and energy analysis of a naval unmanned surface vessel

by

Truls Ballo Sørnes and Sondre Østensen

Submitted as a part of the requirements for the degree:

BACHELOR IN MILITARY STUDIES WITH SPECIALIZATION IN LEADERSHIP

- NAVAL ENGINEERING

Word count: 15 237

Submitted: December 2023

**Godkjent for offentlig publisering**

## Publiseringsavtale

### En avtale om elektronisk publisering av bachelor/prosjektoppgave

Kadetten(ene) har opphavsrett til oppgaven, inkludert rettighetene til å publisere den.

Alle oppgaver som oppfyller kravene til publisering, vil bli registrert og publisert i Bibsys Brage når kadetten(ene) har godkjent publisering.

Oppgaver som er graderte eller begrenset av en inngått avtale vil ikke bli publisert.

| | | |
|---|---|---|
| Jeg (Vi) gir herved Sjøkrigsskolen rett til å gjøre denne oppgaven tilgjengelig elektronisk, gratis og uten kostnader | X<br>Ja | <br>Nei |
| Finnes det en avtale om forsinket eller kun intern publisering?<br><br>(Utfyllende opplysninger må fylles ut) | <br>Ja | X<br>Nei |
| Hvis ja: kan oppgaven publiseres elektronisk når embargoperioden utløper? | <br>Ja | <br>Nei |

### Plagiaterklæring

Vi erklærer herved at oppgaven er mitt eget arbeid og med bruk av riktig kildehenvisning. Vi har ikke nyttet annen hjelp enn det som er beskrevet i oppgaven.

Vi er klar over at brudd på dette vil føre til avvisning av oppgaven.

Dato: 02-12-2023

_Truls. B.Sornes_
_____
Sørnes, Truls Ballo

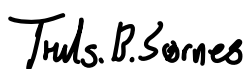_Sondre Østensen_
_____
Østensen, Sondre

# Preface

This thesis is written by Truls Ballo Sørnes and Sondre Østensen as a requirement for the study "Bachelor in military studies with specialization in leadership – naval engineering" at the Royal Norwegian Naval Academy. The thesis was written between September and December 2023 during the Erasmus exchange program at Helmut Schmidt Universität, Hamburg, Germany.

We would like to take the opportunity to thank Associate Prof. Alexander Sauter for providing supervision and guidance throughout the entire work.

Furthermore, we would like to thank Univ.Prof. Dr. Ing. Christian Kreischer, and PhD. Student Florian Dreishing for facilitating for, supporting, and supervising our work at Helmut Schmidt Universität.
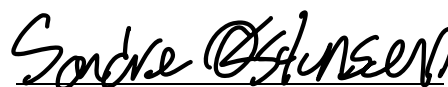
Finally, we would like to thank everyone else who supported us during the work by contributing with knowledge or data.

Bergen, Royal Norwegian Naval Academy, 02-12-2023

Sørnes, Truls Ballo                                    Østensen, Sondre

# Abstract

Norway's geographical location and vast ocean areas contains both national and international areas of interest. Continuous surveillance of these ocean areas both on and below the surface can prove difficult with limited resources and personnel. The implementation of unmanned surface vessels with intelligence, surveillance, and reconnaissance (ISR) capabilities could be a promising possibility for greater coverage at a lesser cost. Such a concept would require high standards for vessel performance, survivability, and redundancy. When addressing these, the drivetrain, its performance, weight and efficiency becomes increasingly important.

The thesis conducts a study on the dynamic behavior of the drivetrain from *A naval design study on a small, unmanned surface vessel by Andressen & Mykland 2022*. The drivetrain is investigated based on the operational capabilities and requirements found by Andressen & Mykland. The thesis provides an analysis of the components in the drivetrain, emphasizing the sizing, weight and efficiency of each, and its correlations to the load and speed of the vessel. For some components, empirical data was gathered to further analyze these dependencies.

The results emphasize how each part affects the overall weight, fuel capacity and performance of the drivetrain. The results showcase the different characteristics of different types of electric motors and how these are affected by varying loads and speeds. Further, it displays the complexity when addressing dynamic behavior of multiple components working to fulfill operational requirements in a given operational area (AO). The answer is not straight forward, and the decisive variables are many.

The results and discussion provide a recommendation of the best configuration for the overall efficiency, weight and fuel capacity for the drivetrain. The configuration has lower efficiency, higher fuel consumption and weight compared to the work of Andressen & Mykland but is assumed to provide more reliable data for further work. The increase in weight will inflict hydrostatic data, factors such as sea keeping and stability, and the performance of the vessel.

Although the thesis presents a recommendation, further work should include physical testing of reference model of drivetrain, as well as addressing subjects of the vessel and drivetrain, not included in this work for further optimization.

[INTENTIONALY LEFT BLANK]

# Content

# Figures

# Tables

# Nomenclature and symbols

**Nomenclature:**

AC                Alternating current

AO                Area of operation

D.G               Diesel generator

DC                Direct current

ETA               Efficiency

FPP               Fixed Pitch Propeller

IEP               Integrated Electric Propulsion

IM                Induction machine

ISR               Intelligence, Surveillance and Reconnaissance

PMSM              Permanent magnet synchronous machine

RPM               Rotation per minute

SM                Synchronous machine

USV               Unmanned Surface Vessel

**Symbols:**

| Symbol | Description | Unit |
|---|---|---|
| ŋ | Efficiency | % |
| $P_{out}$ | Exploitable power out | W |
| $P_{in}$ | Power in | W |
| D | Diameter | m |
| P | Pitch | m |
| BAR | Blade area ratio | $m^2$ |
| $A_D$ | Developed area | $m^2$ |
| $A_o$ | Disc area | $m^2$ |

| w | Wake fraction coefficient | |
|---|---|---|
| $C_b$ | Block coefficient | |
| t | Thrust deduction fraction | |
| $T_{shaft}$ | Thrust per shaft | kN |
| $R_{ts}$ | Towing resistance | kN |
| $n_{shafts}$ | Number of shafts | |
| $T_{max}$ | Maximum thrust | kN/m$^2$ |
| $V_1$ | propeller's speed through water | m/s |
| $V_s$ | Ship speed | m/s, knots |
| $K_T$ | Thrust coefficient | |
| J | Advance ratio | |
| $\rho$ | Density | kg/$m^3$ |
| n | Rotational speed propeller | RPM |
| P.C | Propulsion coefficient | % |
| $\eta_o$ | Open water efficiency | % |
| $\eta_R$ | Relative efficiency | % |
| $\eta_H$ | Hull efficiency | % |
| $\eta_{shaft}$ | Shaft efficiency | % |
| $P_e$ | Power required to propeller | kW |
| $P_E$ | Towing power | kW |
| $\tau$ | Torque | Nm |
| F | Force | N |
| a | Arm | m |

| P | Power | W |
|---|---|---|
| $n_{sync}$ | Synchronous speed | RPM |
| f | Frequency | Hz |
| $p_p$ | Number of pole pairs | |
| $P_{fe}$ | Iron losses | W |
| $P_{hysterisis}$ | Hysteresis losses | W |
| $P_{eddy\ current}$ | Eddy current losses | W |
| $\sigma_h$ | Hysteresis coefficient | |
| $\sigma_e$ | Eddy current coefficient | |
| $B_m$ | Magnetic flux density | T |
| $P_{cu}$ | Copper losses | W |
| $R_{cu}$ | Resistance windings | Ω |
| I | Current | A |
| $\rho_{cu}$ | Resistivity copper | Ω/m |
| l | Length | m |
| d | Diameter | m |
| $k_{coil}$ | Constant depending on location of end windings | |
| $n_s$ | Number of conductors per stator slot | |
| q | Number of stator slots per pole and per phase | |
| $A_{cond}$ | Cross sectional area of one conductor | $m^2$ |
| $P_N$ | Nominal power | kW |

| | | |
|---|---|---|
| $\hat{A}_m$ | Electric loading | A/mm^2 |
| ω | Angular velocity | Rad/s |
| s | Relative slip | % |
| $n_{slip}$ | Slip speed | RPM |
| $n_2$ | Rotor speed | RPM |
| $P_{FR+V}$ | Power losses friction and ventilation | W |
| $\eta_{engine}$ | Efficiency diesel engine | % |
| $\eta_{generator}$ | Efficiency electric generator | % |
| $\tau_{em}$ | Electromagnetic torque | Nm |
| $P_e$ | Shaft power | W |
| $\dot{m}_B$ | Fuel consumption | Kg/s |
| $h_n$ | Lower heating value | MJ/kg |
| $k_1$ | Gear ratio old design | |
| $k_2$ | Gear ratio new design | |
| | Specific Energy density | Wh/kg |
| U | Voltage | V |
| T | Thrust | kN |
| $\eta_{rectifier}$ | Efficiency rectifier | % |
| $\eta_{inverter}$ | Efficiency inverter | % |
| $\eta_{gear}$ | Efficiency gear | % |
| p | Number of poles | |

# 1    Introduction

The Norwegian coastline stretches far from the north, by the Barents Sea, to the North Sea in the south. This makes for a long coastline and connecting ocean areas that are even bigger, which together form the Norwegian ocean areas. These ocean areas contain both national and international areas of interest. The Barents Sea is home to the Russian North fleet stationed on the Kola Peninsula. The fleet is known to have nuclear capabilities, intercontinental missiles, and an ice-free path to the Atlantic- and Polar Sea through the year (FFI, 2020, p.3). The Southern Ocean areas of Norway contain one of the world's largest oil and gas productions. Oil and gas are transported to Norway and other countries through pipes on the ocean floor. The war in Ukraine and the corresponding attack on the Nord Stream pipelines in 2022 (Bryant, 2023), emphasizes the importance of maintaining surveillance of these ocean areas.

The Norwegian Minister of Defense states in its long-term plan that the Norwegian Military must obtain the ability to surveil activities on and below the surface in the Norwegian sea territory, and if needed, different capacities should be able to work together for continuous surveillance of a given area. The Norwegian Armed Forces main anti-submarine capabilities is provided by the frigates, and the maritime patrol aircrafts (Forsvaret, 2023). With limited resources, and accounting for periods of maintenance, it is challenging to establish continuous presence and surveillance, both on and below the surface, in these vast ocean areas.

The development of unmanned surface vessels (USV) is rapidly increasing throughout the world, also in military applications. From a military point of view, detection, tracking and classification of submarines is especially challenging. From the depths of the Norwegian Sea or below the artic ice the Russian submarines have great coverage from planes, satellites, and surface vessels. Given Norway's geographical placement, they play a vital role in early detection and surveillance before they can reach these areas (Hattrem, 2021).

A USV utilizing towable sonar like shown in Figure 1 to detect submarines is a promising possibility for greater coverage for a lesser cost, as well as providing a positive contribution to risk management when considering human lives and material losses (Andressen & Mykland, 2022, p.14)
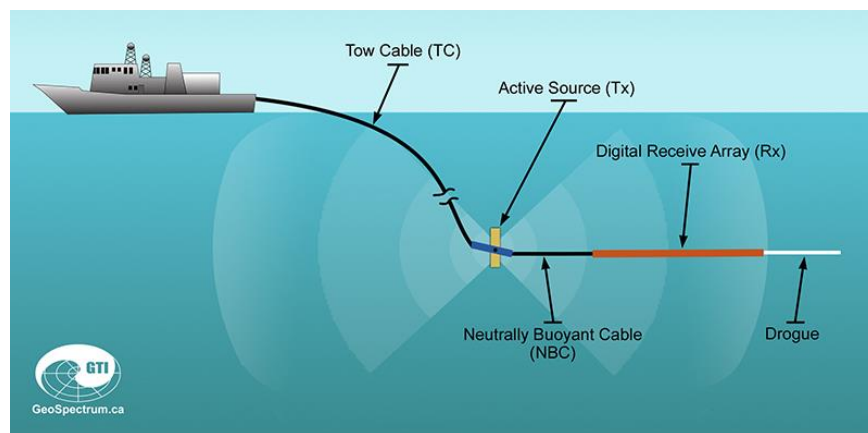
**Figure 1: Illustration of towable sonar (GeoSpectrum, 2018)**

The implementation of such a concept in larger numbers would demand a design specifically suited for the given operations. Parameters such as survivability, redundance and autonomy all play a vital role in the concept. Survivability and autonomy create high standards for the vessels' capability to survive on their own. Some central requirement is the vessel ability to power itself and contain enough fuel or battery power to meet the criteria given by the operational needs and conditions in the area of operation (AO). The power need and fuel consumption of such a vessel would impact the sizing and weight of its components and therefore the overall size and weight of the vessel, which again affects the hydrostatic data and performance. When looking at the power need and fuel consumption, the efficiency of the drivetrain becomes increasingly important when considering the larger number of vessels and long periods of continuous operations. Different kinds of drivetrain configurations provide different pros and cons. These can vary depending on the need for redundance, complexity or simplicity next to other operational restraints. Regardless of the configuration, overall efficiency is always something that should be considered.

The power for the drivetrain origins from a power source, either in the form of a battery or a fuel capacity. Through a series of components, this power is transmitted to the propeller which propels the ship forward. Each of the components in the drivetrain has its own efficiency. All these together form the overall efficiency of the drivetrain. Furthermore, the efficiency is dynamic and will vary depending on the load, and thus on the speed of the vessel, and the sea state it operates in.

To find the optimum drivetrain configuration for a given application in a certain environment is challenging. Often in the early stages of development, rules of thumb are the only easily accessible tools. However, the conduction of a more detailed analysis is important to emphasize the dynamic behavior and changes happening withing the system. A detailed analysis depends on the given needs withing the operation and other external conditions, but also on each component of the drivetrain. One of the biggest research areas for electric drivetrains is how to optimize the sizing and weight of the components while still being able to meet the operational requirements. Both size and weight, in addition to the overall efficiency, are especially of concern when developing small vessels like USVs.

## 1.1  Background

The configuration of the USV is dependent on the required operational capabilities, and nature of operational area. Therefore, in order to conduct a deeper analysis of the drivetrain for a USV, an initial concept is required.

Midshipmen Andressen & Mykland wrote in 2022 a bachelor thesis regarding: *A naval design study on a small, unmanned surface vessel.* The thesis was a concept study regarding the use of a passive USV stationed in large numbers around the Norwegian coastal waters. These were to provide surface and sub-surface intelligence, surveillance, and reconnaissance (ISR) capabilities. The concept included a drivetrain configuration (Figure 2) with associated estimations based on rules of thumb. Although their thesis provides valid estimations, it lacks the necessary depth within its part which is needed to address the dynamic behaviors of the drivetrain.
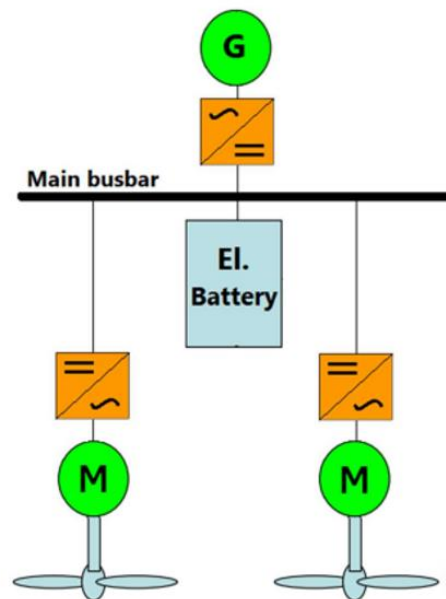
**Figure 2: Model of IEP drivetrain (Andressen & Mykland, 2022, p.72)**

Their drivetrain consists of one M-SQ Pro 25 Maritime diesel generator connected to a rectifier which delivers the power to the main busbar. From the main busbar the power is distributed to two inverters, each supplying power to their own Drivemaster 15W, 10 kW electrical motor. Each motor is connected to the propellers through a shaft. The drivetrain also contains a battery package, estimated from the Tesla's 4680-Type battery, to enable a running mode without the use of the generator, which could lower acoustic signature, and provide increased redundancy. Further a 10-kW hotel load was estimated to supply sensors, navigation equipment, de-icing, and other necessary equipment. The concept study also presented an estimated operation profile for the USV shown in Table 1, and a weight breakdown of the vessel and drivetrain which can be seen in Appendix A (Anderssen & Mykland, 2022). The estimated operation profile considers a certain amount of transit to the operation area, deploying and conducting of search operation with the towing sonar, before making the same transit to return, either its original or a different location.

*Table 1: Estimated operation profile for USV (Andressen & Mykland, 2022, p.81)*

| Operation | Speed [knots] | Distance [Nm] | Hours [h] |
|---|---|---|---|
| Transit | 7 | 350 | 50 |
| Transit | 3 | 10 | 3,33 |
| Winching | 3 | 1 | 0,33 |
| Towing | 5 | 1000 | 200 |
| Winching | 3 | 1 | 0,33 |
| Transit | 3 | 10 | 3,33 |
| Transit | 7 | 350 | 50 |

Some requirements were also set based on the identified capabilities given for the USV. The necessary capability for the concept was defined by given operational needs, missions, tasks, operation scenario, and survivability (Andressen & Mykland, p.34-37). Some of these include the capability to handle ISR operations utilizing a passive towable sonar, and the capability to tow the sonar at vessel speed of 5 knots. Further the vessel should obtain the capability to conduct long term operations in rough sea (Andressen & Mykland, s.54-57).

The sea state in Norwegian oceans can be graded on a scale between 0-9 with respect to the observed wave amplitude. 9 being the harshest, and 0 being dead calm. The sea states are defined by height of waves and are shown in Table 2.

*Table 2: Sea States in Norwegian Ocean (Sivle, 2018).*

| Sea state | Description | Wave height |
|-----------|-------------|-------------|
| 0 | Calm (glassy) | 0 m |
| 1 | Calm (rippled) | 0 -0.1 m |
| 2 | Smooth (wavelets) | 0.1 – 0.5 m |
| 3 | Slight | 0.5 – 1.25 m |
| 4 | Moderate | 1.25 – 2.5 m |
| 5 | Rough | 2.5 – 4 m |
| 6 | Very rough | 4 – 6 m |
| 7 | High | 6 – 9 m |
| 8 | Very high | 9 – 14 m |
| 9 | Phenomenal | Over 14 m |

## 1.2  Purpose

The need for continuous monitoring of the Norwegian and adjacent sea areas is of high importance for both Norwegian and allied command and control. A concept was developed by midshipmen Andressen & Mykland to meet these operational needs. Necessary capabilities were composed to fulfill the operational needs, and from these capabilities a set of requirements was made. The requirements specify the needs for survivability and endurance of the USV. The endurance of the vessel depends on the drivetrain's efficiency and its composition of components. Further, the continuation of this concept would require a deeper understanding of the dynamic behavior occurring within the drivetrain.

This thesis is to investigate further into the drivetrain concept chosen by Andressen & Mykland, in order to investigate the overall efficiency of the drivetrain given the requirements to fulfill the necessary operational capabilities and the estimated operation profile.

The following requirements found by Andressen & Mykland will have an impact on the drivetrain's performance, weight, or configuration.

- Be able to transit in 7 knots in sea state 3.

- Be able to tow sonar in 5 knots in sea state 3.

- The vessel must have two drive trains and means of propulsion.

- 12 hours operating in 5 knots towing condition with battery in case of disrupted energy supply.

- 20 days operating in 5 knots towing condition in sea state 3, with 35% remaining fuel.

While considering these requirements, the thesis will conduct a deeper analysis of the components in the drivetrain. The analysis aims to provide information on how each part of the drivetrain is affected by the load and speed of the vessel. The dynamic behavior of propeller efficiency will be investigated. Further the utilization of a gear, and its effect on the drivetrain will be studied. The electrical motor is studied in detail with regards to different performance characteristics for different types and sizes. In addition, the thesis aims to present updated weight and fuel calculations for the drivetrain based on the results from the analysis. The thesis aims to confirm or find potential for improvement within the already existing drivetrain.

> *The thesis aims to provide further investigation on the drivetrain concept from "A naval design study on a small, unmanned surface vessel" to find the configuration of components that provide the optimum combination of efficiency and weight for the drivetrain.*

## 1.3   Limitations

Due to limited time, the following aspects will not be considered:

- Model construction and testing
- Comprehensive calculations of electrical components outside the drivetrain
- How stability is affected by potential changes in the drivetrain.
- Advanced battery calculations or accounting for battery management system
- Other fuel options
- Rudder configurations and its effect on drivetrain efficiency
- Comprehensive calculations regarding the sea states effect on the vessel

## 1.4   Structure

The thesis will be initiated in chapter 1 by presenting the introduction and identified needs for this thesis. Further the background, task description and limitations are displayed. Chapter 2 starts off with an introduction to the components in the drivetrain. Then, each component of the drivetrain, starting from the propeller, is investigated as a part of a literature study. The study emphasizes the relevant theory regarding each of the components, the available technologies and the efficiency losses connected to each component. Chapter 3 describes how the relationships found in the literature study are comparable with available empirical data or processed based on correlations found. Further, chapter 4 displays the results obtained by the relevant theory, data gathered and the conducted methods. In chapter 5, a discussion of the results found in chapter 4 is conducted. Lastly, in chapter 6, a summary and conclusion of the thesis is provided with recommendations for further work.

# 2   Theory

In this chapter the relevant theory regarding each component in the integrated electric propulsion (IEP) drivetrain (Figure 3) will be presented. It will be concentrated around theory of operation, size, weight, and efficiency for each component.
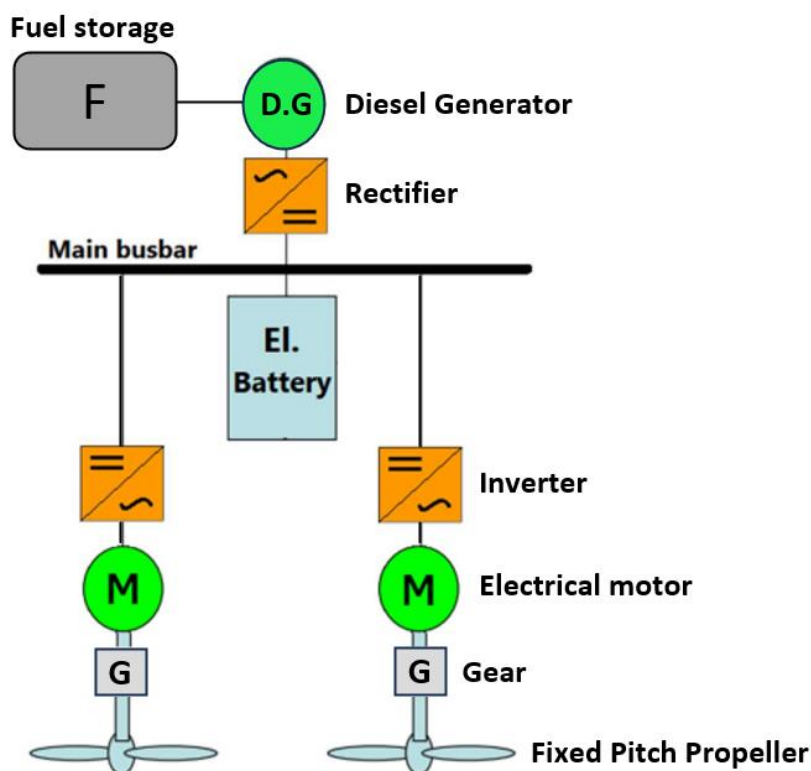


**Figure 3: Drivetrain concept investigated.**

The efficiency, ŋ, is a measure of how efficient a machine or a process is, and is defined as the relationship between exploitable power out and consumed power in. The efficiency for a process is then given by (Grønn, 2022):

$$\eta = \frac{P_{out}}{P_{in}} \tag{2.1}$$

For some machines, an Efficiency map (Figure 4), or iso-efficiency contours are provided by the manufacturer. An efficiency map provides a way to visualize the machines operating area, and how deviations from this will affect the efficiency. They can aid when selecting and optimizing a machine as a part of a larger system, and for a given application. Efficiency maps are used to analyze existing systems, and in design and modeling of machines (Haines, 2019, s.232).
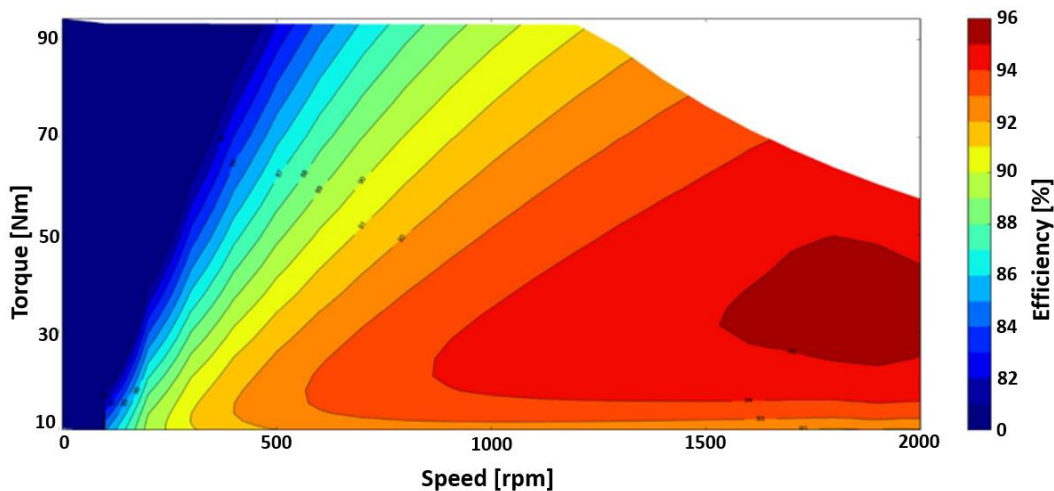
**Figure 4: Example of efficiency map for electrical motor (Appendix B)**

## 2.1 Propeller

The function of a propeller is to convert rotational momentum to axial thrust. This thrust generation is quite similar to how an airplane wing generates lift. The rotational movement of the propeller pushes the water along the blade faces backwards, resulting in an increase in pressure acting on the propeller faces, pushing the propeller forward. At the same time the pressure at the blade backs decreases, creating a vacuum pulling the propeller forward. (Whiteford, 2022)
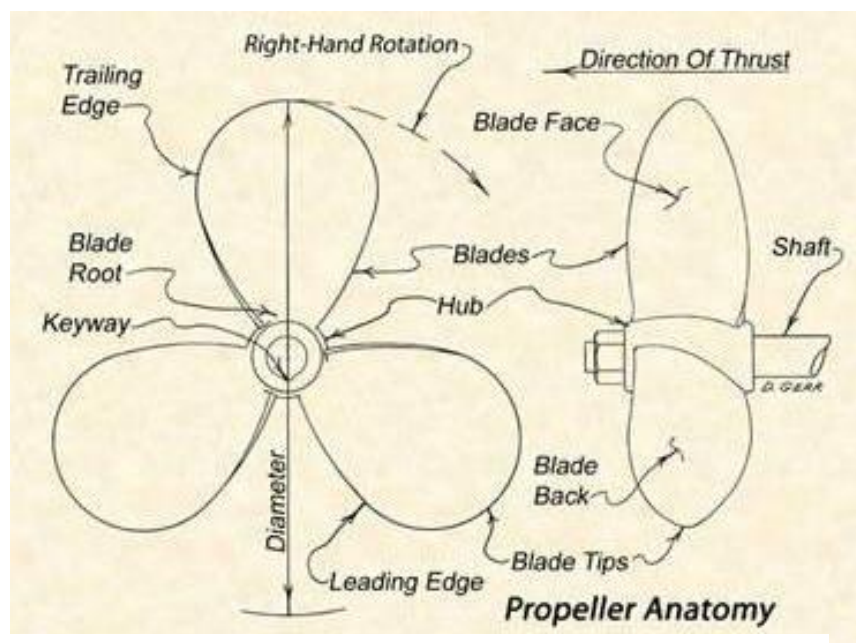


**Figure 5: "*Propeller anatomy*", 2018, unknown creator. (Propeller Anatomy – Accutech (accutechmarine.com)).**

There are many factors affecting how much fluid is moved per time unit, and thereby how much power is generated. Some of these factors are diameter, pitch and rotational speed. The diameter of a propeller (D), illustrated in Figure 5, determines the amount of water moved by dictating the area of water affected by the propeller. Pitch (P) is defined as the distance a propeller advances in the direction of the axis per revolution in an ideal situation (Rawson & Tupper, 2001, p. 395 - 397), as illustrated in Figure 6. The pitch of a propeller is related to the angle of which the propeller blades are mounted to the propeller hub. On a propeller with a larger diameter, the increase in circumference will lead to a lesser angle between the propeller blades and the propeller hub to achieve the same pitch. The angle of the propeller blades is therefore dependent on the relation P/D.



Low pitch

High pitch

Pitch control
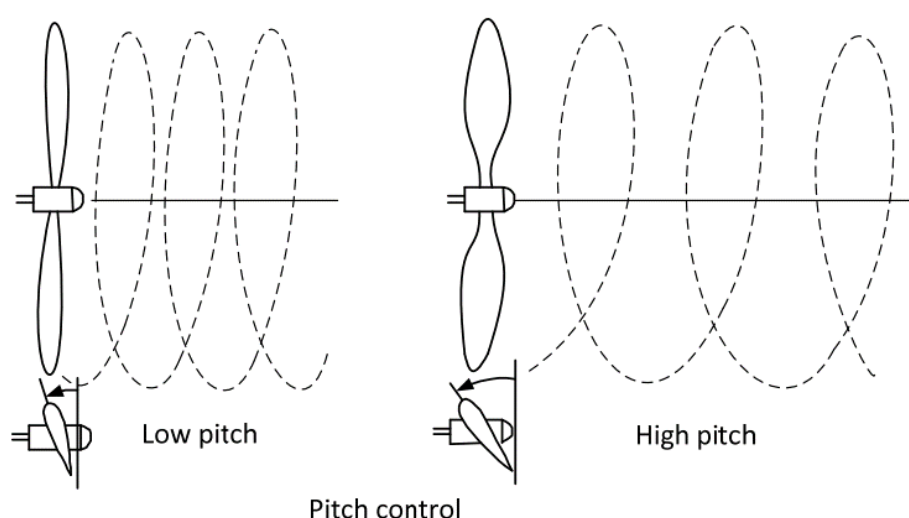
**Figure 6: Definition of propeller pitch. (Czyż, Karpiński, Skiba & Wendeker, 2021, p. 2)**

The rotational speed of the propeller affects how much water is dragged through the propeller and how much thrust is generated by determining the speed of which the water are dragged into and pushed out of the propeller.

Another factor affecting the power generated by the propeller, and power needed to propel the vessel, is the propulsion coefficient (P.C), describing the efficiencies and losses of propeller and hull. The formulas and coefficients in equation 2.2 – 2.10 are used to calculate the propulsion coefficient. Firstly, the wake fraction (w) must be calculated. An estimation of w can be done using the block coefficient ($C_b$), as shown in equation 2.3 (Society of Naval Architecture and Marine Engineers, 1970, p. 394-395). The block coefficient is defined as a ship's displacement volume divided by the volume of the cuboid with the same length, width and height as the ship's length, beam and draught. The block coefficient is extracted from hydrostatic data.

The wake fraction is the relation between the ship speed and speed of which the water surrounding the ship flows along with the ship when it moves.

$$w = 2 * C_b^5 * (1 - C_b) + 0{,}004 \qquad (2.2)$$

From the wake fraction coefficient, the thrust deduction fraction (t) is given by:

$$t = 0{,}7 * w + 0{,}06 \qquad (2.3)$$

Thrust deduction fraction indicates the relation between the towing resistance of a ship and the thrust needed to propel it (Eslamdoost et al., 2015, p. 1). Thrust is the name of the force generated by the propeller, propelling the ship. Equation (2.5) shows the formula used to calculate the thrust needed per propeller shaft to propel the ship, $T_{shaft}$,

$$T_{shaft} = \frac{R_{ts}}{n_{shafts}(1 - t)} \qquad (2.4)$$

where $R_{ts}$ is the towing resistance of the ship when towed through water depending on the speed. The values for $R_{ts}$ are found in Appendix C. $n_{shafts}$ is the number of propeller shafts the thrust is distributed on. The developed area ($A_D$), which is the sum of the face areas of all the blades on a propeller, is calculated from equation (2.6),

$$A_D = \frac{T_{shaft}}{T_{max}} \qquad (2.5)$$

where $T_{max}$ is the maximal allowed force concentration set for the propeller.

Blade area ratio (BAR) is the relation between the developed blade area, $A_D$, and the disc area ($A_0$) of the propeller, which is the area of a circle with the same diameter as the propeller. In other words, the BAR describes how much of the propeller's disc area is contributing to pushing the water backwards. The BAR of a propeller is given by the propeller series and is mainly used for finding the required disc area and diameter of the propeller. The formula for BAR is given in formula 2.6: (Rawson & Tupper, 2001, p. 396).

$$BAR = \frac{A_D}{A_0} = \frac{4A_D}{\pi D^2} \qquad (2.6)$$

From equation (2.6), the diameter of the propeller can be calculated.

$$D = \sqrt{\frac{4 * A_D}{\pi * BAR}}$$

Lastly the propeller's speed through water when considering wake, $V_1$, is calculated using the wake fraction,

$$V_1 = V_s(1 - w) \tag{2.7}$$

where $V_s$ is the ship speed.

When $T_{shaft}$, $D$ and $V_1$ are found, the ratio $K_T/J^2$ can be found. The thrust coefficient $K_T$ describes how much thrust the propeller generates, and the advance ratio J describes how far the ship advances per rotation of the propeller compared to the diameter of the propeller. The ratio $K_T/J^2$ is given by equation (2.8) with a following adaption to find $K_T(J)$ (Rawson & Tupper, 2001, p. 453).

$$\frac{K_T}{J^2} = \frac{T_{shaft}}{\rho * D^2 * V_1^2} \rightarrow K_T = \frac{T_{shaft}}{\rho * D^2 * V_1^2} * J^2 \tag{2.8}$$

With the formula for $K_T(J)$ a curve can be plotted for $K_T$ in the propeller sheet shown in Figure 7. Propeller sheets is a tool made by the propeller manufacturer for finding the open water efficiency ($\eta_o$) and J for a propeller in any loading condition. Open water efficiency is the efficiency of the propeller operating in open water without the hull affecting the flow of water around the propeller. This is used in the calculation of the propulsion coefficient later.
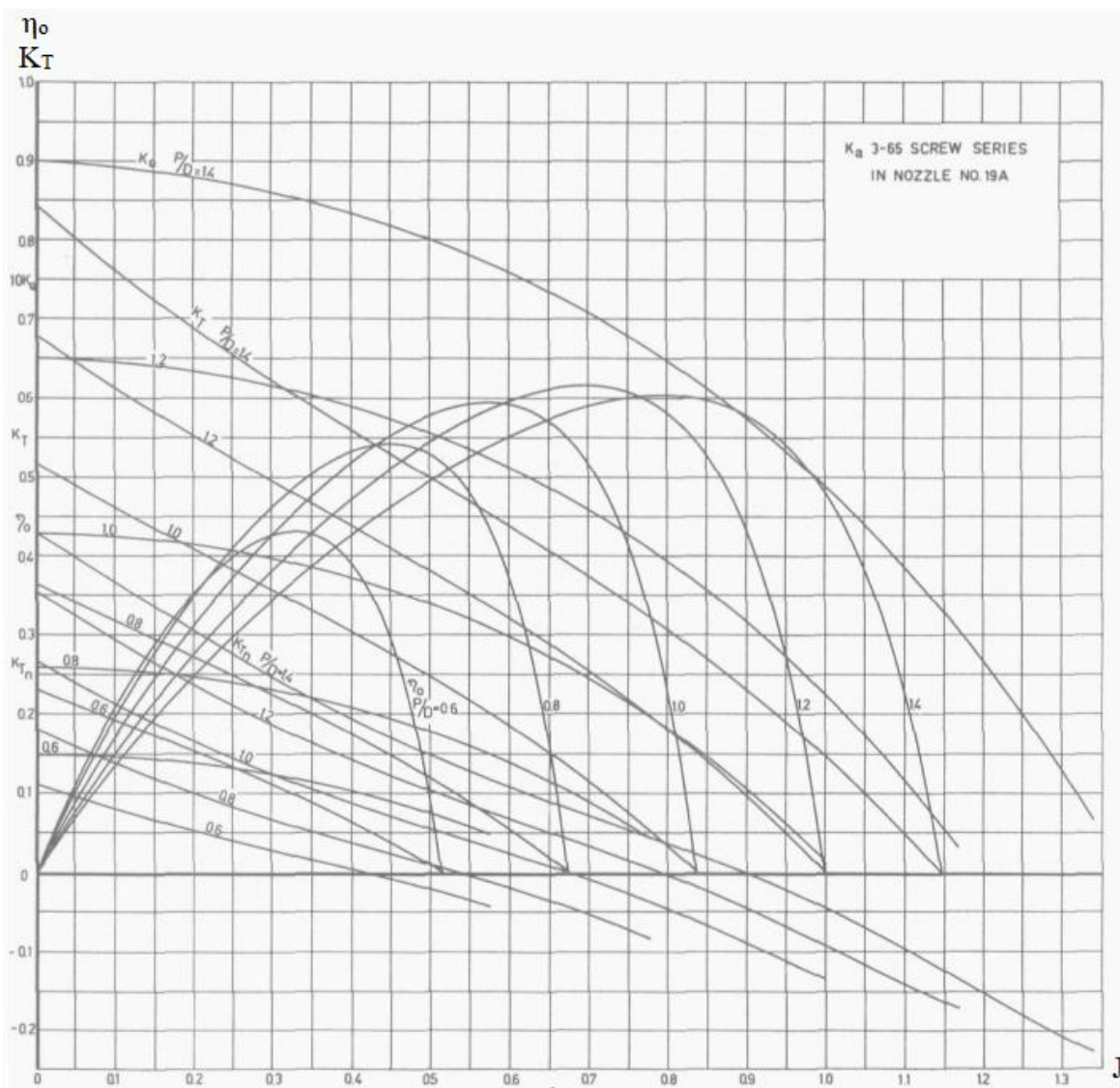
**Figure 7: Propeller curve sheet for the Wageningen Ka 3-65 propeller series with nozzle 19A (Oosterveld, M. W. C., 1970, p. 33).**

The x-axis shows values of the advance ratio, J, while the y-axis shows values of both the thrust coefficient, $K_T$, and the open water efficiency, $\eta_o$. All the curves on the propeller sheet are functions of $J$ and related to different values of $P/D$. The arches going from the origin, up, and then fanning out along the x-axis are plots of $\eta_o$ for different values of $P/D$. The diagonal curves going from the y-axis to the x-axis are curves showing the values of $K_T$ for the same values of $P/D$.

When the values for J, the relationship $P/D$ and $\eta_o$ have been extracted from the propeller sheet, the calculations to find rotational speed of the propeller (n) is given by,

$$n = \frac{V_1 * 60}{D * J} \tag{2.9}$$

where $V_1$ is the vessels speed through water, $J$ is the advance ratio of the propeller and $D$ is the diameter of the propeller. At last, the propulsion coefficient ($P.C$) for the vessel is calculated.

$$P.C = \eta_O * \eta_H * \eta_R * \eta_{shaft} \tag{2.10}$$

Where $\eta_O$ is the open water efficiency of the propeller extracted from the propeller curve, $\eta_H$ is the hull efficiency, which is constant for the hull, $\eta_R$ is the relative efficiency which is dependent on the propellers placement on the hull, and $\eta_{shaft}$ represents the mechanical efficiency in the system. The mechanical efficiency usually includes $\eta_{motor}$ and $\eta_{gear}$ but these are left out and processed individually. When the propulsion coefficient is found the power needed for the propeller to propel the vessel ($P_e$) is calculated,

$$P_e = \frac{P_E}{P.C} = \frac{R_{TS} * V_s}{P.C} \tag{2.11}$$

where $P_E$ is the towing power, dependent on the vessels towing resistance $R_{TS}$ and speed $V_S$. The propeller theory is complex and involves many parameters. Most of them are constant for a given vessel and given propeller series. The important parameters to keep in mind when addressing the efficiency of the propeller is the vessels towing resistance, the diameter of the propeller and the propellers rotational speed.

## 2.2  Shaft and bearings.

The shaft and bearings connect the rotating machine, either through a gear or directly to the propeller. The shaft is usually held in place by support and thrust bearings, as well as the stern tube bearing like shown in Figure 8.
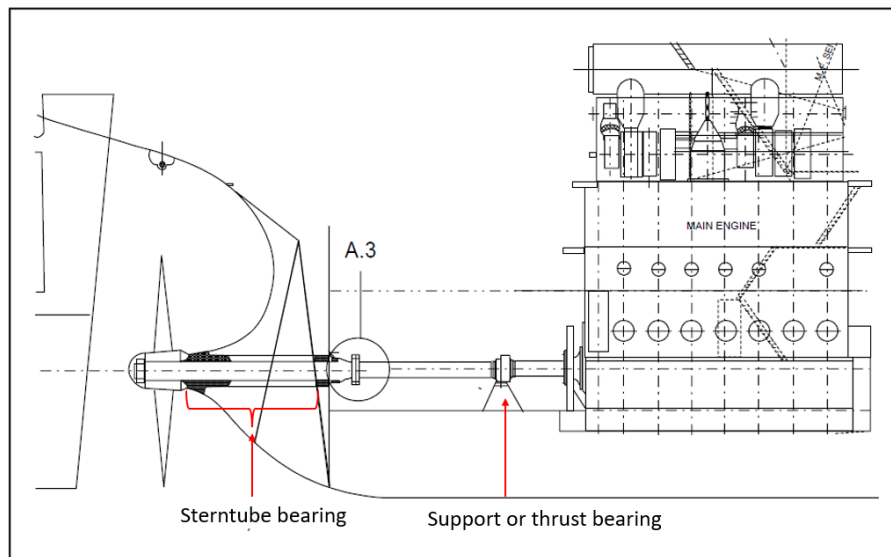
**Figure 8: Example of direct driven fixed pitch propeller (DNV, 2007, p.34)**

The shaft is a strict mechanical connection and transmits all the speed and torque from one end to the other. The main source of losses in shafts and bearings occur due to friction. Even though there are some efficiency losses, they are very small. The shaft and bearing provide a high transmission efficiency for all load and speed conditions (Shi W et al, 2009, p.5), and will for this thesis be set to a constant of 99%. The total weight of the shafts is set to be similar to what found by Andressen & Mykland (Appendix A) for all configurations. When implementing a gear, one part of the shaft would rotate faster and have a smaller diameter, but this will not be considered when addressing the over all weight of the drivetrain.

## 2.3   Gears

Gears serve many purposes in mechanical appliances, especially in the use of changing the rotational speed, and thus the torque, of a rotating system. A gear can also be utilized to change the rotational axis of components driven by the same power source. The magnitude of the changes is dependent on the gear ratio of the gear, which usually is a fixed value. For gear ratios from 1:1 to 1:7 usually a spur gear (Figure 9) is utilized.
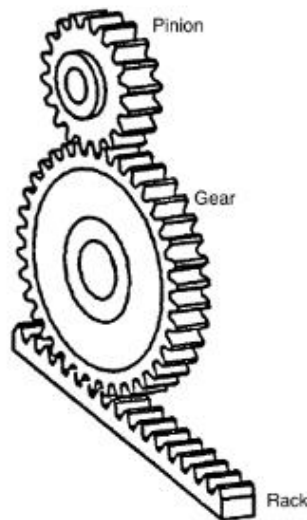
**Figure 9: Pinion and rack configuration of a spur gear (Davis, 2005, p.4)**

For larger gear ratios, a planetary or worm gear should be used. A gear can allow for a wider variety of prime movers with the same power, but different rotational speeds, to operate within their ideal operating area. Gears operate on the fundamental formula for torque and power generation in a rotating system. The torque is defined by,

$$\tau = F * a \tag{2.12}$$

where F is the force acting on the system and a is the arm of the acting force to the point of rotation. Further, the power of the rotating system is given by,

$$P = \tau * \omega \tag{2.13}$$

where P represents the transmitted power, $\tau$ the torque working on the system, and $\omega$ is the angular velocity of the rotation.

Power losses in gears are affected by the rotational speed and load of the gear, the size, number of gears in series, and the manufacturing of each gear. Calculating losses is therefore difficult, and the need for experiments and measurements are required. In 2009 Delft University of Technology and Netherlands Defence Academy published an article where the efficiency of a spur gear was estimated, based on measurements conducted. The gears dependency on load and speed is shown in Figure 10 5.
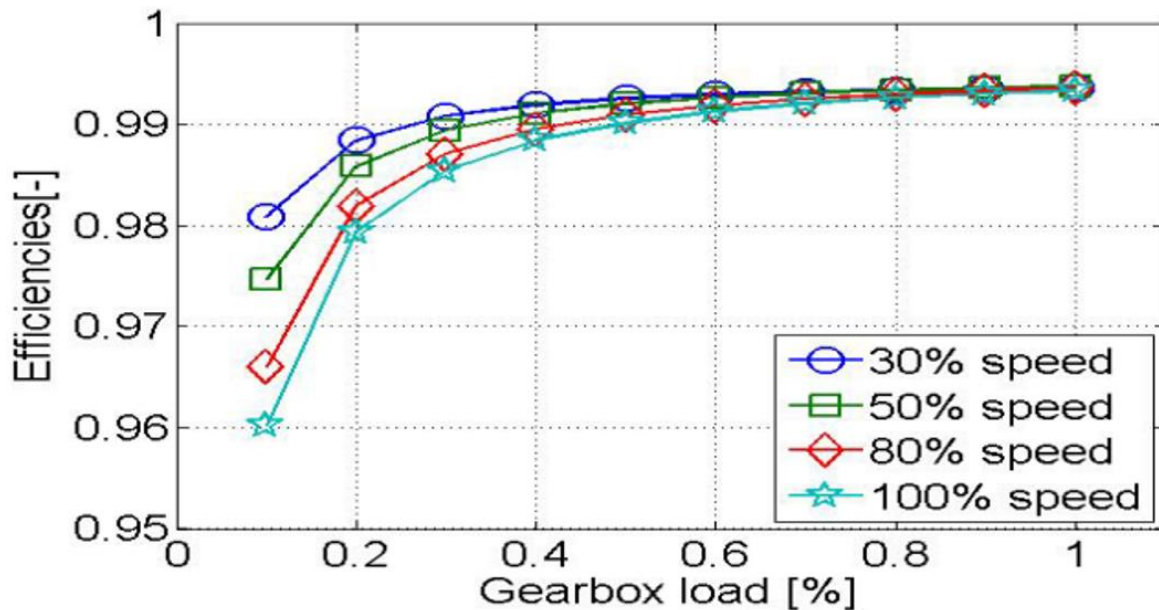
**Figure 10: Spur gear efficiency dependency on load and speed (Shi et al, 2009, p. 452)**

As can be seen in the graph in Figure 10, the efficiency of one gear exchange is dependent on speed and load, but usually very high. Some variations occur for low speed and low load conditions. However, for high loads it is more or less constant.

Due to difficulties retrieving data for gearboxes developed for maritime use in the required power range for our drivetrain, the gearbox from a Renault Twizy, which has a similar power range, is used. The weight of this gear box is 10,85 kg.

## 2.4   Electrical machines

Electrical machines are devices used to transform power from an electrical to a mechanical form or the other way around. These electrical machines, or power converters, exist in different forms. The ones transforming electrical energy to mechanical energy are called electrical motors, whereas the ones that transform from mechanical to electrical are called generators. There are also power converters that transform from one sort of electrical energy to another, like from direct to alternating current. The use of electrical machines is widely spread across a broad specter of applications and power ranges (Slobodan N, 2013, p 1).

The operation principle of electromechanical energy transformation in these kinds of machines is based on utilizing the interaction between the conductors carrying electrical current, the windings, and the magnetic coupling field. Magnetic flux passes through a magnetic circuit made of

ferromagnetic materials. The magnetic circuit is created by stacking thin iron sheets together, which are separated by layers of insulation like shown in Figure 11 (Slobodan, 2013, p.3).
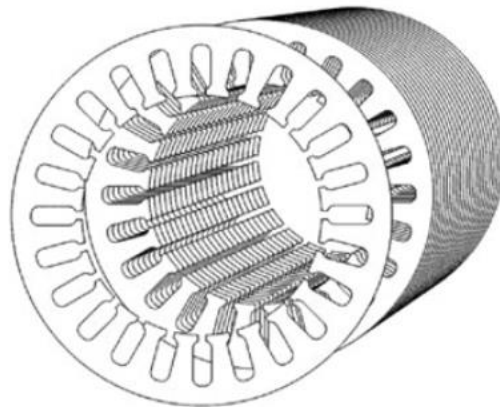


**Figure 11: Stator magnetic circuit of rotating electrical machine (Slobodan, 2013, s.367)**

Common for all rotating electrical machines is that they consist of a stator and a rotor. The stator is the electrical machine's non-moving part, whereas the rotor is the machine's moving part which rotates around the machine axis. Both the stator and the can be equipped with magnetic and electrical circuits. In addition to the above-mentioned characteristics of the electrical machine, it also contains parts such as a shaft for mechanical connection, bearings, terminal for current connections, as well as a housing (Slobodan, 2013, p.4)

The three most established electrical machines are the DC current machine, the asynchronous, or induction machine, and the synchronous machine (Slobodan N, 2013, p 3-4). The DC machine is the oldest electrical machine and has been preferred over the AC machines for a long period of time. This changed after the implementation of power electronics, which facilitates for controlled drives using AC machines. Further, the DC machine is more sensitive to changes in the load, has increased maintenance cost and is less reliable than the AC machine (Melkebeek, 2018, s.49). For these reasons this thesis will only look at the alternating current electrical machines (asynchronous and synchronous). The similarities between these are displayed, before moving on to the difference between them.

The stator windings and the magnetic circuit are similar for both the induction machine (IM) and the synchronous machine (SM). The stator consists of a core made out of ferromagnetic material (thin irons sheets stacked together with insulation between them) and slots in which

the conductors (windings) will go, see Figure 11. In the stator there are usually three sets of windings which each correspond to a phase. The magnetic axes of the three phases are shifted 120 degrees for each phase. When currents are running through the shifted windings the rotating magnetic field is created. The magnetic field rotates at synchronous speed given by,

$$n_{sync} = \frac{f * 60}{p_p}$$
(2.14)

where $f$ is the supply frequency of the three-phase voltage source in Hz and $p_p$ is the number of pole-pairs. This field is what exerts a force on the rotor and makes it turn (Slobodan N, 2013, p 59-60).

Power losses in the stator consist of iron losses in the core, and copper losses in the windings. The iron losses $P_{fe}$, consist of hysteresis losses and eddy current losses. The magnetic field in the stator oscillates according to the operating frequency. The variation of the magnetic field implies moving magnetic diploes and changing their orientation. This operation demands a certain amount of energy due to internal friction between neighboring dipoles and is what is refer to as hysteresis losses. Eddy currents are currents induced within the iron core when the changing magnetic field runs through it. These currents oppose the flux changes and create heat which leads to energy losses.

The total power loss in the magnetic circuit is therefore the sum of hysteresis losses and eddy current losses,

$$P_{fe} = P_{hysterisis} + P_{eddy\ current} = \sigma_h * f * B_m{}^2 + \sigma_e * f^2 * B_m{}^2$$
(2.15)

where $\sigma_h$ is hysteresis coefficient dependent on the nature and mass of the ferromagnetic material, $\sigma_e$ is the eddy current coefficient dependent on the conductivity and mass of the material, f is the operating frequency and $B_m$ is the peak value of flux density in the core (Slobodan N, 2013, p 71-74).

The copper losses of the windings in the stator are referred to as $P_{cu1}$. The copper losses depend on the resistivity of the material, the winding configuration of the machine as well as the physical parameters of the machine,

$$P_{cu} = 3 * R_{cu} * I^2$$
(2.16)

where I is the current running in the stator winding, and $R_{cu}$ is the resistance of the winding given by,

$$R_{cu} = \frac{(\rho_{cu} * l + d * g * k_{coil}) * n_s * q}{A_{cond}} \tag{2.17}$$

where $\rho_{cu}$ is the resistivity of copper, l is the length of the windings and d is the inner diameter of the stator. $k_{coil}, n_s$ and q are variables depending on winding configuration and $A_{cond}$ is the cross-sectional area of the conductor (Anisimov et al, 2021, p.2). The physical parameters also affect the electric properties of the machine.

The correlation between the physical parameters and nominal power $P_N$ of an electrical machine can be given by the formula,

$$P_N = \frac{2\pi}{8} * d^2 * l * B_m * Â_p * \omega \tag{2.18}$$

where d is the inner diameter of the stator, l is the length of the rotor, $B_{mp}$ is the magnetic flux density, and $Â_p$ is the electric loading (Anisimov et al, 2021, p.2). The physical parameters of a machine are also affected by the number of poles for the machine. From equation (2.13), it can be seen that to choose a machine with a high number of poles would lower rotational speed and could be beneficial to minimize or remove the need for a gear. However, the increase of pole pairs increases the mass of the rotor (Pyrhönen. 2008, p.286-287). The majority of available electrical machines for ship propulsion exist within the 1500-3000 rpm range (i.e., with 4 or 2 poles).

Common for both types of AC machines are the construction of the stator, and therefore also the losses connected to this. Also, the correlation between physical parameters and nominal power show similarities, and for both machines the number of poles affects the characteristics of the machine. These are all factors that must be considered when conducting a deeper analysis of the electrical machine in the drivetrain. The differences between the IM and SM will be displayed in the next sub chapters.

### 2.4.1 Induction machine

The induction machine, also known as asynchronous machine, is a commonly used electrical machine that exists in a variety of power ranges. The machine is robust, has favorable operating

characteristics, simple starting conditions, good overload capabilities as well as being relatively simple and cheap to manufacture (Sivertsen, 2019, p.87). These are factors that make it attractive for shipboard propulsion applications.

The magnetic circuit of the rotor is constructed the same way as the magnetic circuit for the stator. The rotor of an IM, similar to the stator, contains slots for the rotor windings as illustrated in Figure 12.
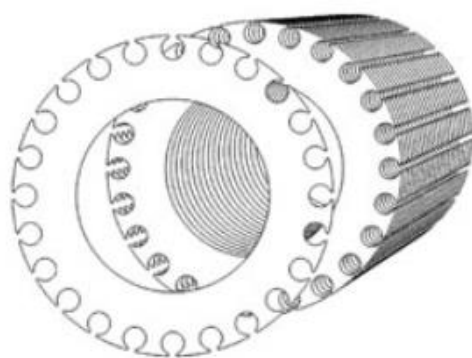


**Figure 12: Magnetic circuit of rotor IM (Slobodan, 2013, p. 367)**

There are primarily two different configurations for rotors windings in asynchronous machines. The short-circuited and the wound rotor configuration. The wound rotor uses copper windings, similar to the stator, on the rotor as well. Wound motors are rarely met nowadays. The copper windings on the rotor make for more complex manufacturing, as well as being larger in size (Slobodan, 2013, p. 369). This makes the wound rotor less attractive for the USV, and therefore will not be further investigated. For the short-circuited rotor, or *squirrel cage* configuration, the slots in the rotor are filled with cast aluminum bars, which then are short-circuited on each end with aluminum rings (Slobodan N, 2013, p. 365-369). See Figure 13.
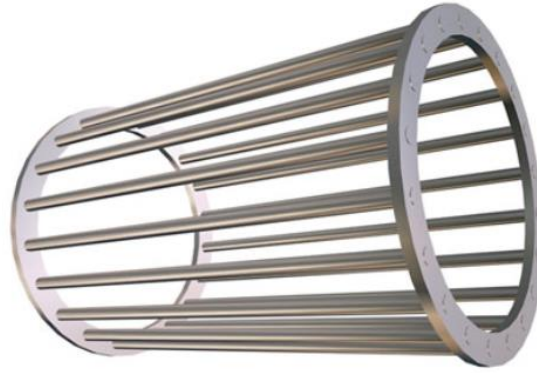
**Figure 13: Squirrel cage of IM (Slobodan, 2013, s.368)**

When the stator-field rotates, according to equation (2.14) relative to the rotor, it induces currents and voltages in the rotor cage. It is this electromagnetic interaction between the rotating stator-field and the induced rotor currents that creates a torque on the rotor and makes it turn (Sivertsen. L, 2019, p. 88-90).

The induction machine is thus dependent on a difference in the rotational speed of the rotating field, and the revolutions of the rotor. If they move at the same speed, there is no relative displacement between them. Then there would be no change in the flux in the rotor windings, and therefore no current in the windings. This difference is called *relative slip.* The relative slip is given by,

$$s = \frac{n_{slip}}{n_{sync}} = \frac{n_{sync} - n_2}{n_{sync}} \tag{2.119}$$

where $n_2$ is the rotors rotating speed in rpm. The slip affects the copper losses occurring in the rotor according to,

$$R_{cu2} = \tau * \omega * s \tag{2.20}$$

Where $\tau$ is the produced torque and $\omega$ is the synchronous angular velocity of the magnetic field. The iron losses in the rotor have the same relations presented in equation (2.15), but due to its dependence on the slip frequency, which is much lower than the supply frequency, it is normally neglected (Sivertsen, 2019, p.95). Other power losses that often are neglecter are friction and ventilation power losses $P_{FR+V}$.

The overall efficiency of an IM is then given by (Sivertsen. L, 2019, p. 94):

$$P_{out} = P_{in} - P_{cu1} - P_{FE} - P_{cu2} \qquad (2.21)$$

## 2.4.2 Synchronous machines:

Contrary to the IM, the rotor of a synchronous machine rotates at the synchronous speed given by equation (2.14). The construction of the rotor is also somewhat different. The magnetic circuit is similar, but rotor of a synchronous machine may contain excitation windings which are supplied by a DC current or built in permanent magnets. In the cases of permanent magnets, the rotor does not contain any windings. The permanent magnet excitation for the SM has numerous advantages over the DC excitation. Firstly, the copper losses in the rotor are eliminated. This is especially beneficial for lower power ratings where efficiency tends to be lower. Secondly, it can make for more compact machines (higher power-density) at low power ranges. Thirdly, the use of slip rings or brushes for DC excitation reduces time between maintenance (Melkebeek, 2018, p.489). For these reasons, only the permanent magnet synchronous machine (PMSM) is investigated further.

The PMSM has been around for over 100 years, but it is during the last 20-30 years that the technology regarding these machines and the associated converters have been good enough to compete with the induction machines. The use of PMSM as electrical motors for electrical vehicles has grown largely during these years. Large number of poles, low rpm, high efficiency, high torque and low operation and maintenance costs are the main benefits for this kind of machine. The stator is in most cases formed as a typical alternating current machine. It contains a slotted ferromagnetic part with a three-phase winding. The rotor has mounted permanent magnets, either internal or surface mounted. See Figure 14.
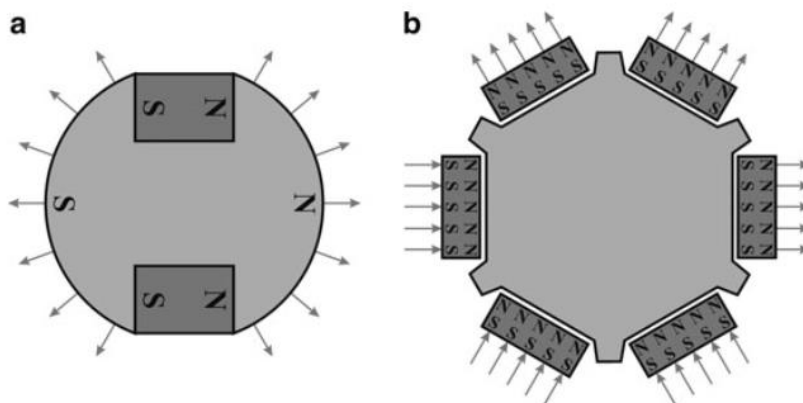
**Figure 14: a) internally mounted magnets PMSM, b) surface mounted magnets PMSM (Slobodan, 2013, p. 546)**

Since the rotor of a synchronous machine revolves in synchronism with the stators magnetic field, there is no variation in the magnetic induction in the rotor core, and therefore no iron losses. Further, by utilizing a PMSM, the rotor windings are removed. This removes the generation of heat from the windings, and the cooling can be adjusted more efficiently towards the stator (Slobodan N, 2013, p.536-537). The total power loss of the PMSM is therefore similar to the IM, but without rotor losses.

$$P_{out} = P_{in} - P_{cu1} - P_{FE} \qquad (2.22)$$

The analysis of the drivetrain will thus focus on the squirrel cage IM and the PMSM, and what each of these could contribute to the drivetrain. The PMSM is presented as more efficient, and the IM is considered more reliable and robust. The performance characteristics for both machines are dependent on physical parameters, operation speed and load. Although the variation in efficiency behaves differently for the two machines.

## 2.5   Inverter & rectifier

In order to utilize the benefits of electric drivetrains with AC machines, power electronics such as inverters and rectifiers are needed.

The IEP configuration has its main power supply coming from fuel and a diesel generator. The diesel generator generates an AC voltage. To convert this to the DC voltage utilized in the main busbar, a rectifier is needed. The rectifier consists of a diode-bridge, Figure 15 a), to smooth out the sinusoidal AC voltage and turn it into DC voltage. It does so by only letting the AC

voltage exit at its maximum point and enter at its lowest point as shown in Figure 15 b). Utilizing a capacitor in the rectifier further smoothens the DC voltage (Melkebeek, 2018, p.233).
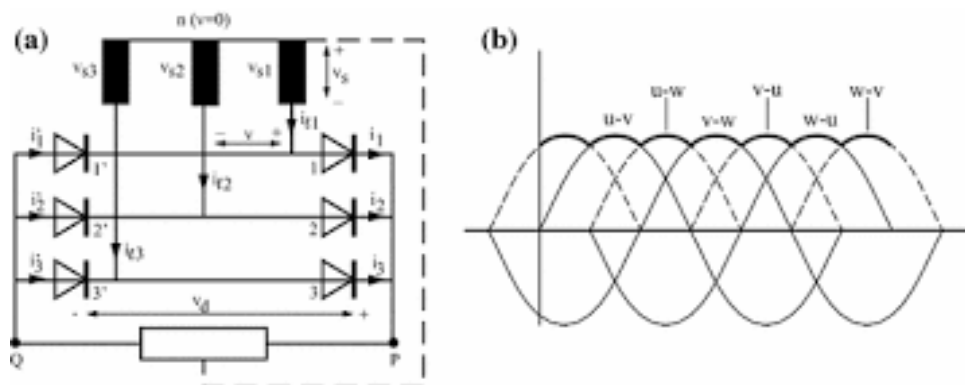


**Figure 15: a) three-phase rectifier bridge. b) line-to-line voltages of the voltage AC voltage (Melkebeek, 2019, p.237)**

The efficiency of the rectifier does vary in some degree based % of full load. However, it is seen that efficiency is more or less constant above 10% of full load and is therefore considered constant (Mikhaylov, 2012, p. 410). The value of efficiency is set to 92% and weight estimated to 153 kg based on commercially available rectifiers for marine application within our power range (Appendix D).

In most uses of electrical motors, it is desirable to have the opportunity of a variation of rotor speeds. The energy efficient way to obtain variable speed operations for AC machines is by feeding them with a variable frequency. Inverters are used when converting DC to AC with variable frequencies (Melkebeek, 2018, p.307). Figure 16 a) displays how the three-phase inverter consists of 6 power transistors operating in 3 pairs, as switches between the + and – side of the DC source. Switching the upper transistor will result in a positive, and the lower in a negative potential of the DC source. Figure 16 b) further shows how switching sequences are used to form new AC voltages.
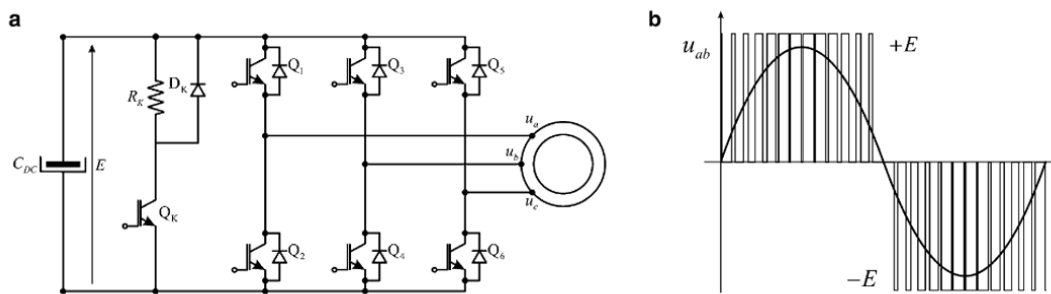
**Figure 16: a) Three-phase DC-AC inverter b) Typical waveform of line-to-line voltages (Slobodan, 2013, p.495)**

Power electronics such inverters are very efficient. They do have some losses due to heat generation during power conversion, but still have efficiencies of approximately 97% for a power area between 8-12 kW with a weight of approximately 20kg (California Energy Commission, 2023).

## 2.6  Battery

When addressing batteries for electric vessels, the energy density of the battery (i.e., energy per weight), is of high importance, due to limited available space within the vessel. The energy density depends on the type and construction of the battery. This thesis will only assess the lithium-ion type battery, as chosen by Andressen & Mykland, due to its superior energy density compared to other batteries (Figure 17).
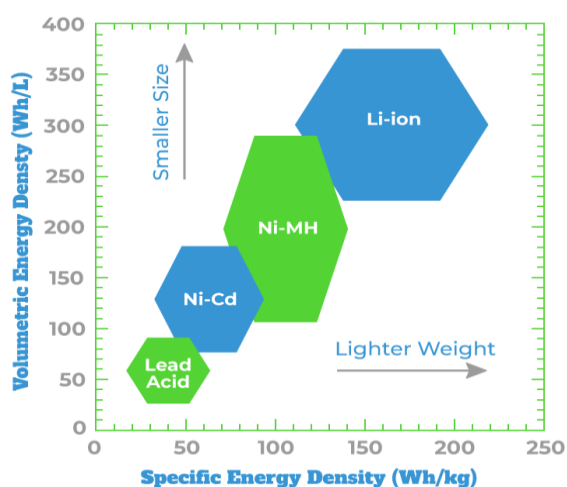


**Figure 17: Battery comparison of volumetric and specific energy density (Dragonfly Energy, 2022)**

Knowing the energy density [Wh/kg] and the necessary capacity [kWh], the weight of the battery can be calculated by the formula (Andrea, 2020, p.28):

$$Weight = \frac{Necessary\ capacity}{Energy\ denisty} \tag{2.23}$$

The necessary capacity is dependent on the efficiency and configurations of the drivetrain and will naturally be a part of further investigation.

## 2.7   Diesel generator

A diesel generator is, simply explained, a diesel combustion engine driving an electrical generator to produce an AC voltage (Figure 18). The engine part operates under the principle of diesel engine combustion. The synchronous generator works under the same operating principles described for the synchronous machine (Jones, 2007, p.13-18).
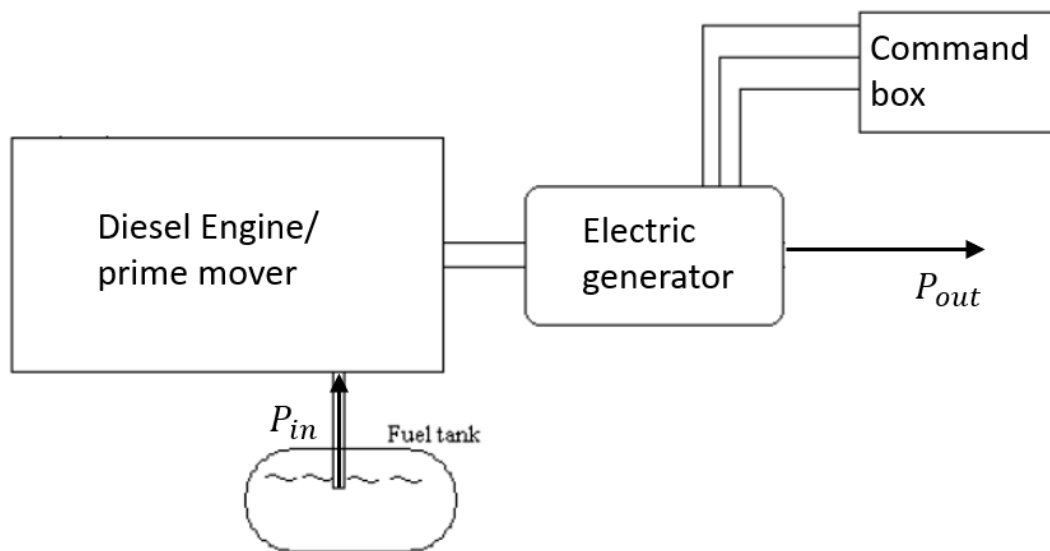


**Figure 18: Simplified block diagram of diesel generator set (Jones, 2007, p.14)**

An estimation of the overall efficiency of the diesel generator can then be derived from the power output compared to the power input.

$$\eta_{D.G} = \frac{P_{out}}{P_{in}} = \frac{P_{in} * \eta_{engine} * \eta_{generator}}{P_{in}} = \eta_{engine} * \eta_{generator} \tag{2.24}$$

41

The efficiency of the generator $ŋ_{generator}$ is based on the same theory presented for the synchronous machine, in section 2.4 and 2.4.2, because the operating principle and losses are similar for synchronous motors and generators.

The electromagnetic torque working on the shaft connecting the diesel engine to the generator is determined by the angular velocity and power output of the generator.

$$\tau_{em} = \frac{P_{out}}{\omega} \tag{2.25}$$

Angular velocity is determined by the synchronous speed of the generator, which is determined by the frequency of the voltage produced. For the generator to rotate at a given speed, the diesel engine must do the same. For the diesel engine to rotate at the same speed the torque generated by the engine must be equal to the electromagnetic torque induced in the generator.

$$\tau_{enigne} = \tau_{em} \tag{2.26}$$

From the required torque the power delivered to the shaft can be calculated:

$$P_e = \tau_{enigne} * \omega \tag{2.27}$$

From this the efficiency of the diesel engine can be calculated.,

$$ŋ_{engine} = \frac{P_e}{\dot{m}_B * h_n} \tag{2.28}$$

where $\dot{m}_B$ is fuel consumption in kg/s and $h_n$ is the lower heating value of the fuel in MJ/kg. This accounts for the thermodynamic losses when transforming energy in fuel to mechanical energy. Other losses in the diesel generator include mechanical losses due to friction, and energy consumed by auxiliary systems such as cooling, lubrication, and fuel oil pumps (Lund A & Strand G, 2013, p.38), but these will not be accounted for in this thesis.

Marine gas oil (MGO) has a density of 855 kg/$m^3$ and a lower heating value of 42,7 MJ/kg (Andressen & Mykland, 2022, p.80)

It is here demonstrated how the efficiency of the diesel generator will be affected by required power output, which again corresponds to the speed or loading of the vessel. Further, efficiency will also determine the fuel consumption for the diesel generator. This must be addressed to complete the analysis of the drivetrain configuration.

# 3    Method

So far, relevant theory regarding each component of the IEP drivetrain has been presented. The theory presents general relationships between factors such as weight or efficiency of each component. In this chapter the methods used to process the previous theory, as well as how the collection and processing of data was performed are described. The method aims to provide information regarding the dynamic behaviors of efficiency within the drivetrain. The dynamic behaviors will further affect aspects such sizing of component and amount of fuel needed.

In order to conduct the main goal of the thesis, a literature study to acquire the necessary theory regarding the drivetrain and all its components, was conducted. The theoretical background from this literature study is presented in the theory part. Further, for correlations not described by theoretical formulas, own models based on collected data are made. The general process for every part is outlined in the following sections.

## 3.1    Propellers

The propeller theory presented is used to calculate efficiency for all loading conditions presented in the estimated operation profile shown in Table 1. The efficiencies are extracted from the relevant propeller sheet by first plotting the $K_T(J)$ curve into the diagram. From the intersections between the $K_T(J)$ curve and the $K_T, P/D(J)$ curve, a vertical line is drawn up to the $\eta_o, P/D(J)$ curve with the same ratio of P/D. The y-value of the intersection point between the vertical line and the $\eta_o, P/D(J)$ curve tells the efficiency for this ratio of P/D. A visual explanation of this process is shown in Figure 19: Illustration of the different curves in the propeller diagram, where the $K_T(J)$ curve is shown in green, a $K_T, P/D(J)$ Curve is shown in blue, the vertical line from the intersection point is  shown in pink and the corresponding $\eta_o, P/D(J)$ is shown in red.
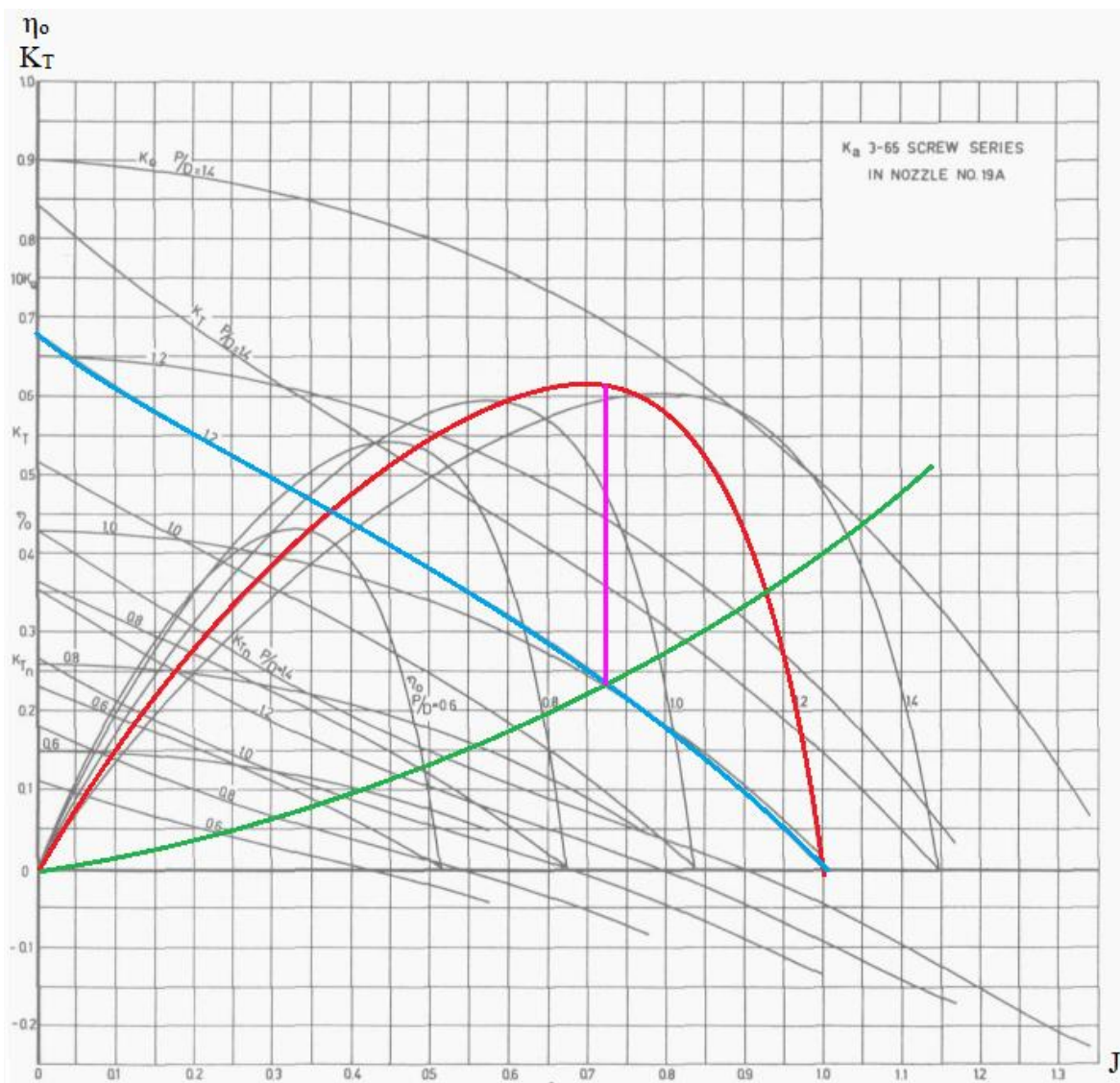
**Figure 19: Illustration of the different curves in the propeller diagram**

When this process is done for all ratios of P/D, the $\eta o(J)$ curve can be plotted between the intersection points on the $\eta_o, P/D(J)$ curves. From the $\eta o(J)$ curve the highest efficiency for the propeller in the loading condition can be determined. The point on the $\eta o(J)$ curve with the highest value on the y-axis, also has the optimal value of J as its value on the x-axis. A hypothetical example of this extraction is presented in Figure 20.
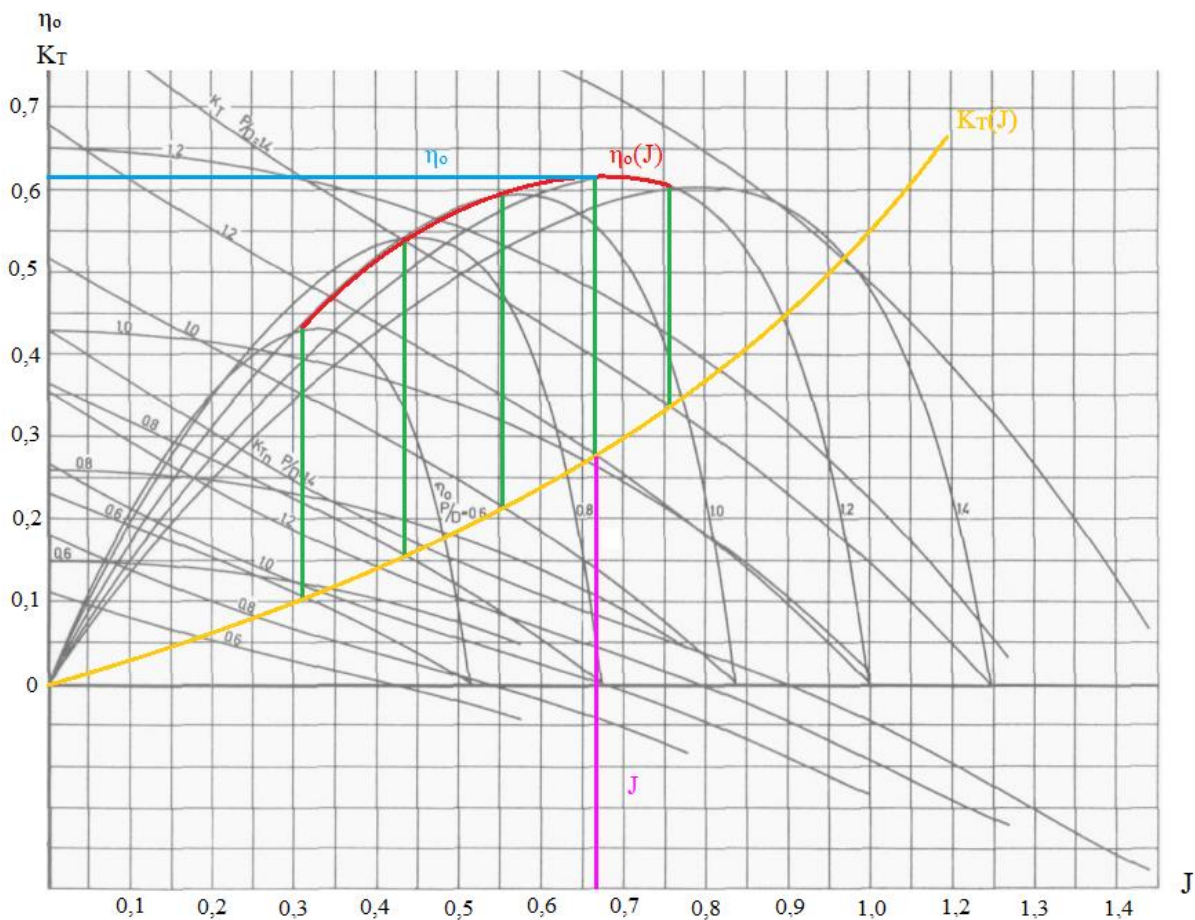
**Figure 20: Example of extraction from Wageningen KA 3-65 screw series propeller diagram.**

To determine changes in overall efficiency dependent on the propeller, a new propeller design is investigated. The same calculations are conducted for both designs to see if a propeller optimized for a different load and speed will result in better overall efficiency $\eta_o$.

## 3.2 Gear

Based on the theory presented, a recreation of the curve found in the paper published by Delft University of Technology and the Netherlands Defence Academy in Figure 10 is made. An interpolation of the curve's datapoints are done in MATLAB (see Appendix E) to find efficiency values not defined by the published data. The rotation speed and torque working on the gear from the propeller is calculated. The resulting speed and torques are inserted into the script and the resulting efficiency is extracted.

## 3.3   Electrical machines

When investigating relevant relationships between the factor's efficiency, nominal power and weight of electrical machines, a combination of a qualitative and quantitative approach was used. Quantitatively, different manufacturers for both industrial machines and machines designed for ship propulsion were contacted. Data regarding the size, weight and efficiency have been collected in a broad range of machine sizes and rated powers, for both IM and PMSM (Appendix F & G). However, the majority of which is concentrated around the 10-kW nominal power range. The data collected was utilized to show the correlation between both the machines' power output and size, as well as the efficiency's dependencies on the size. The data retrieved are plotted using MATLAB (see Appendix H) and fitted curves are found utilizing the MATLAB's fitting tool. The correlation found by the data is then further used to calculate weight, nominal power and efficiency further used in the analysis.

Qualitatively, the efficiency maps of machines with the desired power outputs were studied as a way to present updated efficiency values at different speed- and loading conditions. The efficiency maps were evaluated utilizing MATLAB (see Appendix I) to obtain speed, torque, and efficiency values for each given power requirement. The code reads the values from the efficiency map and matches them with the corresponding colormap. The efficiency map scale is adjusted to fit previous calculations on the electrical machine. Further, the load curve for a given power output is plotted into the efficiency map, as well as a new curve representing the correlation between speed and efficiency for that given power.

## 3.4   Battery

The battery choice was investigated further with respect to marine application and operations in cold weather environments. The data is retrieved from a manufacturer specifically designing battery packages for marine application (Appendix J). The updated values are used in combination with the updated necessary battery capacity to recalculate estimated battery weight.

## 3.5   Diesel generator

The diesel generator is studied further based on the knowledge gained by the literature study done on electrical machines and diesel engines, in section 2.4 and 2.7. The efficiency of the generator is determined by the correlations found from the data collected of the PMSM.

The efficiency of the diesel generator for different loading conditions is calculated. The diesel generators fuel consumption relative to load is given by data Andressen & Mykland retrieved from manufacturer. Given the fuel consumption of the diesel generator and updated values for power requirement for each operating mode and configuration, fuel capacity for the vessel is calculated.

# 4    Results

The theory regarding each component has been presented, and the methods utilized to connect them to the drivetrains' weight or efficiency has been described. The following chapter will display the results from the conducted methods, in order to create the groundwork for the discussion in chapter 5.

## 4.1    Propeller optimization

To determine the overall efficiency for the propeller from Andressen & Mykland's thesis, the propeller calculations shown in their thesis were replicated for all loading conditions and the curves for $\eta_o(J)$ of all conditions are plotted into the propeller sheet in Figure 21.
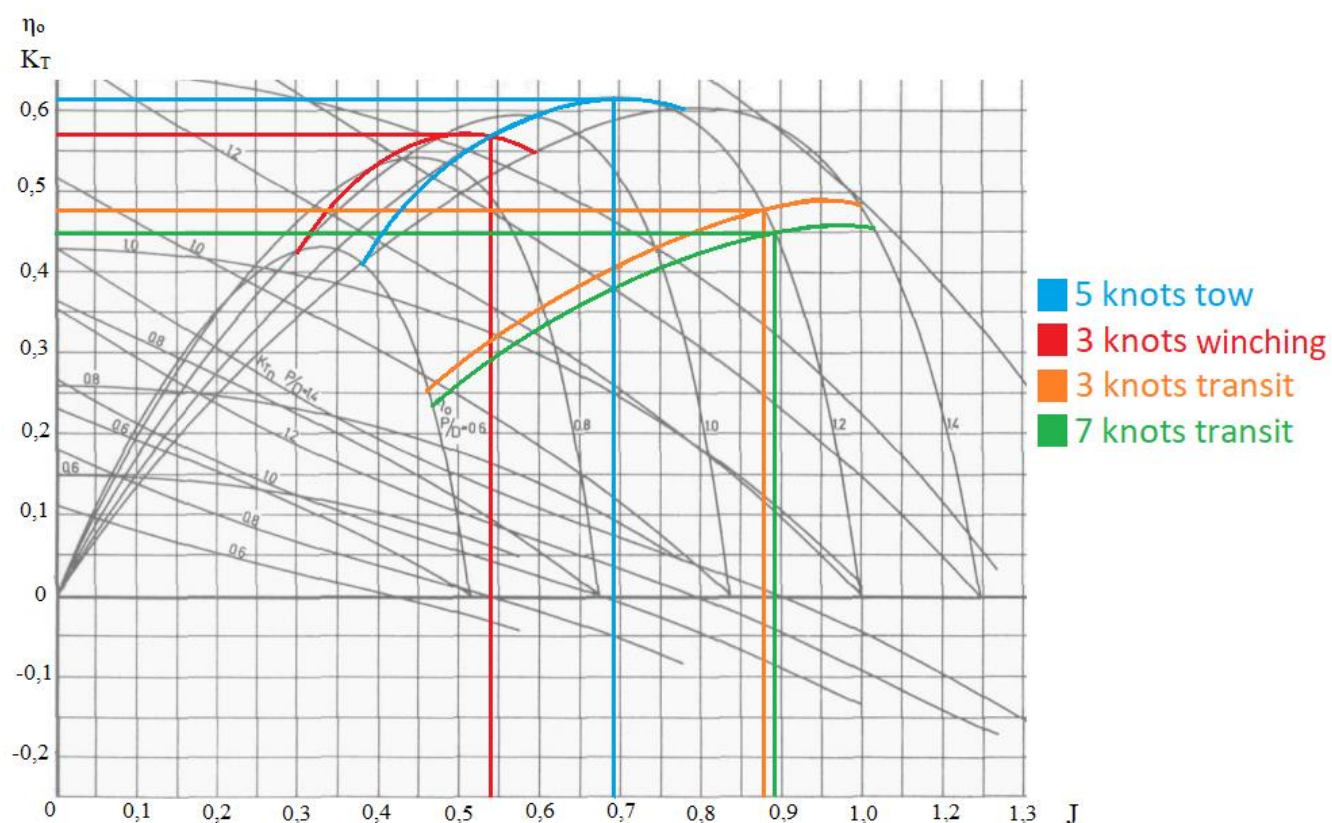
**Figure 21: Efficiency curves for the propeller chosen by Andressen & Mykland**

The colored curves in Figure 21 show how the efficiency of the propeller changes for each loading condition as J increases along the x-axis. Andressen & Mykland propeller design was optimized for the 5 knots towing condition. The figure shows that the efficiency for this loading condition tops out in the point of intersection with the curve for P/D = 1,2.  Therefore, P/D is

set to 1,2 for all the loading conditions. From these points, $\eta_o$ and J values are extracted, which is used for finding optimum rotational speed for the propeller in each loading condition.

A new propeller design has been developed by dividing $T_{shaft}$ for 7 knots transit by $T_{max}$ as shown in equation (2.5) to find the resulting $A_D$. This results in a diameter of 0,343 m for the new propeller design. Figure 22 shows the efficiency curves for a new propeller design.
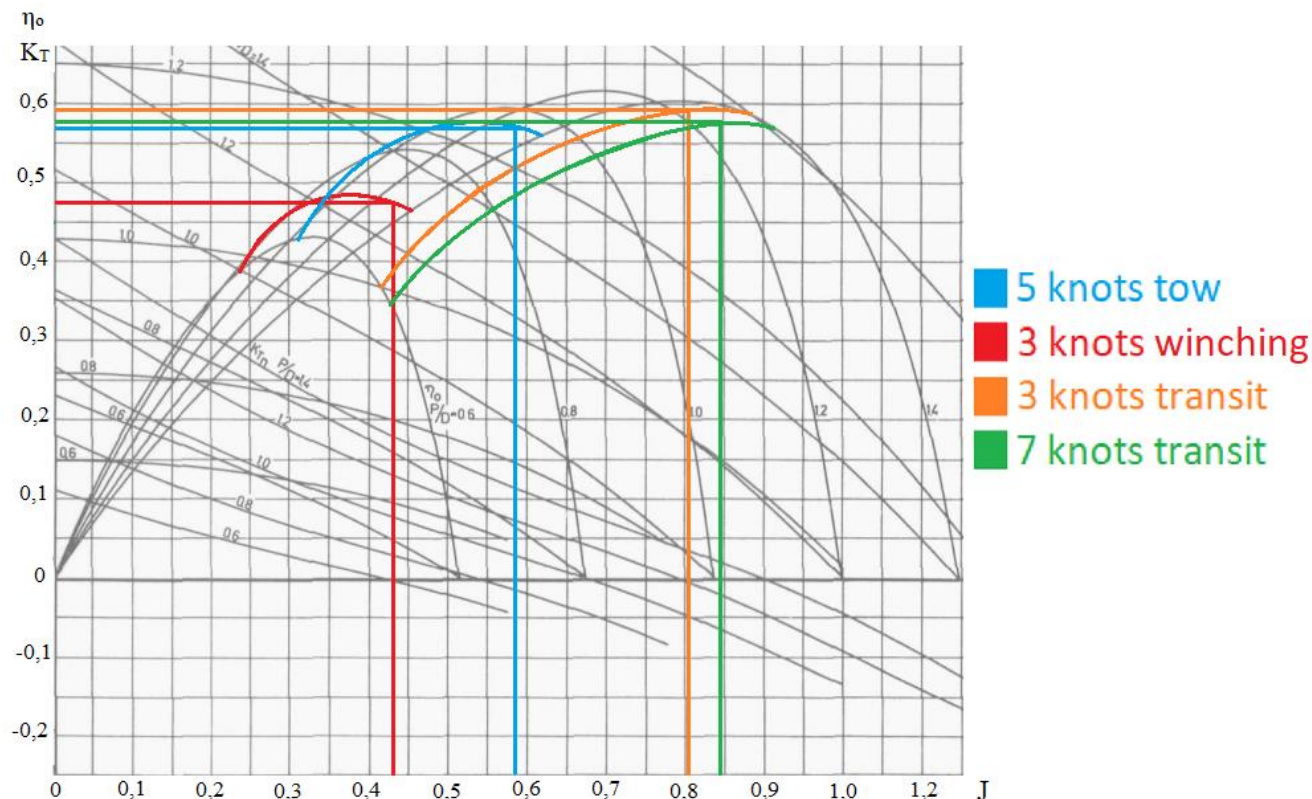


**Figure 22: Efficiency curves for the new propeller.**

For the propeller optimized for 7 knots transit the optimal P/D ratio has changed to 1,3 and one can see that the efficiency curves of the loading conditions are shifted to the left. This shift results in a change in the optimal efficiencies for all loading conditions. Table 3 shows the optimal efficiencies, J-values and rotational speeds for all loading conditions for each propeller designs. In addition, the propulsion coefficient is calculated for the vessel.

*Table 3: Collection of data extracted and calculated from propeller curves, plus the rest of the propulsion coefficient.*

| Loading condition | Old propeller design | | | | | New propeller design | | | | |
|---|---|---|---|---|---|---|---|---|---|---|
| | $\eta_{O:}$ | P/D | J | P.C | RPM | $\eta_{O:}$ | P/D | J | P.C | RPM |
| 3 knots transit | 0,48 | 1,2 | 0,88 | 0,4498 | 195,00 | 0,597 | 1,3 | 0,805 | 0,55938 | 308,87 |
| 3 knots winching | 0,57 | 1,2 | 0,535 | 0,5341 | 320,74 | 0,475 | 1,3 | 0,43 | 0,44507 | 578,23 |
| 5 knots tow | 0,62 | 1,2 | 0,7 | 0,5809 | 408,57 | 0,57 | 1,3 | 0,58 | 0,53408 | 714,49 |
| 7 knots transit | 0,45 | 1,2 | 0,895 | 0,4216 | 447,37 | 0,58 | 1,3 | 0,845 | 0,54345 | 686,58 |

| | |
|---|---|
| $\eta_R$ | 0,995 |
| $\eta_H$ | 0,961 |
| $\eta_m$ | 0,98 |

By combining the propulsion coefficients found for the loading conditions with the needed power for propulsion, $P_E$ (equation 2.11), the required power to the propellers can be calculated. The calculations are shown in Table 4.

*Table 4: Required power to the propeller shafts, based on the propulsion coefficient.*

| | Comparison of delivered power need to propeller | | | | |
|---|---|---|---|---|---|
| Loading condition | $P_E$ [kW] | $P_e$ old propeller [kW] | $P_e$ new propeller [kW] | $P_e$ old design, both propellers [kW] | $P_e$ new design, both propellers [kW] |
| 3 knots transit | 0,206 | 0,229 | 0,184 | 0,459 | 0,369 |
| 3 knots winching | 1,750 | 1,638 | 1,966 | 3,276 | 3,931 |
| 5 knots tow | 3,448 | 2,968 | 3,228 | 5,935 | 6,456 |
| 7 knots transit | 2,296 | 2,723 | 2,113 | 5,446 | 4,226 |
| | Sum: | 7,558 | 7,491 | 15,116 | 14,982 |

## 4.2 Gears – speed, torque and efficiency

A three-dimensional recreation of the data retrieved from Delft University of Technology and the Netherlands Defence Academy was made with MATLAB shown in Figure 23. (Appendix C)
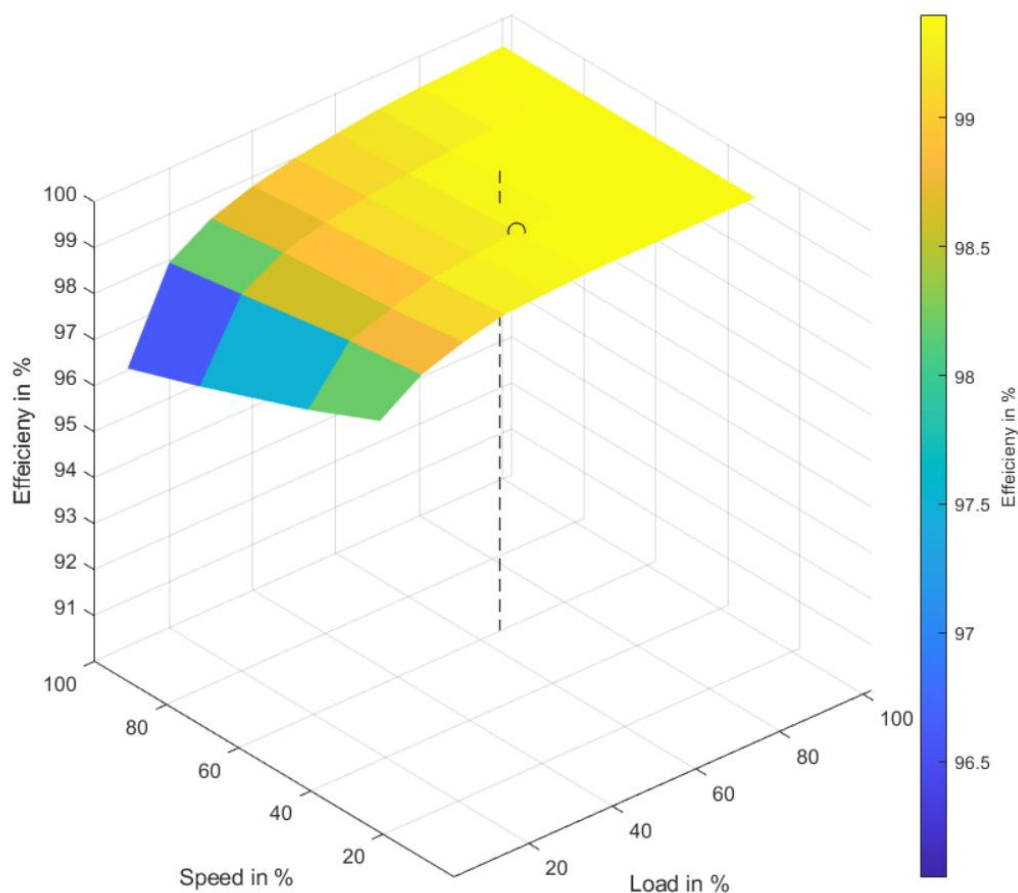
**Figure 23: Recreation of the estimation of gear efficiency in three dimensions**

This plot was later interpolated in MATLAB to increase the accuracy for efficiency results for all values of speed and torque. The original data determines 4x10 datapoints, while the interpolated plot estimates 200x200 datapoints. The enhanced plot is shown in Figure 24.
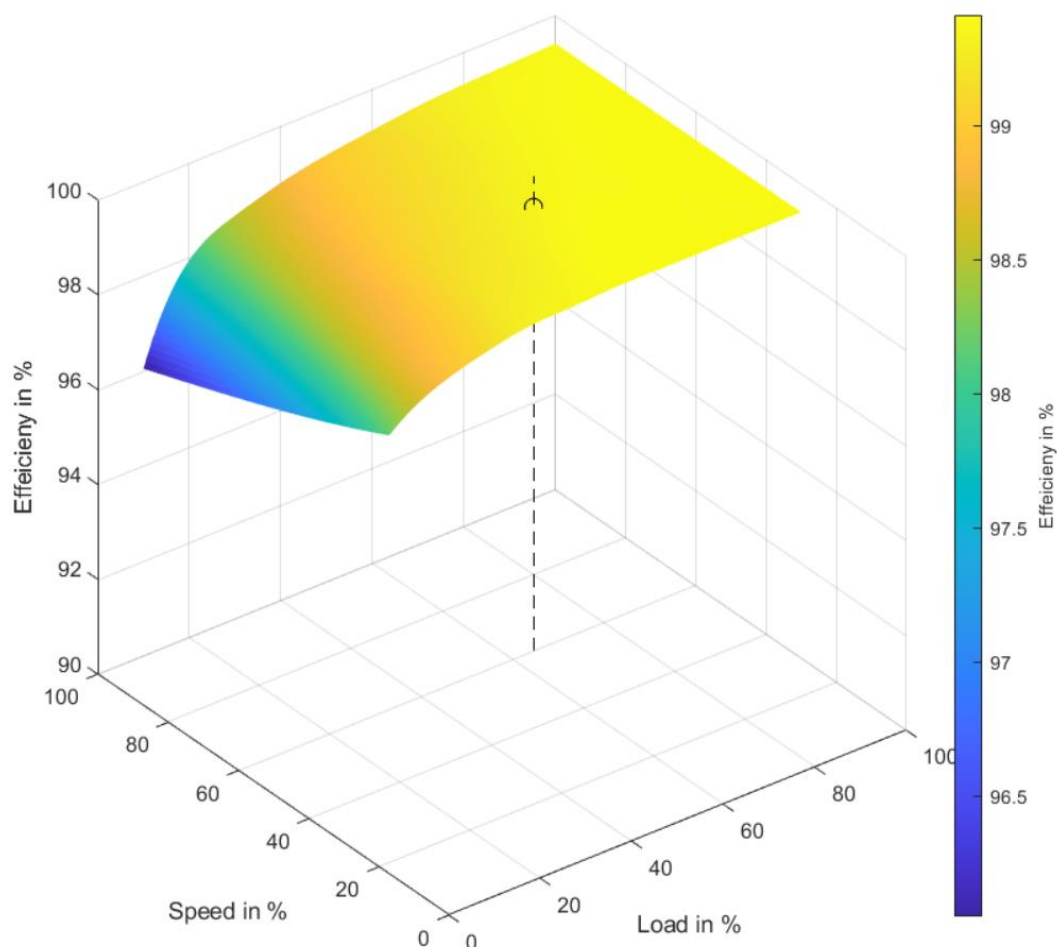
**Figure 24: Interpolated gear efficiency plot**

The dashed lines in Figure 23 and Figure 24 show the inserted values for torque and speed, while the circles show the datapoint on the plot closest to the inserted values.

The torque of the propeller is calculated for all loading conditions for both propeller designs. The speed of the propeller is collected from Table 3. The maximum torque and speed for the gear is set to the highest calculated value for the given propeller design with a 20% addition. The results are shown in Table 5 and Table 6.

*Table 5: Speed and torque calculations for the propeller optimized for 5 knots.*

| Torque and speed percentages | | | | |
|---|---|---|---|---|
| Old design | Gear speed | | Gear torque | |
| Loading condition | Speed [RPM] | Speed [%] | Torque [Nm] | Torque [%] |
| Formula/ source | | $\frac{RPM*100}{(RPM\ max\ /\ 0,80)}$ | $\frac{P_E * 60 * 1000}{(2 * \pi * RPM)}$ | $\frac{Torque * 100}{(torque\ max\ /\ 0,80)}$ |
| 3 knots transit | 195 | 34,90 | 11,23 | 12,97 |
| 3 knots winching | 321 | 57,45 | 48,73 | 56,26 |
| 5 knots tow | 409 | 73,20 | 69,29 | 80,00 |
| 7 knots transit | 447 | 80,00 | 58,18 | 67,17 |

*Table 6: Speed and torque calculations for the propeller optimized for 7 knots.*

| Torque and speed percentages | | | | |
|---|---|---|---|---|
| New design | Gear speed | | Gear torque | |
| Loading condition | Speed [RPM] | Speed [%] | Torque [Nm] | Torque [%] |
| Formula/ source | | $\frac{RPM*100}{(RPM\ max\ /\ 0,80)}$ | $\frac{P_E * 60 * 1000}{(2 * \pi * RPM)}$ | $\frac{Torque * 100}{(torque\ max\ /\ 0,80)}$ |
| 3 knots transit | 309 | 34,62 | 5,70 | 10,56 |
| 3 knots winching | 578 | 64,76 | 32,47 | 60,18 |
| 5 knots tow | 714 | 80,00 | 43,17 | 80,00 |
| 7 knots transit | 687 | 76,97 | 29,37 | 54,42 |

The speed and torque percentages are then inserted into the script in appendix C to plot the values into data from the 3D curve shown in Figure 24 and find the efficiency. The resulting efficiencies are listed in Table 7.

*Table 7: Gear efficiencies for both propeller designs.*

| Loading conditions | Old propeller design | New propeller design |
|---|---|---|
| 3 knots transit | 98,02% | 98,14% |
| 3 knots winching | 99,23% | 99,18% |
| 5 knots towing | 99,38% | 99,37% |
| 7 knots transit | 99,09% | 99,17% |

## 4.3   Electrical motor – weight, power and efficiency

Due to difficulties retrieving a satisfactory amount of valid data from electrical machines specifically designed for ship propulsion, industrial machines were considered. This will be taken into account when discussing the results.

The collected data (Appendix F & G) regarding the sizing of the machine relative to the power output and efficiency are plotted into separate curves both for an IM and for a PMSM. The data gathered is concentrated around the design area of weight and power requirement. Some datapoints are collected well beyond and below our desired area, in order to get a broader understanding of the tendencies.

The correlation between efficiency and weight (Figure 25) and between nominal power and weight (Figure 26) for induction machines is plotted from the retrieved data. (Appendix F). A fitted curve is obtained to further utilize these correlations.
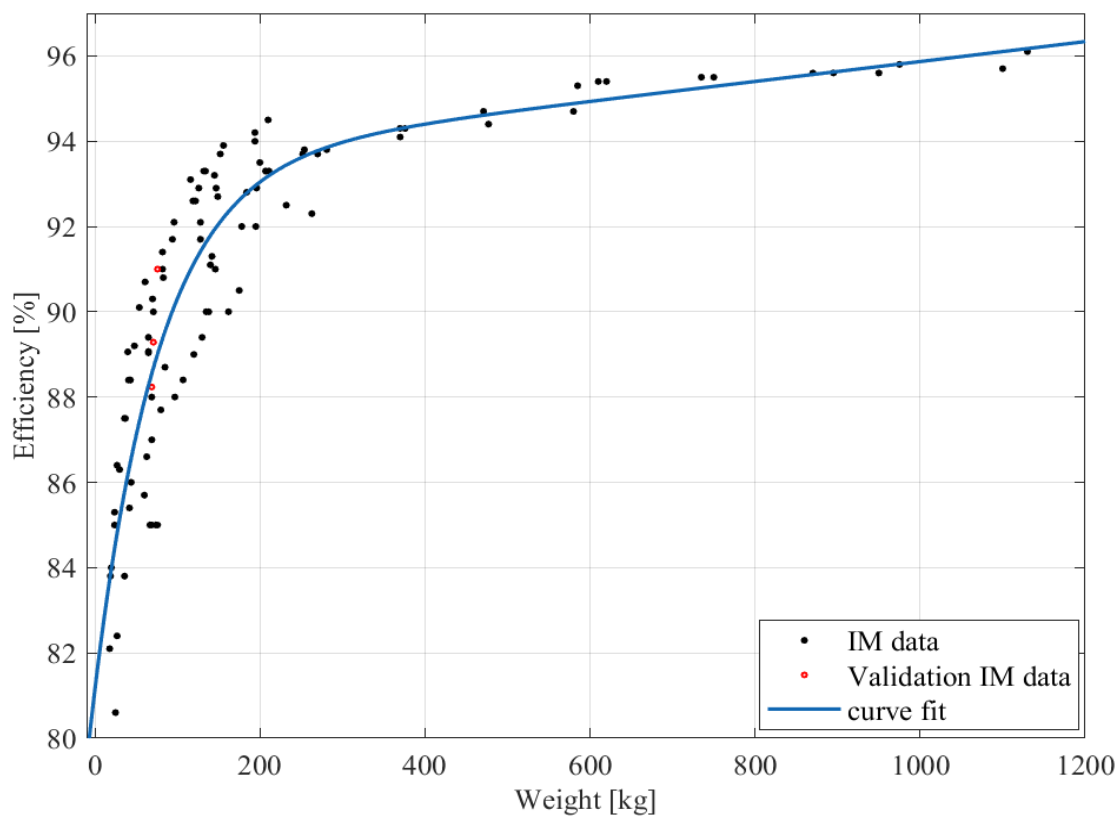
**Figure 25: Efficiency [%] and weight [kg] of an IM.**
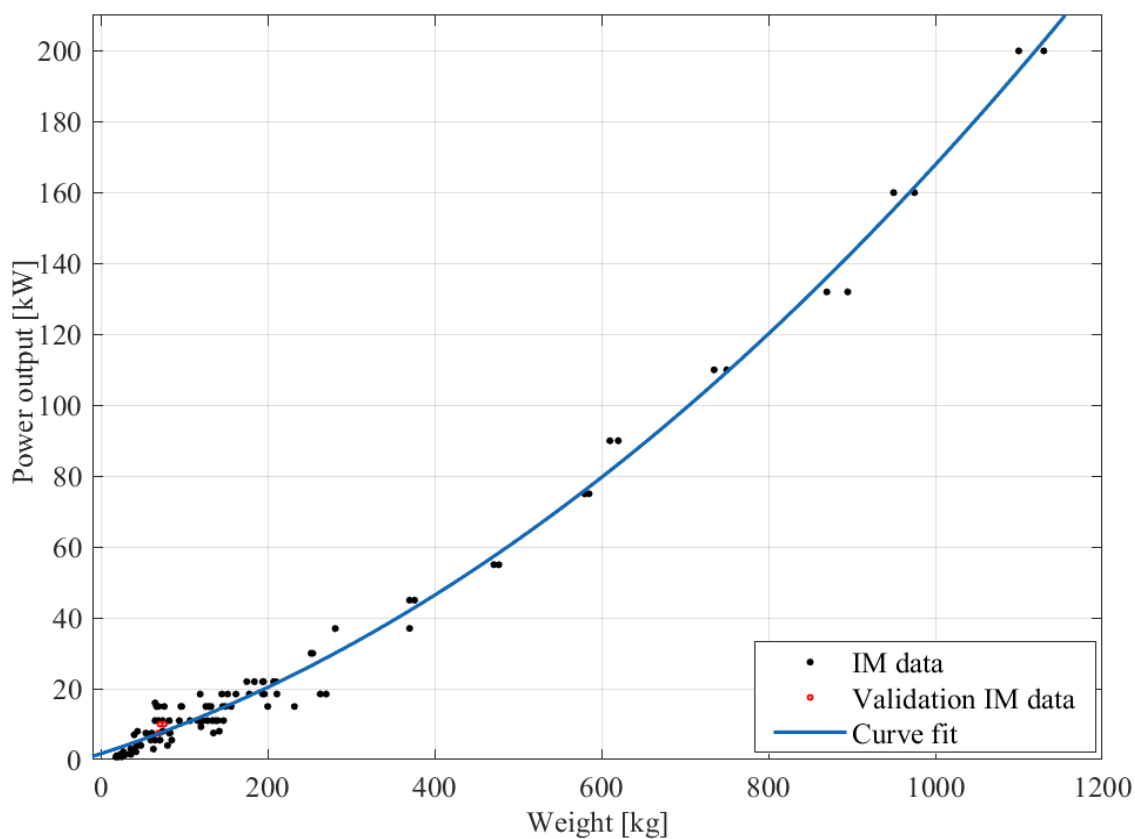


**Figure 26: Power output [kW] and weight [kg] of an IM.**

By utilizing the curve fitting tools in MATLAB, the given fits are obtained.

For efficiency and weight for induction machine (Figure 25),

$$f(x) = a + c * e^{(d*x)} \qquad (4.1)$$

where a = 93.5590, c = -12.4390, d = -0.0127 and x = weight [kg].

For power output and weight for induction machine (Figure 26),

$$f(x) = p1 * x^2 + p2 * x + p3 \qquad (4.2)$$

where p1 = 0.0001, p2 = 0.0755, p3 = 1.6823 and x = weight [kg].

The same correlations are plotted for PMSM. Efficiency and weight shown in Figure 27 and nominal power and weight in Figure 28 (Appendix G).
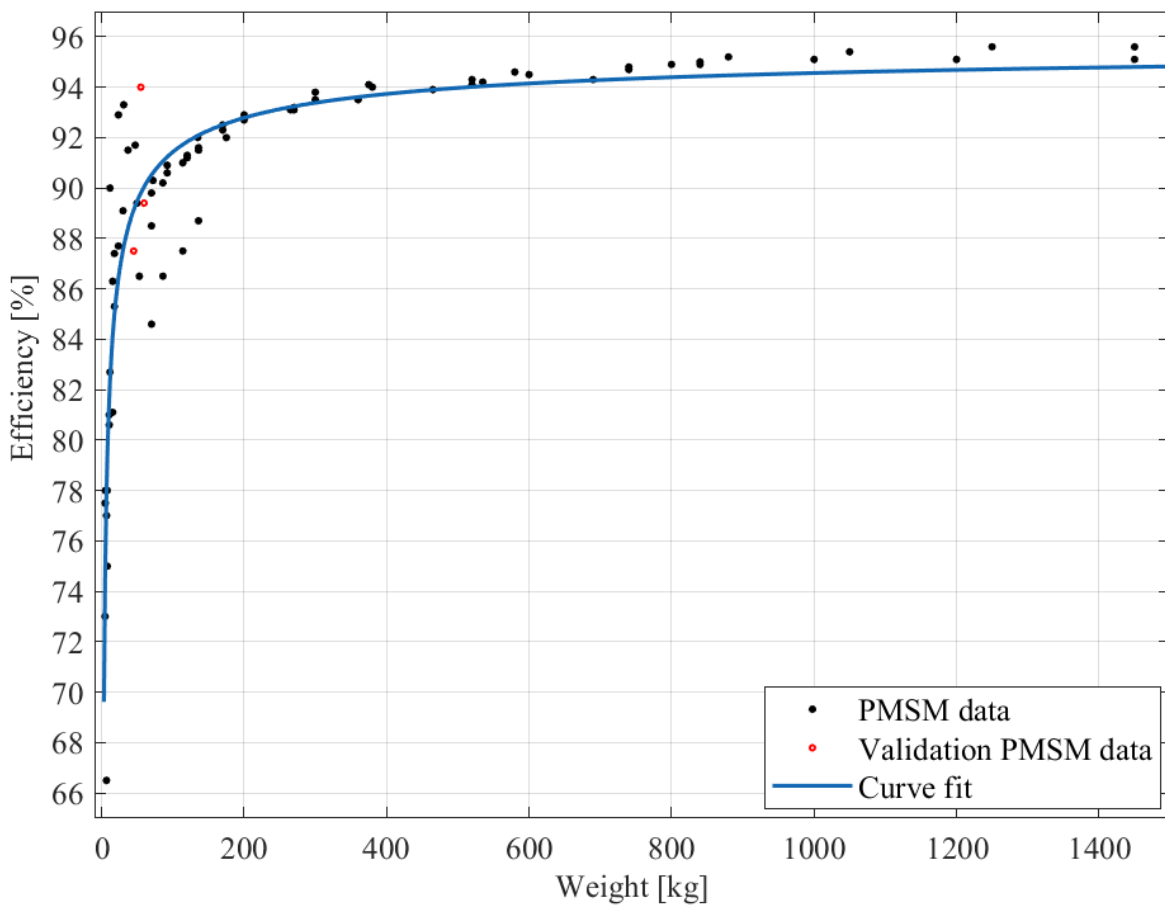


**Figure 27: Efficiency [%] and weight [kg] of a PMSM.**
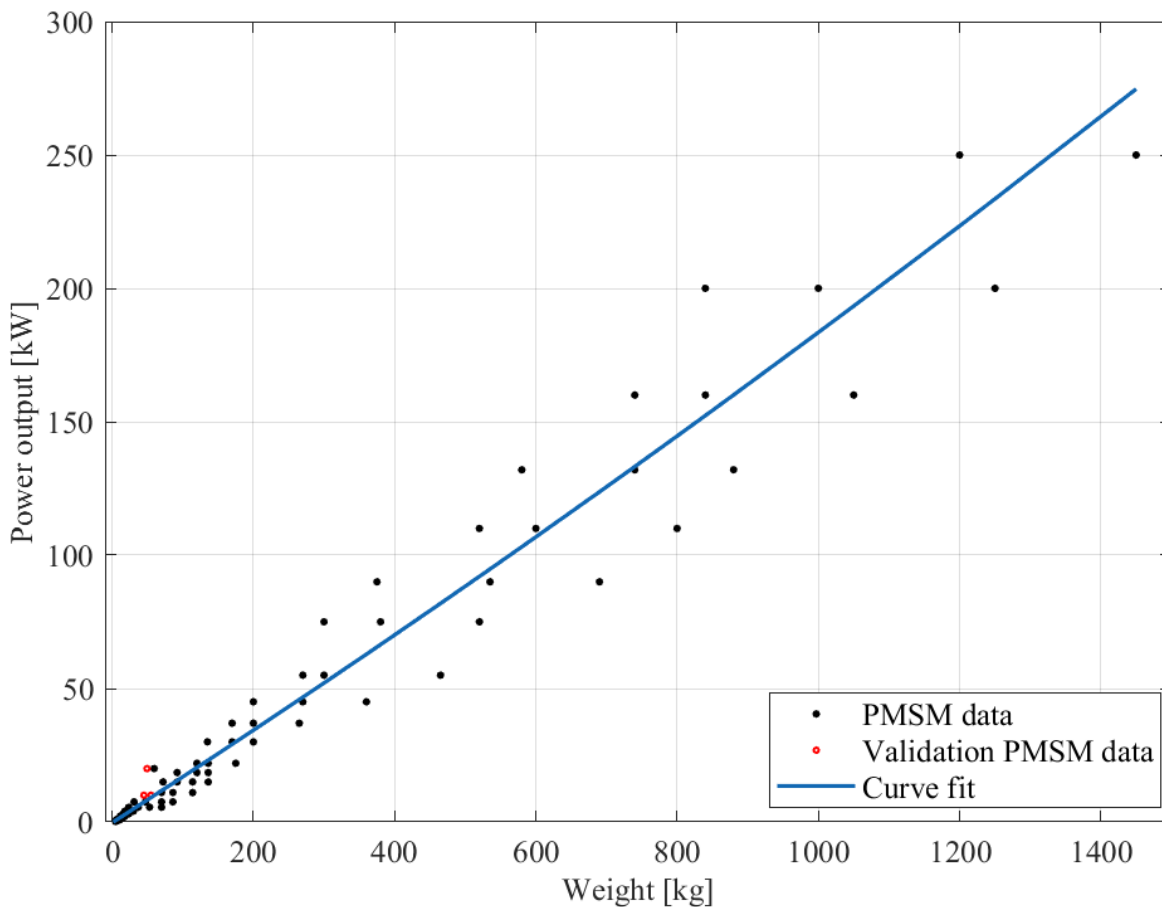
**Figure 28: Power output [kW] and weight [kg] of a PMSM.**

By utilizing the curve fitting tools in MATLAB, the given fits are obtained.

For efficiency and weight PMSM (Figure 27):

$$f(x) = a * x^b + c \qquad (4.3)$$

Where a = -48.5894, b = -0.5165, c = 95.9315 and x = weight [kg].

For power output and weight PMSM (Figure 28):

$$f(x) = p1 * x + p2 \qquad (4.4)$$

Where p1 = 0.1707, p2 = -0.3003 and x = weight [kg].

Given the equations (4.1-4.4) retrieved from curve fittings, the calculations for power, weight and efficiency for each machine are conducted. The calculations are based on previous weight estimations of 75 kg per electrical machine (Appendix A) as a maximum limit, and the mini-

mum power needed to still fulfill the operational requirements, as a minimum. Since the requirement demands two drivetrains and means of propulsion, the minimum power need is calculated based on all power being delivered from 1 propeller for the most demanding condition with a 20% service addition. The calculations are done for all configurations of new and old propeller design, gear and no gear and IM or PMSM.

*Table 8: Weight and efficiency of IM & PMSM at maximum weight and minimum power need.*

| Decisive factors | | | Electrical machine type | Power [kW] | Weight [kg] | Efficency [%] |
|---|---|---|---|---|---|---|
| old design | no gear | weight limit | induction machine | 7,907 | 75 | 88,76 |
| | | minimum power need | | 7,048 | 65,4 | 88,14 |
| | | weight limit | permanent magnet synchronous machine | 12,502 | 75 | 90,71 |
| | | minimum power need | | 7,048 | 43 | 88,97 |
| | gear | weight limit | induction machine | 7,907 | 75 | 88,76 |
| | | minimum power need | | 7,416 | 69,5 | 88,41 |
| | | weight limit | permanent magnet synchronous machine | 12,502 | 75 | 90,71 |
| | | minimum power need | | 7,416 | 45,2 | 89,14 |

| Decisive factors | | | Electrical machine type | Power [kW] | Weight [kg] | Efficency [%] |
|---|---|---|---|---|---|---|
| new design | no gear | weight limit | induction machine | 7,907 | 75 | 88,76 |
| | | minimum power need | | 7,531 | 70,8 | 88,50 |
| | | weight limit | permanent magnet synchronous machine | 12,502 | 75 | 90,71 |
| | | minimum power need | | 7,531 | 45,9 | 89,20 |
| | gear | weight limit | induction machine | 7,907 | 75 | 88,76 |
| | | minimum power need | | 7,927 | 75,2 | 88,77 |
| | | weight limit | permanent magnet synchronous machine | 12,502 | 75 | 90,71 |
| | | minimum power need | | 7,927 | 48,2 | 89,37 |

The highest efficiency and lowest weight are highlighted in green, whereas the lowest efficiency and highest weight is red.

The relationship between the number of poles, weight and efficiency of the machine is also visualized by the retrieved data (Appendix F & G) for both types of machines in vicinity of our power area.
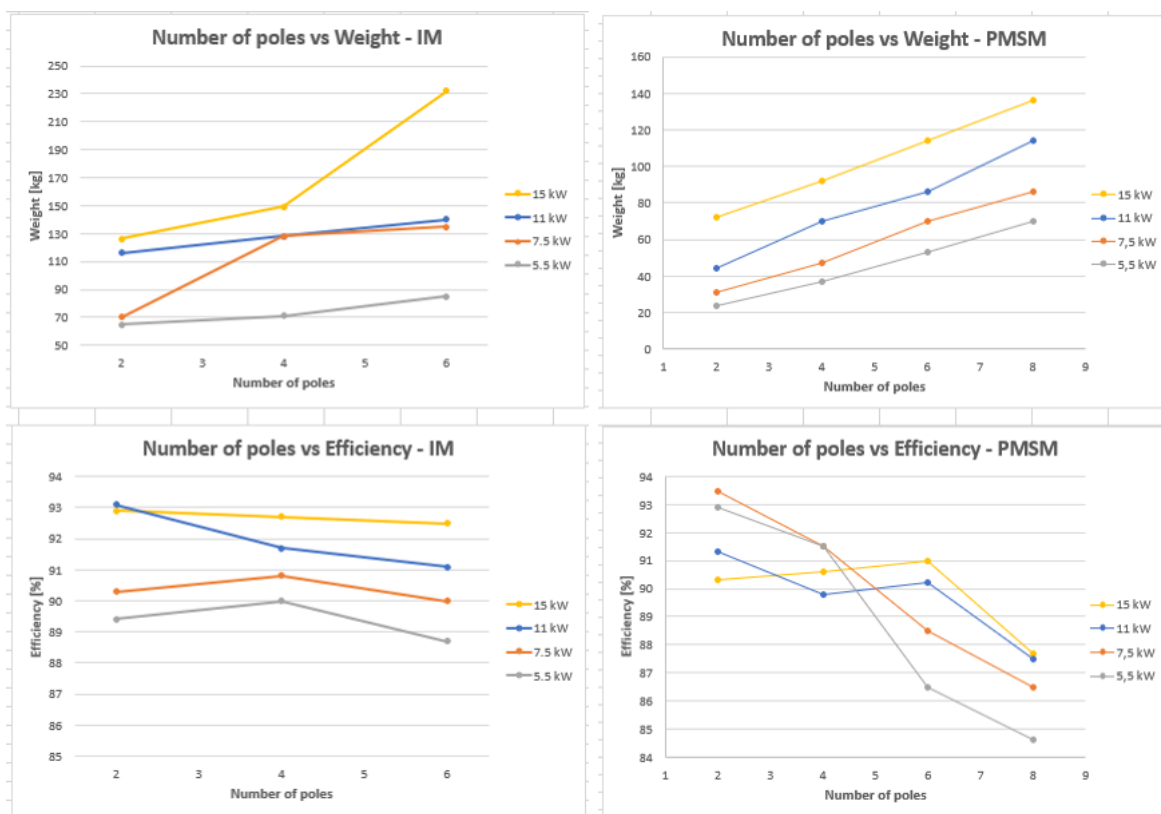
**Figure 29: Weight and efficiency correlation to number of poles IM & PMSM**

## 4.4 Electrical motor – speed vs efficiency

The efficiency's dependency on load and speed condition is displayed utilizing data retrieved from the efficiency maps. The efficiency maps retrieved origins from a 10 kW and 8 kW PMSM and an 8 kW IM (see Appendix B).

The power required by the electrical machine at any given mode is calculated by multiplying the required power to the propeller with the efficiency of the shaft and the gear. The results are shown in Table 9.

*Table 9: Power requirements of electrical motor for different operation modes and configurations*

| Power requiremetns for different operations modes and configurations [kW] | | | | | |
|---|---|---|---|---|---|
| Desicive factors | | 7 knots | 5 knots towing | 3 knots | 3 knots winching |
| old design | no gear | 2,696 | 2,937 | 0,227 | 1,619 |
| | gear | 2,713 | 2,955 | 0,228 | 1,629 |
| new design | no gear | 2,102 | 3,138 | 0,183 | 1,922 |
| | gear | 2,117 | 3,161 | 0,184 | 1,936 |

Further the speed-torque curve for the given power output is plotted into the existing efficiency map using MATLAB (Appendix I). When calculating the torque when a gear is considered, the speed is multiplied by the gear ratio,

$$\tau = \frac{P * 60}{2\pi * rpm * k_{1-2}}$$

where $k_1$ is the gear ratio for the old propeller design, and $k_2$ for the new design. This process is done for all configurations. Some examples are shown below for the 5 knot towing condition (which gives a power requirement of 2,937 kW) with a PMSM (Figure 30), and with an IM (Figure 31). In both figures the upper markings represent when no gear is utilized, and the lower filled marking when a gear is used.
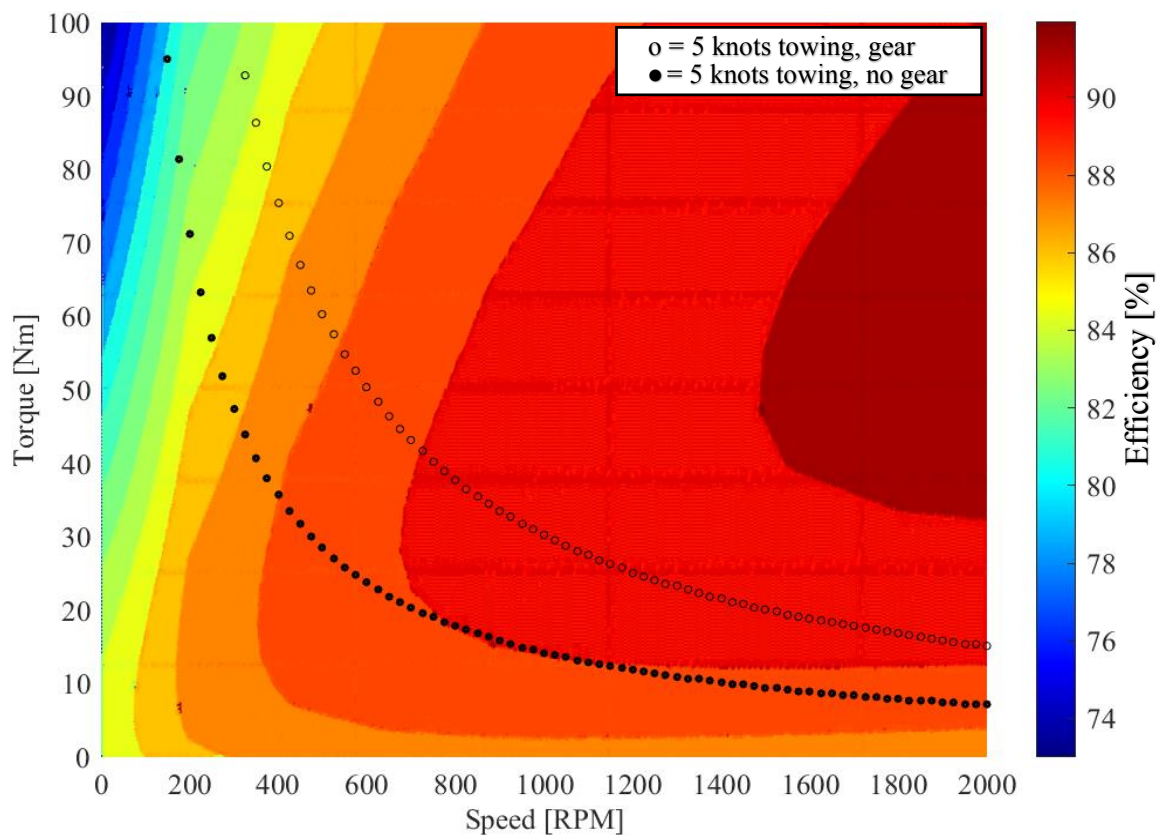


**Figure 30: Efficiency map with load curve 10 kW PMSM, 5 knots towing.**
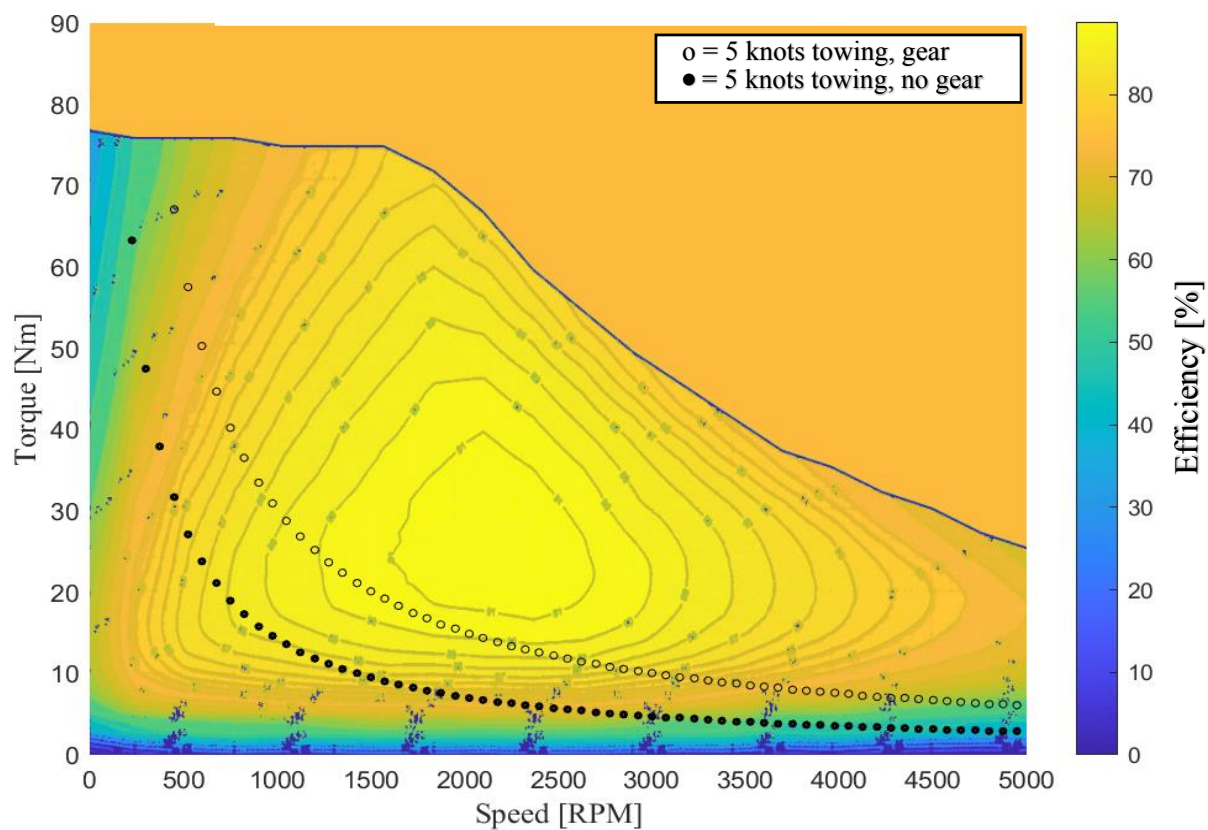
**Figure 31: Efficiency map with load curve, 8 kW IM, 5 knots towing.**

The MATLAB script reads out how the efficiency changes with speed variations for the given power output and plots it in a separate curve. An example of the 5 knot towing condition, old propeller is shown for both PMSM (Figure 32) and IM (Figure 33), with curves for with and without a gear.
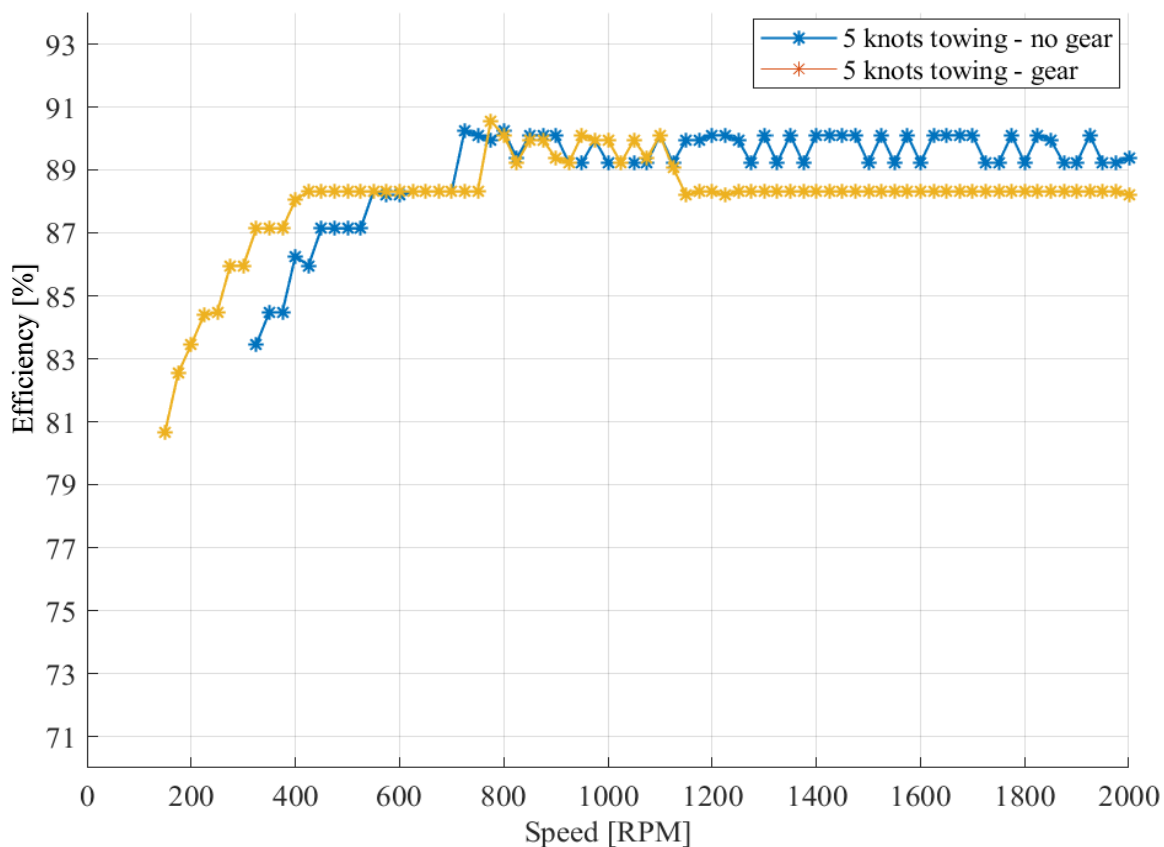
**Figure 32: RPM vs Efficiency curve for 12.5 kW PMSM, 5 knots towing.**
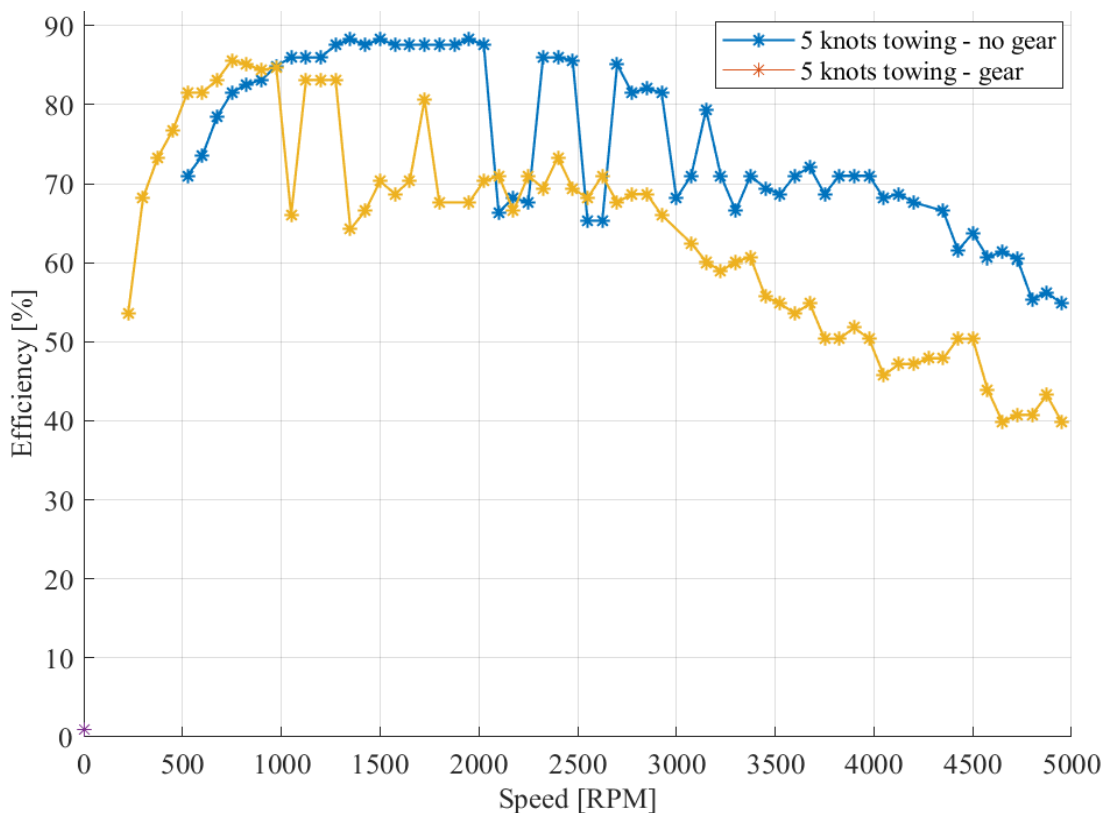


**Figure 33: RPM vs Efficiency curve for 8 kW IM at 5 knots towing.**

Further, an example of the curve fitting for Figure 32 and Figure 33 is displayed in respectively Figure 34 and Figure 35.
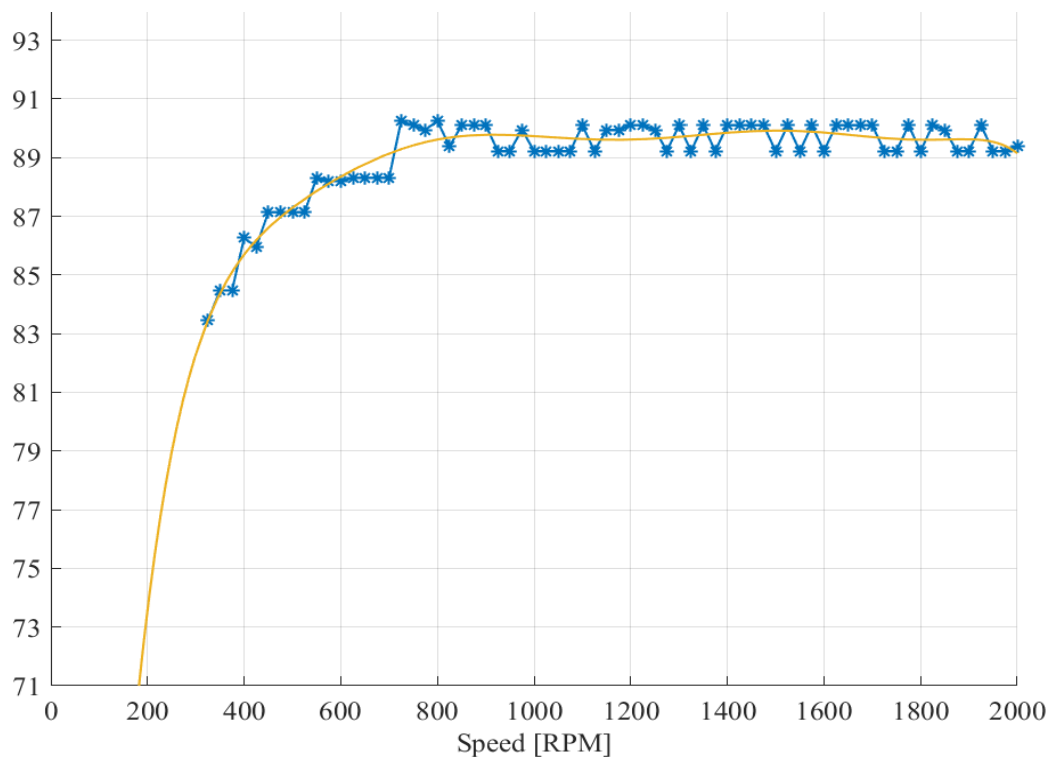


**Figure 34: Curve fit for 5 knot towing, old propeller design, no gear, PMSM.**
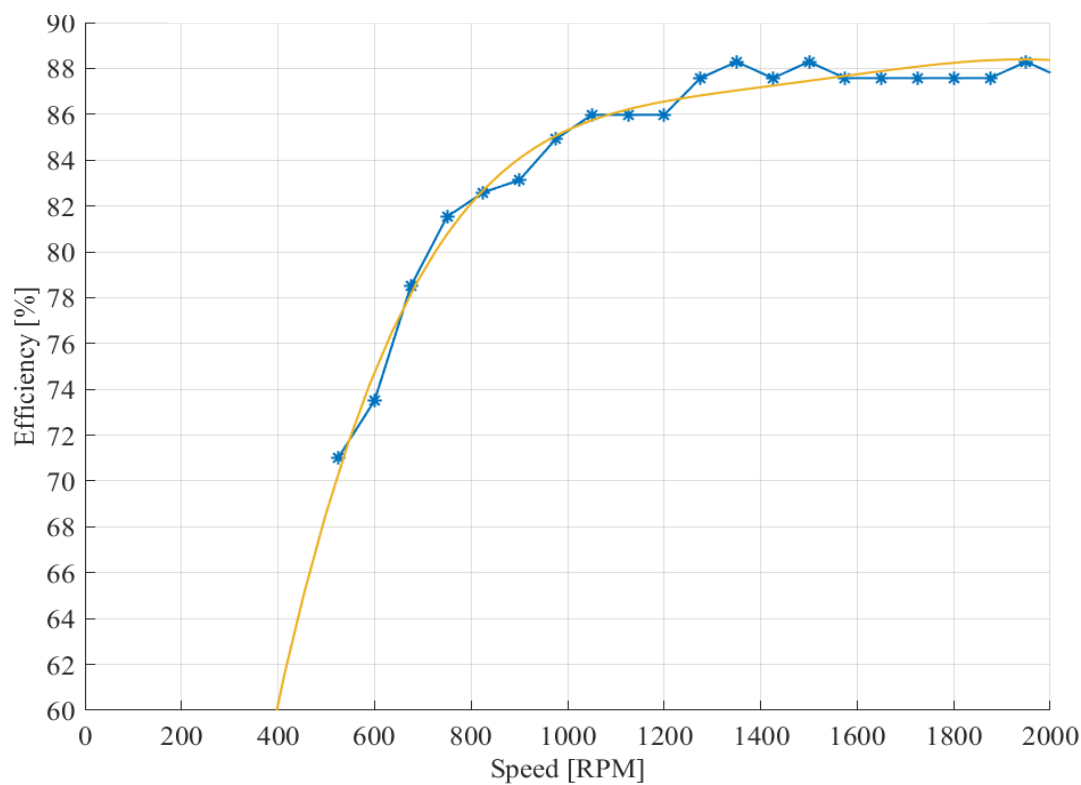


**Figure 35: Curve fit for 5 knots towing, old propeller design, no gear, IM.**

By using MATLABS' curve fitting and interpolation tools, efficiency data for each given speed and given power is extracted. This process is repeated for each loading condition, each operation mode and for the different types of machines. The results are shown in Table 10.

*Table 10: Extracted efficiency values for all configurations.*

**12.5 kW PMSM**

| old propeller design with new efficiencys - with and without gear | | | | |
|---|---|---|---|---|
| operation mode | rpm - no gear | efficiency @ rpm - no gear | rpm - gear | efficiency @ rpm - gear |
| 7 knots | 453 | 0,872 | 1663 | 0,884 |
| 5 knots towing | 409 | 0,865 | 1500 | 0,886 |
| 3 knots | 195 | 0,873 | 714 | 0,873 |
| 3 knots winching | 320 | 0,868 | 1175 | 0,886 |
| new design with new efficiencys - with and without gear | | | | |
| operation mode | rpm - no gear | efficiency @ rpm - no gear | rpm - gear | efficiency @ rpm - gear |
| 7 knots | 668 | 0,892 | 1413 | 0,884 |
| 5 knots towing | 708 | 0,891 | 1500 | 0,884 |
| 3 knots | 298 | 0,872 | 630 | 0,874 |
| 3 knots winching | 606 | 0,889 | 1283 | 0,884 |

**8 kW PMSM**

| old propeller design with new efficiencys - with and without gear | | | | |
|---|---|---|---|---|
| operation mode | rpm - no gear | efficiency @ rpm - no gear | rpm - gear | efficiency @ rpm - gear |
| 7 knots | 453 | 0,793 | 1663 | 0,887 |
| 5 knots towing | 409 | 0,765 | 1500 | 0,875 |
| 3 knots | 195 | 0,805 | 714 | 0,867 |
| 3 knots winching | 320 | 0,772 | 1175 | 0,877 |
| new design with new efficiencys - with and without gear | | | | |
| operation mode | rpm - no gear | efficiency @ rpm - no gear | rpm - gear | efficiency @ rpm - gear |
| 7 knots | 668 | 0,863 | 1413 | 0,886 |
| 5 knots towing | 708 | 0,855 | 1500 | 0,889 |
| 3 knots | 298 | 0,850 | 630 | 0,868 |
| 3 knots winching | 606 | 0,858 | 1283 | 0,890 |

**8 kW IM**

| old propeller design with new efficiencys - with and without gear | | | | |
|---|---|---|---|---|
| operation mode | rpm - no gear | efficiency @ rpm - no gear | rpm - gear | efficiency @ rpm - gear |
| 7 knots | 453 | 0,659 | 1663 | 0,654 |
| 5 knots towing | 409 | 0,611 | 1500 | 0,681 |
| 3 knots | 195 | 0,687 | 714 | 0,279 |
| 3 knots winching | 320 | 0,678 | 1175 | 0,609 |
| new design with new efficiencys - with and without gear | | | | |
| operation mode | rpm - no gear | efficiency @ rpm - no gear | rpm - gear | efficiency @ rpm - gear |
| 7 knots | 668 | 0,818 | 1413 | 0,730 |
| 5 knots towing | 708 | 0,792 | 1500 | 0,811 |
| 3 knots | 298 | 0,676 | 630 | 0,380 |
| 3 knots winching | 606 | 0,800 | 1283 | 0,743 |

These updated values for the efficiency of the electrical machine is further used to analyse how the speed and oparating condition of the vessel affects the efficiency of the drivetrain.

## 4.5   Battery

Updated values for energy density are obtained from the KBP63 Kreisel high voltage battery system (Appendix J).

$$Energy\ Density = 163\ \frac{Wh}{kg}$$

Necessary capacity is calculated based on the requirement to operate 12 hours on battery in the 5 knots towing condition in case of power failure. The weight is calculated based on equation (2.23) and the power needed from the battery to maintain 5 knots towing and the estimated hotel load of 10 kW for 12 hours.

*Table 11: Power requirements and necessary capacity of battery for different configurations*

| descisive factors | | | power need from battery at 5 knots towing  [kW] | Necessary capacity for 12 hours [kWh] | weight battery [kg] |
|---|---|---|---|---|---|
| 12,5 kW PMSM | old design | no gear | 17,6 | 211,3 | 1296 |
| | | gear | 17,4 | 209,1 | 1283 |
| | new design | no gear | 17,9 | 214,7 | 1317 |
| | | gear | 18,0 | 215,5 | 1322 |
| 8 kW PMSM | old design | no gear | 18,6 | 223,2 | 1370 |
| | | gear | 17,6 | 210,8 | 1293 |
| | new design | no gear | 18,2 | 218,7 | 1342 |
| | | gear | 18,0 | 215,5 | 1322 |
| 8 kW IM | old design | no gear | 20,8 | 249,3 | 1529 |
| | | gear | 19,7 | 236,7 | 1452 |
| | new design | no gear | 18,9 | 226,6 | 1390 |
| | | gear | 18,7 | 224,7 | 1379 |

The highest and lowest weight are highlighted respectively in red and green. These calculated weights will be used when accessing the overall weight of the drivetrain.

## 4.6   Diesel generator

Based on the updated values for each component of the drivetrain, the new power requirements for the generator are calculated for different loading conditions and configurations. the calculations are given 20% addition in order to maintain power equilibrium in the battery.

*Table 12: Power requirements from diesel generator for different configurations*

| power requirement from diesel generator at different loads and configurations [kW] | | | | | | |
|---|---|---|---|---|---|---|
| descisive factors | | | 7 knots | 5 knots towing | 3 knots | 3 knots winching |
| 12,5 kW PMSM | old design | no gear | 18,3 | 19,1 | 10,7 | 15,0 |
| | | gear | 18,2 | 18,9 | 10,7 | 14,9 |
| | new design | no gear | 16,3 | 19,5 | 10,6 | 15,8 |
| | | gear | 16,4 | 19,5 | 10,6 | 15,8 |
| 8 kW PMSM | old design | no gear | 19,1 | 20,3 | 10,8 | 15,6 |
| | | gear | 18,2 | 19,1 | 10,7 | 15,0 |
| | new design | no gear | 16,5 | 19,9 | 10,6 | 16,0 |
| | | gear | 16,4 | 19,6 | 10,6 | 15,9 |
| 8 kW IM | old design | no gear | 21,0 | 22,9 | 10,9 | 16,4 |
| | | gear | 21,2 | 21,7 | 12,2 | 17,2 |
| | new design | no gear | 16,9 | 20,7 | 10,7 | 16,5 |
| | | gear | 17,8 | 20,5 | 11,3 | 17,0 |

For the M-SQ Pro 25 Maritime Generator the fuel consumption is 1-6 liters/h. The fuel consumption compared to load is given from the work of Andressen & Mykland, and from this a linear correlation for fuel consumption per power output is created (Figure 36).
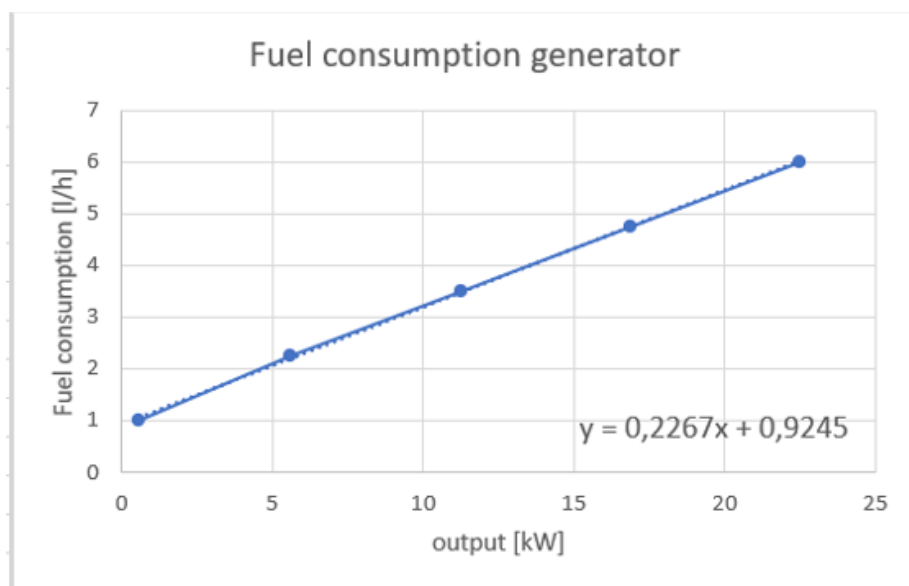


**Figure 36: Linear correlation for fuel consumption of M-SQ Pro Maritime Generator**

The linear correlation is used to calculate fuel consumption for other power values. The efficiency of the diesel engine is calculated with equation (2.28), the values in Table 12, and the linear relation for fuel consumption. The efficiency of the electrical generator is calculated based on the equation (4.3 & 4.4) retrieved from the curve fit of the correlation between the weight, power output and efficiency for a PMSM.

$$22,5\ kW \rightarrow 133,5 kg \rightarrow \text{ŋ}_{generator} = 92\%$$

The efficiency of the generator is assumed to be constant since always running at 1500/1800 rpm, and load variation has little impact on efficiency in designed speed areas (ref efficiency map for PMSM, Appendix B).

The efficiency of the diesel engine is calculated from equation (2.28), with the power requirements from each condition and configuration, and the linear correlation in Figure 36 to find the corresponding fuel consumptions. The result is shown in Table 13.

*Table 13: Efficiency of diesel engine for different operation modes and configurations.*

| total efficiency of diesel engine at different loads and configuratiosn [%] | | | | | | |
|---|---|---|---|---|---|---|
| descisive factors | | | 7 knots | 5 knots towing | 3 knots | 3 knots |
| 12,5 kW PMSM | old design | no gear | 30,4 | 30,7 | 26,9 | 29,2 |
| | | gear | 30,4 | 30,6 | 26,9 | 29,2 |
| | new design | no gear | 29,8 | 30,7 | 26,8 | 29,6 |
| | | gear | 29,8 | 30,8 | 26,8 | 29,6 |
| 8 kW PMSM | old design | no gear | 30,7 | 31,0 | 27,0 | 29,5 |
| | | gear | 30,4 | 30,6 | 26,9 | 29,2 |
| | new design | no gear | 29,8 | 30,9 | 26,8 | 29,6 |
| | | gear | 29,8 | 30,8 | 26,8 | 29,6 |
| 8 kW IM | old design | no gear | 31,1 | 31,6 | 27,1 | 29,8 |
| | | gear | 31,2 | 31,3 | 27,9 | 30,1 |
| | new design | no gear | 30,0 | 31,1 | 26,9 | 29,8 |
| | | gear | 30,3 | 31,0 | 27,3 | 30,0 |

The generator efficiency is multiplied with the efficiency of the diesel engine to calculate the overall efficiency of the diesel generator for each loading condition and configuration (Table 14.)

*Table 14: Efficiency of diesel generator for different operation modes and configurations*

| total efficiency of diesel generator at different loads and configuratiosn [%] | | | | | | |
|---|---|---|---|---|---|---|
| descisive factors | | | 7 knots | 5 knots towing | 3 knots | 3 knots winching |
| 12,5 kW PMSM | old design | no gear | 28,0 | 28,2 | 24,8 | 26,9 |
| | | gear | 28,0 | 28,1 | 24,8 | 26,9 |
| | new design | no gear | 27,4 | 28,3 | 24,7 | 27,2 |
| | | gear | 27,4 | 28,3 | 24,7 | 27,2 |
| 8 kW PMSM | old design | no gear | 28,2 | 28,5 | 24,8 | 27,1 |
| | | gear | 28,0 | 28,2 | 24,8 | 26,9 |
| | new design | no gear | 27,5 | 28,4 | 24,7 | 27,3 |
| | | gear | 27,4 | 28,3 | 24,7 | 27,2 |
| 8 kW IM | old design | no gear | 28,7 | 29,0 | 24,9 | 27,4 |
| | | gear | 28,7 | 28,8 | 25,7 | 27,7 |
| | new design | no gear | 27,6 | 28,6 | 24,8 | 27,4 |
| | | gear | 27,8 | 28,5 | 25,2 | 27,6 |

The highest efficiency for each operating mode is highlighted in green. The efficiencies are added to the calculations for the overall efficiency of the drivetrain.

## 4.7   Efficiency, fuel requirement and weight of drivetrain

Further, the results from the study of the drivetrain are used to calculate the overall efficiency, fuel amount, and weight with regards to the operation profile and the operational requirements.

The total efficiency of the drivetrain is determined by adding all the efficiencies for the components together,

$$\eta_{total} = \eta_{propeller} * \eta_{shaft} * \eta_{gear} * \eta_{motor} * \eta_{rectifier} * \eta_{inverter} * \eta_{D.G} \qquad (4.5)$$

where $\eta_{gear}$ equals 1 when no gear is used.

The total efficiency and fuel consumption for the drivetrain at different operating modes and different configurations is calculated (Table 15).

*Table 15: Drivetrain efficiency for different operating modes and configurations*

| desicive factors | | | total efficiency of drivetrain @ different operation modes | | | | total fuel consumtion for operation profile [liters] |
|---|---|---|---|---|---|---|---|
| | | | 7 knots | 5 knots towing | 3 knots | 3 knots winching | |
| 12,5 kW PMSM | old propeller | no gear | 0,093 | 0,128 | 0,088 | 0,112 | 1590,2 |
| | design | gear | 0,093 | 0,130 | 0,086 | 0,114 | 1577,6 |
| | new propeller | no gear | 0,119 | 0,123 | 0,108 | 0,098 | 1560,7 |
| | design | gear | 0,117 | 0,122 | 0,106 | 0,097 | 1565,4 |
| 8 kW PMSM | old propeller | no gear | 0,085 | 0,114 | 0,081 | 0,101 | 1663,6 |
| | design | gear | 0,093 | 0,128 | 0,086 | 0,113 | 1586,4 |
| | new propeller | no gear | 0,115 | 0,119 | 0,105 | 0,095 | 1583,7 |
| | design | gear | 0,117 | 0,122 | 0,107 | 0,097 | 1566,6 |
| 8 kW IM | old propeller | no gear | 0,072 | 0,093 | 0,069 | 0,089 | 1824,7 |
| | design | gear | 0,071 | 0,102 | 0,029 | 0,080 | 1773,6 |
| | new propeller | no gear | 0,110 | 0,111 | 0,084 | 0,089 | 1628,0 |
| | design | gear | 0,098 | 0,112 | 0,048 | 0,082 | 1641,0 |

The highest total efficiency is highlighted in green, and the lowest in red for each operating mode. The lowest and highest fuel consumption for the estimated operation profile is also highlighted, with the lowest being green and highest red.

Although the fuel consumption for the specific operation profile is calculated above, the decisive factor when determining amount of fuel is the requirement to go 20 days in 5 knots towing in sea state 3, and still have 35% remaining fuel. The fuel amount for 5 knots towing in 20 days is given a 20% addition to account for sea state 3 (Magnussen, 2017, p. VI) and is displayed in the weight breakdown below. The fuel is multiplied by the fuel density of 0.885 kg/liter to find the mass. Due to limited time, changes in weight of the diesel generator were not studied, and will therefore be set to the 650kg of the M-SQ25 pro.

*Table 16: Weight breakdown of drivetrain for different configurations.*

| decisive factors | | | weight of components in drivetrain [kg] | | | | | | | | | total active weight [kg] |
|---|---|---|---|---|---|---|---|---|---|---|---|---|
| | | | fuel | generator | rectifier | battery | inverter | electrical motor | gear | shaft | propeller | |
| 12.5 kW PMSM | old design | no gear | 4000 | 650 | 153 | 1296 | 40 | 150 | 0 | 200 | 200 | 6689,2 |
| | | gear | 3962 | 650 | 153 | 1283 | 40 | 150 | 10,85 | 200 | 200 | 6648,7 |
| | new design | no gear | 4059 | 650 | 153 | 1317 | 40 | 150 | 0 | 200 | 100 | 6669,1 |
| | | gear | 4072 | 650 | 153 | 1322 | 40 | 150 | 10,85 | 200 | 100 | 6697,5 |
| 8 kW PMSM | old design | no gear | 4206 | 650 | 153 | 1370 | 40 | 86 | 0 | 200 | 200 | 6904,3 |
| | | gear | 3991 | 650 | 153 | 1293 | 40 | 90,4 | 10,85 | 200 | 200 | 6628,5 |
| | new design | no gear | 4127 | 650 | 153 | 1342 | 40 | 91,8 | 0 | 200 | 100 | 6704,1 |
| | | gear | 4073 | 650 | 153 | 1322 | 40 | 96,4 | 10,85 | 200 | 100 | 6645,4 |
| 8 kW IM | old design | no gear | 4654 | 650 | 153 | 1529 | 40 | 130,8 | 0 | 200 | 200 | 7557,5 |
| | | gear | 4437 | 650 | 153 | 1452 | 40 | 139 | 10,85 | 200 | 200 | 7281,9 |
| | new design | no gear | 4263 | 650 | 153 | 1390 | 40 | 141,6 | 0 | 200 | 100 | 6937,5 |
| | | gear | 4231 | 650 | 153 | 1379 | 40 | 150,4 | 10,85 | 200 | 100 | 6914,2 |

# 5    Discussion

Chapter 4 display numerus calculations, figures and tables, all with their different results. The next chapter will analyze these results in order to display their correlation to the overall efficiency, weight and configuration of the drivetrain.

## 5.1    Propeller optimization

When choosing a fixed pitch propeller, the optimization must be done for one certain point. Usually this is done for the most demanding conditions. However, since the USV should be able to conduct different types of operation, it might be beneficial with an overall better open water efficiency for variety of speeds and loads. The purpose of designing a new propeller was to identify how the physical parameters of the propeller affect its open water efficiency, and thus the P.C. The changes in the open water efficiencies between the propellers can be seen in Figure 37.
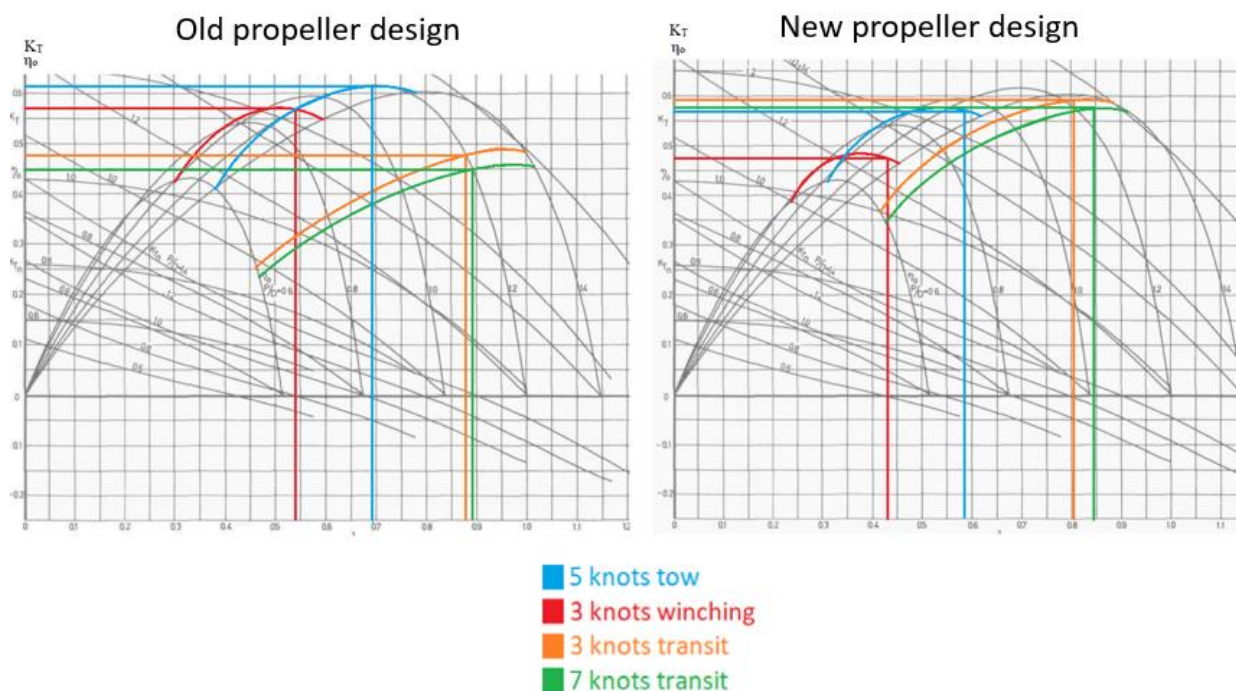


**Figure 37: Comparison of propeller sheet for old and new propeller design.**

Since the old propeller design is optimized for 5 knots towing, it has its highest open water efficiency at this point. However, the efficiency for the less demanding operations, such as transit in 1-7 knots, is significantly lower. Here, the decrease in efficiency of about 15%. The

new propeller design, which is optimized for transit, obtains its highest open water efficiency at the points of 1-7 knots. The increase for these is about 12-13% compared to the old design. However, this leads to a decrease in efficiency for the more demanding operations, such as 5 knots towing, and 3 knots winching. The efficiency drop for the demanding conditions is about 5% for 5 knots towing and towards 10% for 3 knots winching. The 3 knots winching conditions is little used compared to the other conditions and will have little impact on the overall energy consumption of the drivetrain.

The result emphasizes how choosing a smaller propeller increases its rotational speed and pushes the efficiency curves left in the propeller diagram. In the same way, choosing a larger propeller would result in a lower rotational speed, and curves occurring further right in the diagram. The old propeller design gives an inferior open water efficiency for the 5 knots towing condition, which is beneficial when considering fuel requirements, and longer periods of operation in this mode. On the other hand, the new propeller design presents a high efficiency for a spectra of operation modes. The new propeller design also requires a higher rotational speed, which is beneficial for the electric motor. The old propeller design has a developed area of $0.126m^2$, compared to the new design with $0.060m^2$. The reduction in size will also make a positive contribution to the weight of the vessel. The weight of the new propeller is therefore estimated to be half the weight of the old propeller (Appendix A).

Since the developed area $A_D$ for the propeller is halved, the maximum load $T_{max}$ will doble. Andressen & Mykland stated concluded that a lower $T_{max}$ would give a higher open water efficiency (Andresseen & Mykland, 2022, p. 66). This is true to a certain extent. The decrease in $T_{max}$ will give a flatter $K_T(J)$ curve, which will push the optimum open water efficiency points further right on the $\eta_o(P/D)$ curves. When the peak of the $\eta_o(P/D)$ curves are reached, a further decrease in $T_{max}$ will give a decrease in open water efficiency.

## 5.2  Gear

As mentioned, a gear may allow for the electrical engine to operate closer to its ideal operating range, and at the same time maintaining the optimum speed of the propeller, but it comes with some additional power losses. So how does the implementation of a gear affect the drivetrain?

Figure 24 shows that a single gear exchange can introduce losses up to 4%. However, this is only for high speeds and small load conditions, which can be the case for airplane propellers,

but never for ship propellers given the resistance in the water. This gives the results displayed in Table 7, a minimum of efficiency of 98%.

Another question about the gear that arises is "Is it necessary to find the individual gear efficiencies when they are so similar for all loading conditions?". In Table 3, the gear efficiencies for all loading conditions on both propellers are shown to lay between 98,02% and 99,38%. For the most demanding loading condition, 5 knots towing with the propeller optimized for 7 knots transit, the difference between the best and the worst gear efficiency would amount to a difference in power need of 76 watts per motor. With such small variations, would it not be both easier and more time efficient to assume constant gear efficiency? From Table 3 it can be seen that for all the loading conditions except 3 knots transit, the efficiency is greater than 99%. Since both 3 knots loading conditions are limited in time compared to 5 knots towing and 7 knots transit, it is reasonable to set the constant value of efficiency to represent to the two latter loading conditions. If a quick estimation of gear efficiency is wanted, 99% seems like a reasonable value, although this will most likely lead to the calculated power need and energy consumption being slightly higher than the real values for this application.

## 5.3   Electrical motor

### 5.3.1  Weight, power and efficiency

The data collected for different electrical machines was meant to provide a greater understanding of the relationship between weight, power, and efficiency for the two selected machine types. The choice of electrical motor is a complex task. It will now be discussed how the choice of electrical motor affects the drivetrain's efficiency and weight.

The results show an almost linear relationship between the power output and the weight for both types of machines (Figure 36). The bigger the machine, the greater the power output. This relationship is validated through the equation (2.18). The magnetic flux density $B_{mp}$ and electrical loading $\hat{A}_p$ vary within certain ranges. The magnetic flux density is dependent on the magnet's material properties and the size of the airgap. The electric loading depends on the winding configurations within the machine (i.e., the number of coils and the current flowing through). Assuming these parameters vary to a little degree, the physical characteristics of the machine will indeed impact its nominal power (Pyrhönen, 2008, p.282-284).

Though the linear representation gives an indication of how the size will affect the power output, it is not perfect. The results show deviations. Figure 39 and Figure 38 display the same curves represented in Figure 26 and Figure 28, but zoomed to desired nominal power area.

Both figures contain validation data required from electric motors specifically designed for ship propulsion. For the IM, the validation data comes from the Waterworld 10.0i and Vetus e-line 7.5- & 10-kW motors (see Appendix F), and for PMSM the validation data comes from the Drivemaster 15W and Epropulsion I-10 & I-20 motors (see Appendix G).
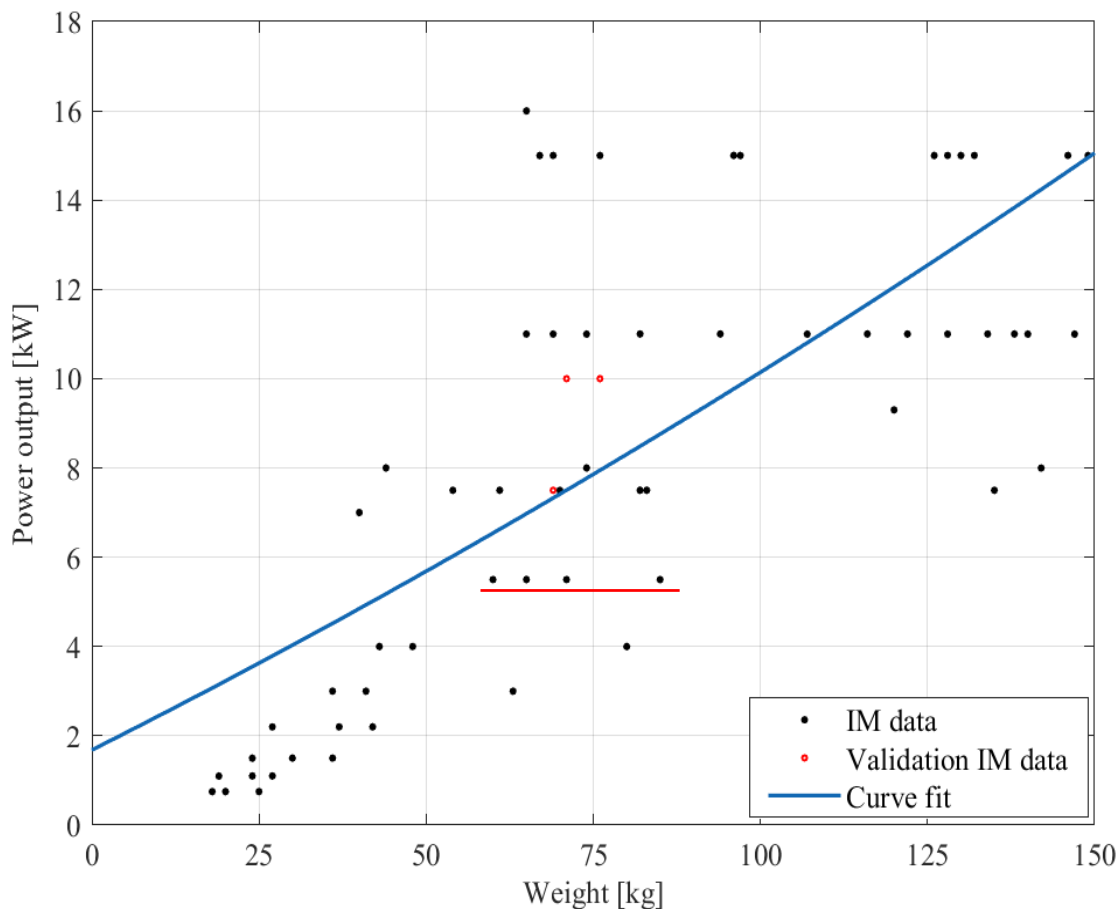


**Figure 38: Figure 26 – IM - zoomed.**
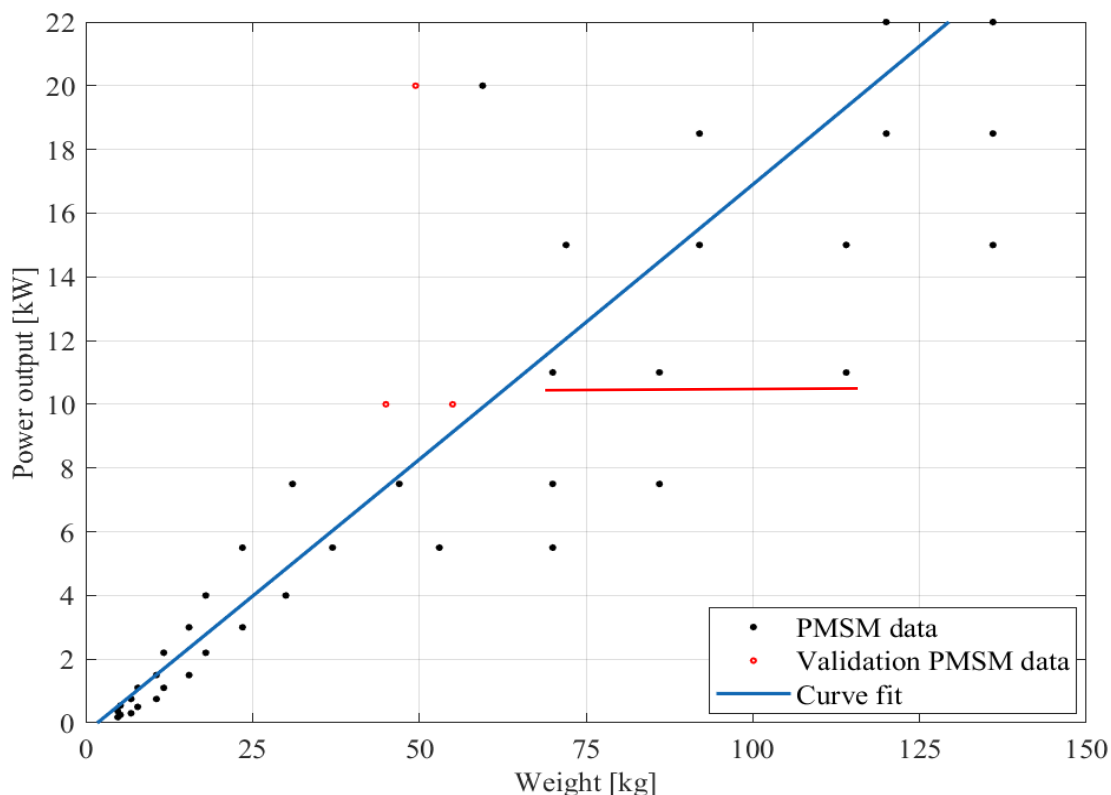
**Figure 39: Figure 28 – PMSM – zoomed.**

Deviations will occur due to different manufactures utilizing different technologies and techniques when designing the electrical machine. Some of the deviations which occur on the same power level, but a variety of weights (marked with a red line in both figures), is due to the difference in number of poles. To choose a machine with a high number of poles to lower the rotational speed would be beneficial to minimize or remove the need for a gear. However, the increase of pole pairs comes with an increase in weight and size (Pyrhönen. 2008, p.286-287), and the weight limit of 75kg is quickly exceeded when trying to keep a power output around 8-12 kW.

Further with an increase in weight, at the same power, efficiency tends to drop (Figure 29). When accessing commercially available electrical motors for ship propulsion, the majority of the machines exist within the 1500-3000 rpm range (i.e., with 4 or 2 poles). In order to keep the weight down and keep the efficiency drop to a minimum, the choice to look at machines with 4 poles and a nominal speed of 1500 rpm was made.

The relationship between efficiency and weight shows other tendencies. Figure 40 and Figure 41 display the same curves as in Figure 25 and Figure 27, but zoomed for the desired weight area.
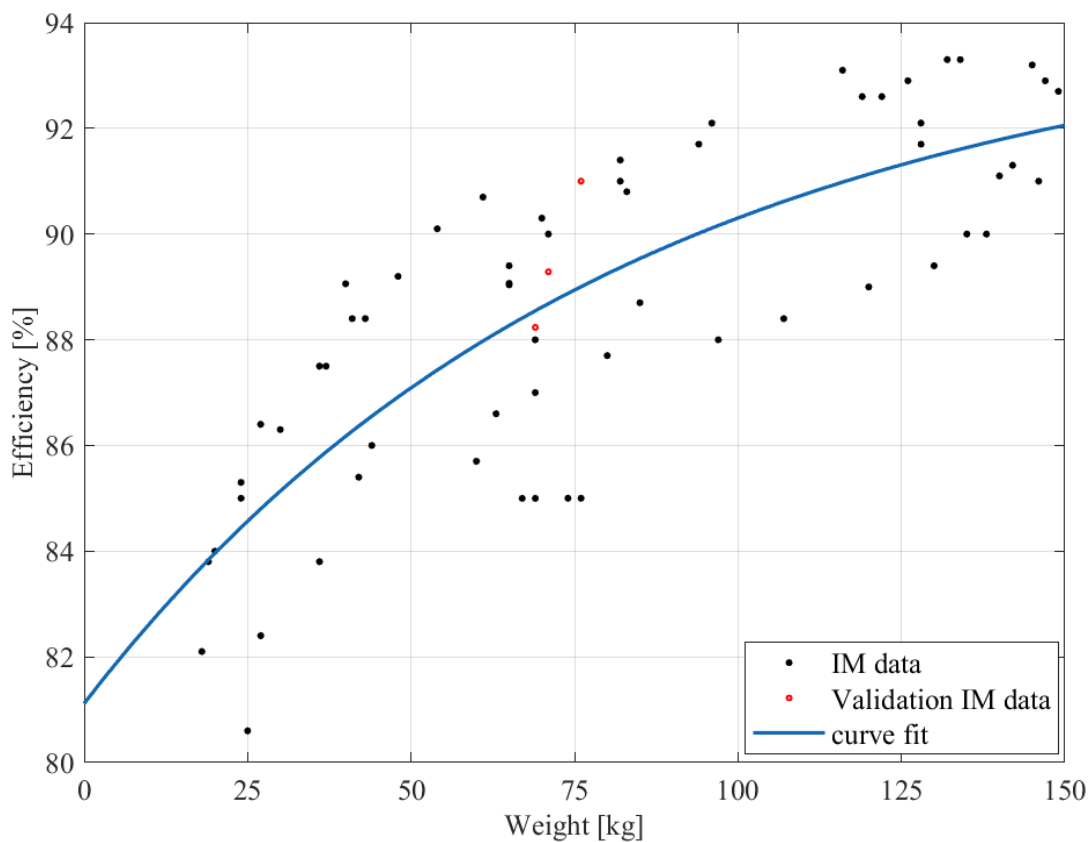
**Figure 40: Figure 25 – IM – zoomed.**
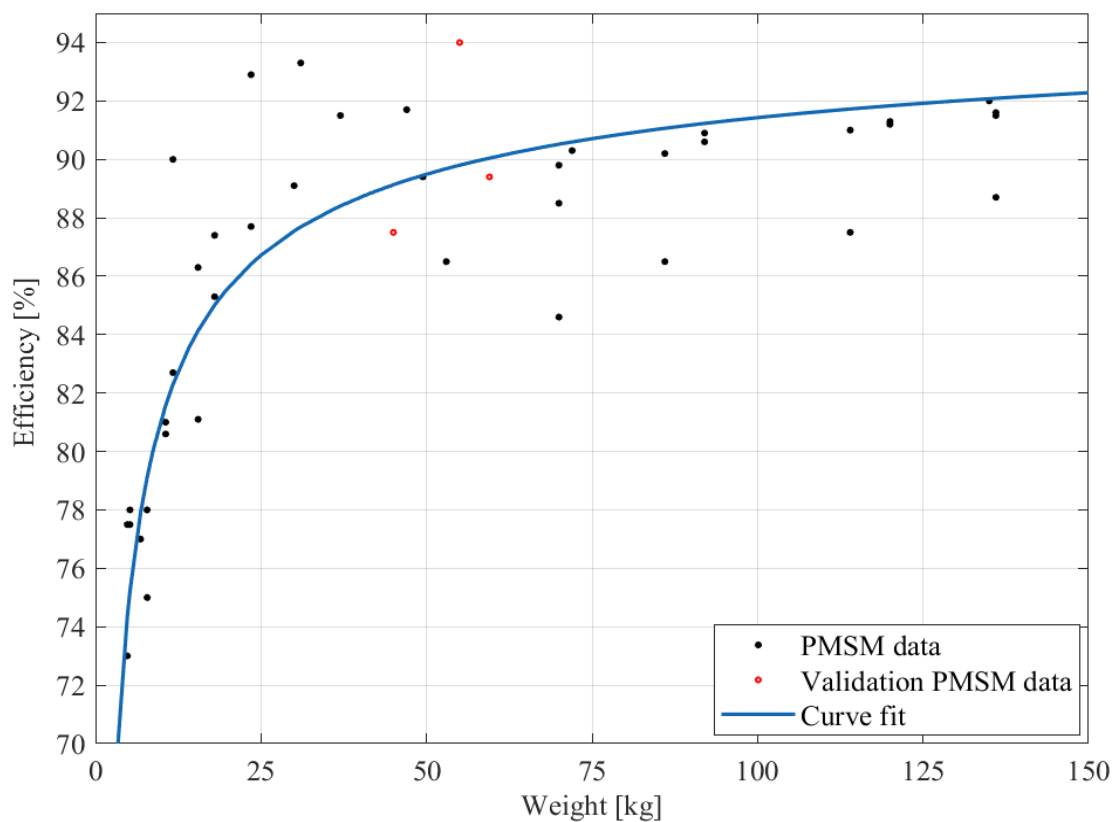


**Figure 41: Figure 27 – PMSM – zoomed.**

Efficiency seems to drop rapidly for smaller machines, and in the other converge towards a maximum efficiency. These tendencies are represented in the equation (4.1 and 4.3) for the curve fit, where large number of x (weight) makes the equations converge towards respectively 93.5590% for IM and 95.9315% for PMSM. So why does the larger machine have better efficiency?

The power losses in the machines mainly consist of copper losses. These losses increase depending on the resistance of the copper, and the current's square (equation 2.16). Further, the resistance of the copper is dependent on the machine's physical parameters as shown in equation (2.17).

The other power losses involve iron losses. Equation (2.15) shows how the iron losses (i.e., the hysteresis and eddy current losses) are dependent on mainly the frequency and not so much the size. Although it might have some variations dependent on size, it is assumed to be minimal compared to copper loss variations (Slobodan N, 2013, p.74).

This emphasizes how the size (and therefore also the weight) affects the losses. When studying equations (2.18) and (2.17), it can be seen that the size (i.e., the length l and the diameter d) have a greater impact on the rated power of the machine. Since the power is dependent on the square of the diameter times the length, whereas the copper resistance is dependent on the length and diameter, but it is also divided by the cross-sectional area, which will also increase with the size. Therefore, the increase in power will be greater than the increase in power loss, which can explain why efficiency tends to increase with the weight of the machine.

These results show how both machines are capable of great efficiencies, if made large enough. On the other hand, it also emphasizes that the efficiency of a PMSM increases more rapidly with increasing the weight compared to an IM for the lower areas of the curve. The PMSM also has an overall greater efficiency, which is expected given the fact that there are no rotor losses connected to its operation (equation 2.22)

From equation (2.18), it can also be derived that an increase in angular velocity of the electric machine, with constant power, will lead to a decrease in the size. The reduction in size will then also reduce the copper losses, but the higher frequency will increase the iron losses. The article by Anisimov presents an analysis of the effects of rotor speed on the sizing and losses of an electric motor. The results also emphasize how this would affect the efficiency of the machine.

The use of high-speed rotating machines to reduce size is an interesting topic to further investigate. Since most of the commercially available electrical machines for our purpose do not fall within these categories, and these machines usually require special manufacturing, the choice to exclude them from this thesis was made. It is, however, recommended to look into this as a part of further optimization of the electrical machine.

As mentioned before, most of the collected data is gathered from industrial machines. Electrical motors for ship propulsion or electric traction drives are often designed to keep the weight to a minimum while still being able to fulfill the given requirements. This can be seen in Figure 38 and Figure 39, where the red dots represent the validation data from machines specifically designed for ship propulsion. As can be seen, these machines also have deviations from each other. Even though the possibility to obtain machines with a high power-density [kW/kg] and a high efficiency, the results also emphasize how these machines might correspond with the curve. But how viable is the curve?

From the calculations for the maximum weight or the minimum power need (Table 8), an efficiency for the 12,5 kW PMSM around 91%, and around 89% for the 8 kW PMSM was obtained. Since the IM is heavier by default, the maximum rated power given by the weight limit of 75kg is almost the same as the minimum rated power needed to still meet the requirements of the operation profile. The efficiency obtained when considering an 8 kW IM is around 88.5%

The European commission regulation of October 2019 states that as of 1 July 2023 the energy efficiency for motors with a rated power equal to or above 0.12 kW and equal to or below 1000 kW, with 2,4,6 or 8 poles, shall correspond to at least IE2 efficiency level. The IE2 efficiency table is shown in Table 17.

*Table 17: Minimum efficiencies for IE2 efficiency level (commission regulation (EU), 2019. ANNEX 1)*

| Rated output power $P_N$ [kW] | Number of poles | | | |
|---|---|---|---|---|
| | 2 | 4 | 6 | 8 |
| 0,12 | 53,6 | 59,1 | 50,6 | 39,8 |
| 0,18 | 60,4 | 64,7 | 56,6 | 45,9 |
| 0,20 | 61,9 | 65,9 | 58,2 | 47,4 |
| 0,25 | 64,8 | 68,5 | 61,6 | 50,6 |
| 0,37 | 69,5 | 72,7 | 67,6 | 56,1 |
| 0,40 | 70,4 | 73,5 | 68,8 | 57,2 |
| 0,55 | 74,1 | 77,1 | 73,1 | 61,7 |
| 0,75 | 77,4 | 79,6 | 75,9 | 66,2 |
| 1,1 | 79,6 | 81,4 | 78,1 | 70,8 |
| 1,5 | 81,3 | 82,8 | 79,8 | 74,1 |
| 2,2 | 83,2 | 84,3 | 81,8 | 77,6 |
| 3 | 84,6 | 85,5 | 83,3 | 80,0 |
| 4 | 85,8 | 86,6 | 84,6 | 81,9 |
| 5,5 | 87,0 | 87,7 | 86,0 | 83,8 |
| 7,5 | 88,1 | 88,7 | 87,2 | 85,3 |
| 11 | 89,4 | 89,8 | 88,7 | 86,9 |
| 15 | 90,3 | 90,6 | 89,7 | 88,0 |
| 18,5 | 90,9 | 91,2 | 90,4 | 88,6 |
| 22 | 91,3 | 91,6 | 90,9 | 89,1 |
| 30 | 92,0 | 92,3 | 91,7 | 89,8 |

According to the table, the calculated values seem to be in line with the minimum requirements. Although some of the values barely make the minimum requirements, the fact that they show correspondence is a good sign for the validity of the curve. The fitted curves are therefore decided valid for further use, keeping in mind that it will be in the lower region compared to machines specifically designed for ship propulsion (commission regulation (EU), 2019. ANNEX 1).

### 5.3.2  Speed, load, and efficiency

The efficiency maps provide valuable information when accessing the dynamic behavior of the electrical machine's performances. especially when considering how speed affects efficiency. The efficiency maps do, however, change with different machine types, and do have some variation when considering machines of the same type as well. So, how much does the change of speed affect efficiency, and how viable is the data.

From the plotted load curve, the curve for the efficiency's dependence of speed is extracted. The validation of this extraction is put to questioning. The data retrieved from this extraction is lacking in terms of accuracy. Since the extraction bases itself on a thorough read of the efficiency map, utilizing code, the data tells nothing about the behavior outside the limits of the efficiency map. Further, the data retrieved comes in varying quality dependent on the nature of the efficiency map. Black lines, numbers, and other impurities create disturbances in the read. An example of how this would inflict the read is shown in Figure 42
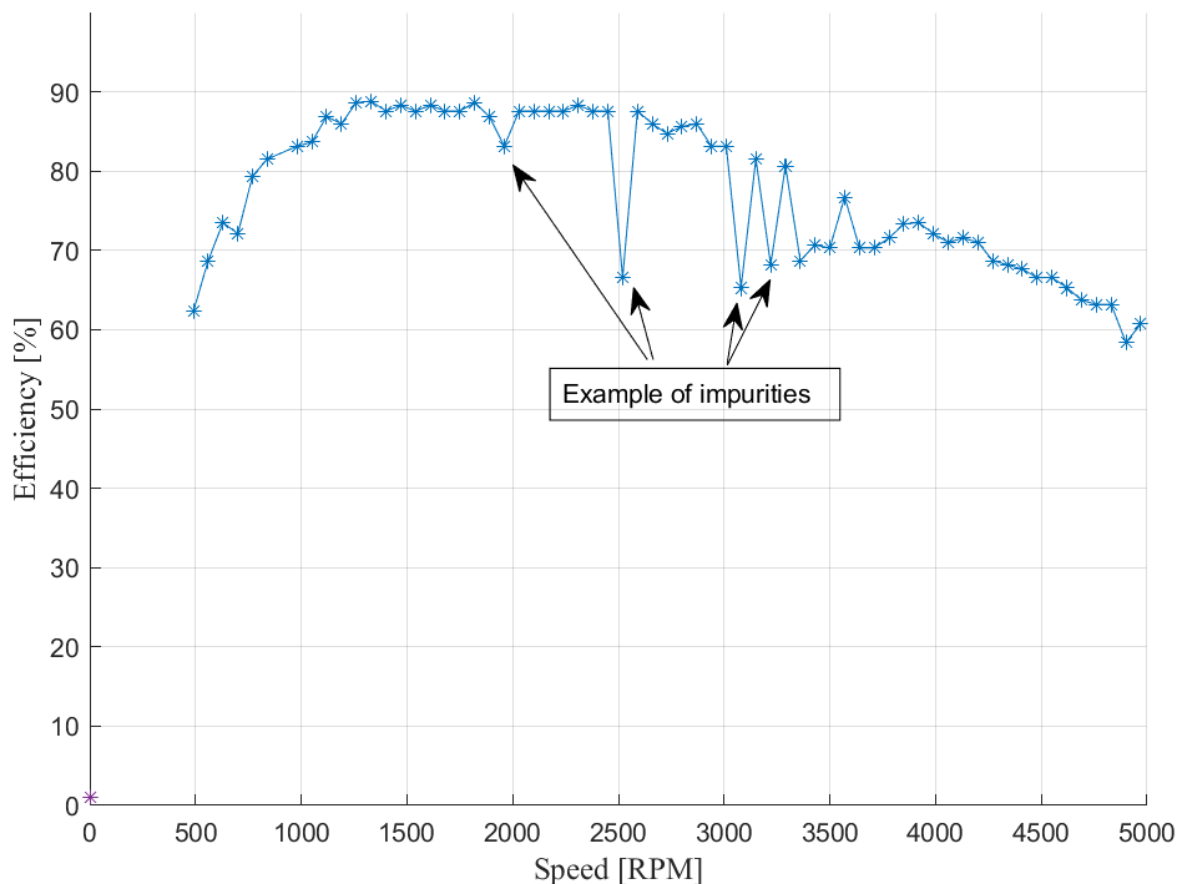


**Figure 42: Example of disturbances in read**

On the other hand, the read provides a greater number of what seems to be accurate reads, especially for the rpm range of interest (0-1500). Utilizing filter functions in the MATLAB gives a positive contribution to decreasing the impurities.

Due to difficulties obtaining efficiency maps for a large variety of power ranges, the few collected close to the desired power range are used as reference. This will result in some errors for the 12.5 kW read. An efficiency map is, as mentioned, individual for each machine. However, the behavior of efficiency within the efficiency map seems to be similar when comparing same

type of machines, for different nominal powers. This can be seen when comparing the 8 kW and 10 kW efficiency maps for the PMSM (Appendix B). For the IM the efficiency map for the 8 kW IM is used.

The first observation made when carrying out these extractions is how the implementation of a gear pushes the loading curve down, due to the reduced torque applied to the electrical machine (Figure 30):
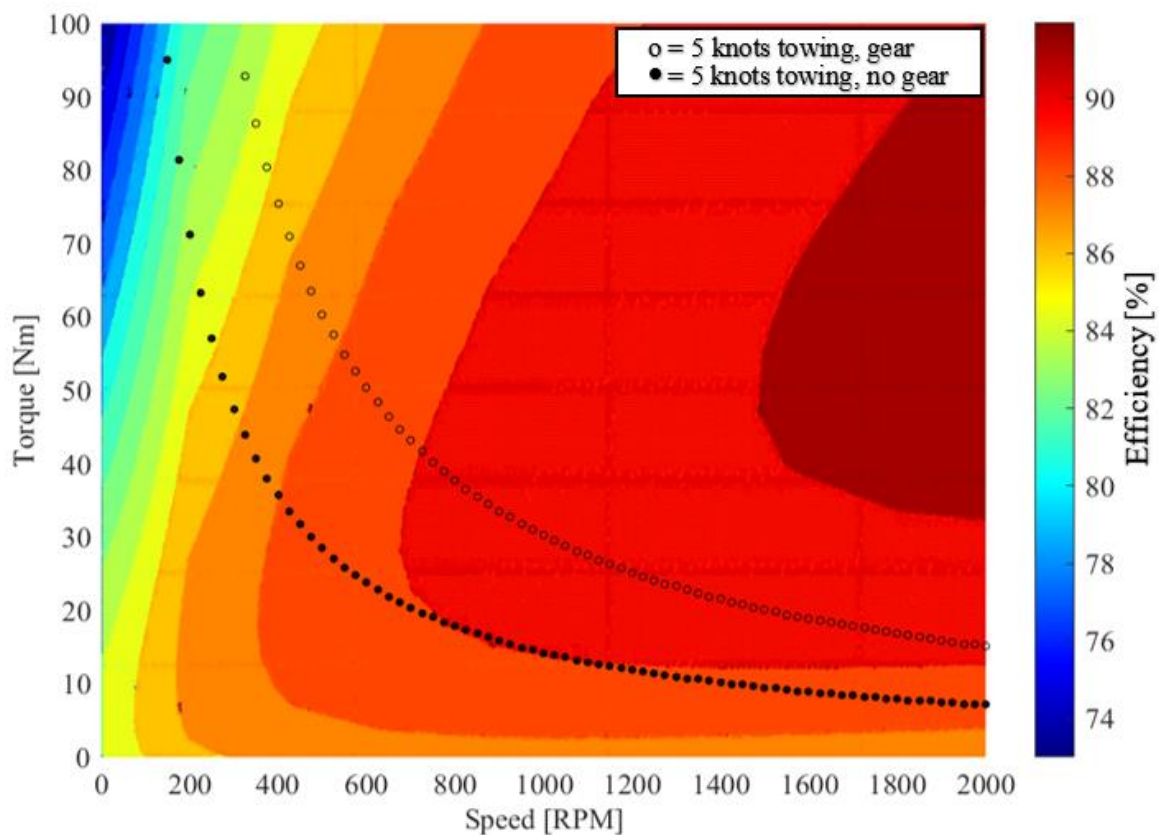


**Figure 30: Efficiency map with load curve 10 kW PMSM, 5 knots** towing.

This is one of the great benefits of utilizing a gear. The reduced torque allows the machine to maintain efficiency over a greater area of speed variation. When the torque becomes too high, the currents in the conductors increase accordingly. Since the copper losses are dependent on the current squared $I^2$, equation (2.16), the efficiency will, for increasing values of torque, decrease rapidly.

The second thing noticed is how none of the curves lay within the optimum operating area. Given the requirement for two drivetrains and means of propulsion, the choice to be able to propel the ship from one electrical motor was made. This is why Andressen & Mykland decided

on two 10 kW machines, one for each propeller. This choice of redundancy has led to the electrical machine being oversized. Most electric motors are designed to run at 50-100% of rated power. The maximum efficiency is usually somewhere near 75%. Outside these loading limits, efficiency tends to drop. However, this range can vary from different designs. This range also seems to increase for larger motors (U.S Department of energy, n.d, p.1). According to the calculations when the ship is propelling on both propellers, each machine has to produce a maximum of about 3 kW, which then corresponds to 30% of rated power. This value is even lower when operating in less demanding operating conditions. The vessel should also be able to drive on one propeller, which in theory would double the power requirement. However, these calculations would be dependent on the rudder configuration and, it is assumed that the operating on one propeller is for redundancy if failure, and not for conducting missions in this mode. This results in all the plotted loading curves being well below the optimum operating area. Further, the implementation of a gear pushes the curve only further away from the optimum point and thus ends up with a lower efficiency. The effects of this vary in degree based on type of machine. The PMSM has a high and relative steady efficiency for large areas of the efficiency map. Whereas the IM is more sensitive to these changes, especially for the less demanding operations.

On the other hand, by utilizing a gear, the torque and thus the current in the conductors, are kept lower for a larger variation of speed. This keeps the power losses smaller and allows it to operate at a larger variable of speeds without great changes in efficiency. It is possible to obtain a high efficiency for a lower rpm the closer the curve is to the bottom left corner. This area of variable speed is much larger at the PMSM compared to the IM. This is a side effect of the machine being oversized. For a smaller sized machine, and thus a loading curve far higher in the efficiency map the machine would be more sensitive towards speed variations, which can be seen in the calculations for the 8 kW machines in Table 10.

## 5.4   Battery

The previous thesis estimated values for energy density and necessary capacity. A rough estimate for the initial necessary capacity was made and set to 250 kWh. The energy density was based on an average energy density for the Tesla 4680-type battery, with a 40% reduction to consider cold environment.

The new calculations regarding the battery seem to provide more accuracy than the previous estimation. The power density of the KBP63 is 163 Wh/kg, which is close to the estimated value of Andressen & Mykland of 170Wh/kg. The battery retrieved from Kreisel electric is a lithium-ion battery designed for marine applications, which is certified by DNV, has a degree of protection of IP67 and has protective measures taken regarding salt misting. Further the ambient temperature range is from -40 to 70 degrees, which will be sufficient for the given AO. Kreisel electric has not manufactured a battery large enough for our use. Therefore, the weight is estimated only on power density and necessary capacity. However, this gives an indication of what the state-of-the-art technology is capable of when it comes to batteries for marine applications and might not require such a substantial development phase as expected when utilizing the Tesla 4680-type battery. Although the investigation of the battery choice might provide more accurate data, it lacks in presenting data regarding charging, discharging, self-discharging and any form of battery management system. This should be investigated in further work.

## 5.5   Diesel generator efficiency

The results for the diesel generator indicate a much lower efficiency value than previously estimated. Further the newly calculated values give a picture of how efficiency is dependent on loading of the diesel generator.

For the 22.5 kW synchronous generator the calculated efficiency value of 92% seems to be in accordance with the IE2 efficiency level presented in Table 17. When the operating speed remains constant at synchronous speed, the only thing affecting efficiency will be the torque, which is dependent on the load. The efficiency map for the PMSM emphasizes how, when operating at higher rpm's, the machine is more capable of handling variations in load, without larger variations in efficiency.

For the diesel engine, efficiency is determined by the amount of power consumed, in the form of fuel, compared to the power delivered shaft connecting to the generator. Given the linear relation for fuel consumption in Figure 36, and equation (2.28) it can be derived that the efficiency of the diesel engine will be greater for higher power outputs.

The results displayed that the highest efficiencies for the diesel generator are retrieved for the 8 kW IM with the old propeller design at around 25-29%. Which is expected given that this is the configuration that requires the most power (Table 12). It can also be seen that the efficiency

of the diesel generator is dominated by the efficiency of the diesel engine given its low efficiency value compared to the generator part. Although these results emphasize the how efficiency varies for the load, they do not account for power losses due to friction or the powering of auxiliary systems connected to the diesel generator. Furthermore, only the M-SQ Pro 25 diesel generator is accessed. However, the linear relationship for fuel consumption seems to be in accordance with fuel consumption charts given by manufacturers of diesel generators (Table 18).

*Table 18: Diesel Generator Fuel Consumption chart in liters (FW Power, n.d)*

| Generator Size | Approximate Diesel Fuel Consumption | | | |
| --- | --- | --- | --- | --- |
| | ¼ Load (litres/hr) | ½ Load (litres/hr) | ¾ Load (litres/hr) | Full Load (litres/hr) |
| 8kW / 10kVA | 1 | 1 | 2 | 3 |
| 10kW / 12kVA | 1 | 2 | 3 | 4 |
| 12kW / 15kVA | 1 | 2 | 3 | 4 |
| 16kW / 20kVA | 1 | 3 | 4 | 5 |
| 20kW / 25kVA | 2 | 3 | 5 | 6 |
| 24kW / 30kVA | 2 | 4 | 5 | 7 |
| 32kW / 40kVA | 3 | 5 | 8 | 10 |
| 40kW / 50kVA | 3 | 6 | 9 | 12 |

So, can the higher diesel generator efficiency make up for a lower efficiency in other parts of the drivetrain?

## 5.6   Efficiency, Fuel requirement and weight of drivetrain

To lower the weight of the drivetrain it is important to find the optimum combinations of components, without compromising too much of the efficiency. It is no use considering a lighter machine if this results in lower efficiency, and one end up having to carry more fuel. When calculating the weight and fuel consumption for the drivetrain, all the previous calculations are considered. The calculations are done for all configurations. Old vs new propeller design, gear vs no gear, 12.5 kW or 8 kW and PMSM vs IM. So, witch configurations can provide the lowest weight, highest efficiency and lowest fuel consumption.

The first observation is that the new propeller design with a 12.5 kW PMSM without a gear retrieves some of the highest drivetrain efficiencies and the lowest fuel consumption for the

given operational profile (Table 15). Further, it shows how most of the PMSM configurations and some of the IM configurations do not stray too far away from the best result. When sizing down from a 12.5 kW PMSM to a 8 kW PMSM, new design, with a gear, one only end up with an increase in fuel of 5.9 liters per operation profile, but since sizing down to an 8 kW machine, the weight of the machine drops about 25 kg per machine (Table 8). If sizing down to an 8 kW IM, new design, no gear, one only gets an increase of 67.3 liters per operation profile, which corresponds to about 57.5 kg. However, the weight benefits of downsizing are reduced due to the heavier nature of the IM. Even though the 8 kW IM is higher in weight and lower in efficiency, and thus has an increased fuel consumption, it could be justified by some of the benefits of choosing an IM. The IM is simple and relatively cheap to produce compared to the PMSM. Further it is considered a robust and reliable machine which will contribute to the vessel's overall reliability and survivability.

Secondly, the result emphasizes how the change in propeller design affects the overall fuel consumption for this operation profile. This occurs due to the new propeller design requiring a higher rotational speed for the propeller, which leads to less speed variations for the electrical machine, and thus smaller efficiency changes. In the extreme cases for the 8 kW IM, old propeller design, the fuel consumption is reduced by 196.7 liters, which corresponds to about 168kg. However, it is important to keep in mind that this is for the given operation profile. The reduction occurs because the new propeller design creates steadier efficiency, which is beneficial when the USV is to operate in a broader spectrum of speeds and loads. Nevertheless, the decisive requirement regarding fuel revolves around the 5 knots towing condition in sea state 3 with a 35% remaining fuel. Therefore, the configuration with the best efficiency for this condition (the old design) will end up with the lowest total required amount of fuel storage. This will of course be a positive contribution to the overall weight as shown in Table 16. On the other hand, when considering the possible diversity occurring in an operational profile, the new propeller design might be able to fulfill the same operation profile with lesser amount of fuel consumed. As a test the old operation profile was updated to 400 hours of 5 knots towing, compared to the previous 200 (Table 19**Error! Reference source not found.**)

*Table 19: Fuel consumption for operation profile updated to 400 hours 5 knots towing.*

| desicive factors | | | total fuel consumtion for operation profile [liters] |
|---|---|---|---|
| 12,5 kW PMSM | old propeller design | no gear | 2645,9 |
| | | gear | 2623,3 |
| | new propeller design | no gear | 2632,0 |
| | | gear | 2640,1 |
| 8 kW PMSM | old propeller design | no gear | 2773,6 |
| | | gear | 2639,8 |
| | new propeller design | no gear | 2673,2 |
| | | gear | 2641,6 |
| 8 kW IM | old propeller design | no gear | 3053,1 |
| | | gear | 2944,7 |
| | new propeller design | no gear | 2753,1 |
| | | gear | 2757,8 |

At this point the old propeller design just surpasses the new design due to the increase in the 5 knots towing condition. The same can be seen when reducing the 7 knots transit time to 50 compared to the previous 100 (Table 20).

*Table 20: Fuel consumption for operation profile updated to 50 hours 7 knots transit.*

| desicive factors | | | total fuel consumtion for operation profile [liters] |
|---|---|---|---|
| 12,5 kW PMSM | old propeller design | no gear | 1335,6 |
| | | gear | 1324,3 |
| | new propeller design | no gear | 1328,6 |
| | | gear | 1332,6 |
| 8 kW PMSM | old propeller design | no gear | 1399,5 |
| | | gear | 1332,5 |
| | new propeller design | no gear | 1349,2 |
| | | gear | 1333,4 |
| 8 kW IM | old propeller design | no gear | 1539,4 |
| | | gear | 1486,3 |
| | new propeller design | no gear | 1389,3 |
| | | gear | 1392,2 |

It seems the difference in these two designs is minimal when the transit to towing ratio is about 1:4. For more transit hours, the new design becomes more beneficial, and for more towing hours the old design is preferred.

Thirdly, the result for the overall weight of the drivetrain shows that the lowest weight is obtained by the 8 kW PMSM, with the old propeller design and a gear. The old propeller design gives it one of the lowest fuel requirements for the 5 knots towing condition (Table 16). A high overall efficiency (Table 15) gives it one of the lowest necessary capacities', and thus one of

the lightest batteries (Table 11). Further, with the reduction in weight from 12.5 kW to 8 kW (Table 8) it obtains the lowest weight. Although this configuration gives the lowest weight, other configurations do not deviate much from the best result. For all the PMSM configurations the largest deviation is 275.8kg and the smallest being 16.9 kg. The IM, however, shows a considerable weight gain, with the lowest being 285.7 kg, and the highest being 929 kg. This is not only due to its lower power density compared to the PMSM, but also due to the lower efficiency, which leads to higher fuel consumption, a higher necessary capacity for the battery, and thus a heavier battery.

Lastly, given the updated efficiency values for most of the components in the drivetrain, the fuel consumption has increased for all configurations, compared to Andressen & Mykland's thesis. However, the updated values for necessary capacity have lowered the battery weight, from the previous 1500kg, for all but one configuration. The weight breakdown for their thesis gives their drivetrain an overall weight of 6205kg (ref Appendix A). The updated weight break-down shows a minimum increase in weight of 423.5kg, and a maximum of 1129kg.

# 6 Conclusion and recommendation for further work

## 6.1 Conclusion

This thesis has aimed to provide a deeper analysis of the dynamic behavior of the drivetrain configuration of a *naval design study of a small, unmanned surface vessel.* The thesis has studied each of the components within the drivetrain, emphasizing factors such as weight, performance, and efficiency. Through relevant theory, and collection of empirical data, the thesis has described the dynamic behavior for each component and its effect on the drivetrain. The change in the drivetrain is also assessed against the requirements to fulfill the operational capabilities. Further, new values are presented for previous estimations, and updated values for fuel consumption, fuel storage and weight of the drivetrain are obtained.

From the result found from this analysis, our recommendation is the configuration involving an 8 kW PMSM, the new propeller design utilizing a gear. The choice of PMSM instead of an IM was made due to its ability to maintain high efficiency over large variation of speeds and torques, as well as it being lighter compared to the IM. Further, the 8 kW PMSM gives a reduction in weight and, also assumed, price compared to the 12.5 kW PMSM. The new propeller design makes for an overall steadier efficiency, which makes it more versatile for the given, and other, operation profiles. Furthermore, it also requires higher speeds for the propeller, which also is beneficial for the electric motor. The implementation of a gear further enhances the rotational operating area for the motor, with a very low loss of efficiency. This configuration with its high overall efficiency gives it a low battery weight, low fuel consumption for the operation profile, and one of the lowest necessary fuel capacities.

However, the configuration of a drivetrain is complex and not always straight forward. Some of the complexities when addressing a drivetrain configuration are showcased in this thesis. It can be seen that many factors regarding capabilities, operating area, choice and sizing of components and probably many more must be accounted for. Optimization would require use of heavy optimization tools which can account for the many variables. Due to this complexity, our choice may not be the optimum solution, and further work will be necessary.

## 6.2   Recommendation for further work

Before moving forward with the design of the drivetrain and the USV, the following aspects is recommended for further work, based on the findings in this study:

- Physical testing of a reference model of the drivetrain.
- Investigate the extent to which the different sea states affect the USV.
- Investigate rudder configurations and its effect on the drivetrain.
- Further optimization of the drivetrain.
- Adress the power requirements of components outside the drivetrain.
- Investigate the use of high-speed or low-speed electrical motors, as a way to optimize weight and efficiency of electric motor.
- Investigate battery management system.
- Investigate diesel generator size, weight and efficiency.
- Investigate newer propeller designs.
- Addressing shaft size and material.

# References

1. Melkebeek, Jan A. (2018) *Electrical machines and drives*, Ghent: Springer international publishing.

2. Andrea, D (2020) *Lithium-ion batteries and applications*. Norwood: Artech House

3. Vukosavic, Slobodan N. (2013) *Electrical machines,* Belgrade: Springer publishing

4. Dragonfly Energy (2022, 22. December) *Why Does Energy Density Matter In Batteries?* [Why Does Energy Density Matter In Batteries? | Dragonfly Energy](#)

5. Det kongelige Forsvarsdepartementet (2020) *Evne til forsvar – vilje til beredskap. Langtidsplan for forsvarssektoren.* p.26-32)

6. Siversten, L (2019) *Elektriske maskiner – oppbygging, virkemåte og drift,* Bergen: Fagbokforlaget

7. Molian, S. (1982) *Mechanism Design: an introductory Text,* Cambridge: Cambridge University Press

8. FFI (2020) *Russiske kjernefysiske styrker.* [Russiske kjernefysiske styrker (knowledgearc.net)](#)

9. Hattrem, E (2021) *En ny og skjult trussel utenfor Norges kyst* [Kinesiske, russiske og amerikanske ubåter i enorsk farvann - Teknologi (klikk.no)](#)

10. Pyrhönen, J., Jokinen, T., & Hrabovcovà, V. (2008) *Desing of rotating electrical machines,* Lappeenranta: Lappeenranta University of Technology

11. Commission regulation (EU), (2019), ANNEX 1

12. DNV (2007) *CALCULATION OF SHAFTS IN MARINE APPLICATIONS.*

13. GeoSpectrum (2018) GeoSpectrum Technologies to Showcase their Towed Reelable Active Passive Sonar (TRAPS) at CANSEC 2018. [GeoSpectrum Technologies to Showcase their Towed Reelable Active Passive Sonar (TRAPS) at CANSEC 2018 | Elbit Systems](#)

14. Grønn, Ø (2022, 22.september) Virkningsgrad, i *Store norske leksikon.* [virkningsgrad – Store norske leksikon (snl.no)](#)

15. Anisimov, V.R, Filatov, V.V, Klimov, A.V & Ryabtsev, F.A. (2021) *Optimisation of the Rotor Speed as a way to Improve Specific Indicators of Traction Electric Motors.* Moscow. [https://doi.org/10.1109/IEEECONF51389.2021.9416120](https://doi.org/10.1109/IEEECONF51389.2021.9416120)

16. Haines, G., Ertugrul, N. & Soong, W.L (2019) *Autonomously obtaining system efficiency maps from motor drive systems.* Australia: The University of Adelaide. IEEE Xplore Full-Text PDF:

17. U.S. Department of Energy (n.d) *Motor challenge – Determining Electric Motor Load and Efficiency.* Retrieved 28. November 2023 from (Determining Electric Motor Load and Efficiency (energy.gov)

18. FW Power (n.d) *Diesel generator fuel consumption.* Retrieved 28. November 2023 from Diesel Generator Fuel Consumption - Diesel Generators | New and Used Generators | FW Power

19. Jones, W.G (2007) *Distribution system operation and planning in the presence of distributed generation technology.* Missouri: University of Missouri-Rolla Distribution system operation and planning in the presence of distributed generation technology (mst.edu)

20. Bryant M (2023, 26. September) Key details behind Nord Stream pipeline blasts revealed by scientists. *The Guardian.* Key details behind Nord Stream pipeline blasts revealed by scientists | Nord Stream 1 pipeline | The Guardian

21. Andressen M & Mykland R (2022) *A naval design study on a small, unmanned surface vessel.* Bergen: Royal Norwegian Naval Academy

22. Shi W, Stapersma D & Grimmelius H.T (2009) *Analysis of energy conversion in ship propulsion system in off-design operation conditions.* Department of Marine & Transport Technology, Delft University of Technology, The Netherlands & Netherlands Defence Academy, The Netherlands. http://dx.doi.org/10.2495/ESU090411

23. Lund A & Strand G (2013) *Kompendium skipsmaskineri drift og vedlikehold,* Bergen: Bergen maritime fagskole

24. Forsvaret (2023) *Kystvakten – «Alltid til stede».* Kystvakten - Forsvaret

25. Forsvaret (2023) *Marinen.* Marinen - Forsvaret

26. Sivle, A. D. (2018, February 27th 2018). Sjøgang. Retrieved from sjøgang – Store norske leksikon (snl.no)

27. Unknown creator. (2018). *Propeller anatomy* [illustration]. Propeller Anatomy – Accutech (accutechmarine.com)

28. Czyż, Z., Karpiński, P., Skiba, K., & Wendeker, M. (2021). Wind Tunnel Performance Tests of the Propellers with Different Pitch for the Electric Propulsion System, p. 2.

29. Rawson, K.J. & Tupper, E.C. (2001). *Basic Ship Theory* (5$^{th}$ ed.). Butterworth-Heinemann

30. Davis, J.R. (2005) *Gear Materials, Properties, and Manufacture.* Materials Park, Ohio : ASM International.

31. Magnussen, A.K (2017) *Rational calculation of sea margin.* Trondheim: Norwegian University of Science and Technology. Rational calculation of sea margin (ntnu.no)

32. Eslamdoost, A., Larson, L. & Bensow, R. (2015, June). *Waterjet Propulsion and Negative Thrust Deduction*, Fourth International Symposium on Marine Propulsors smp'15, Austin, Texas. MA3-3.pdf (marinepropulsors.com)

33. Whiteford, S. (2022, January 8). *Ship propellers – how do they work?.* One Step Power. Ship propellers - how do they work? (onesteppower.com)

34. Mikhaylov, K, Tervonen, J & Faddev, D (2012) *Development of Energy Efficiency Aware Applications Using Commercial Low Power Embedded Systems.* In book: Embedded Systems - Theory and Design Methodology. DOI:10.5772/38171

35. California Energy Commission (2023) *Solar Equipment Lists - Grid Support Solar Inverters.* Solar Equipment List - CA Energy Commission

36. Oosterveld, M. W. C. (1970, 25$^{th}$ June) *WAKE ADAPTED DUCTED PROPELLERS.* H. Veenman & Zonen N.V.

# Appendixes

Appendix K will come as a separate file due to its format.

- Appendix A - Weight breakdown of vessel from Andressen & Mykland
- Appendix B – Efficiency maps
- Appendix C – Resistance curve of USV
- Appendix D – rectifier
- Appendix E - MATLAB scrip for adaption of gear efficiency curves
- Appendix F – Motor data IM
- Appendix G – Motor data PMSM
- Appendix H –MATLAB script for plotting of nominal power, weight, and efficiency of collected motor data.
- Appendix I – MATLAB script for extracting data from efficiency maps
- Appendix J – KBP63 Battery
- Appendix K – Drivetrain calculations weight, fuel consumption & efficiency